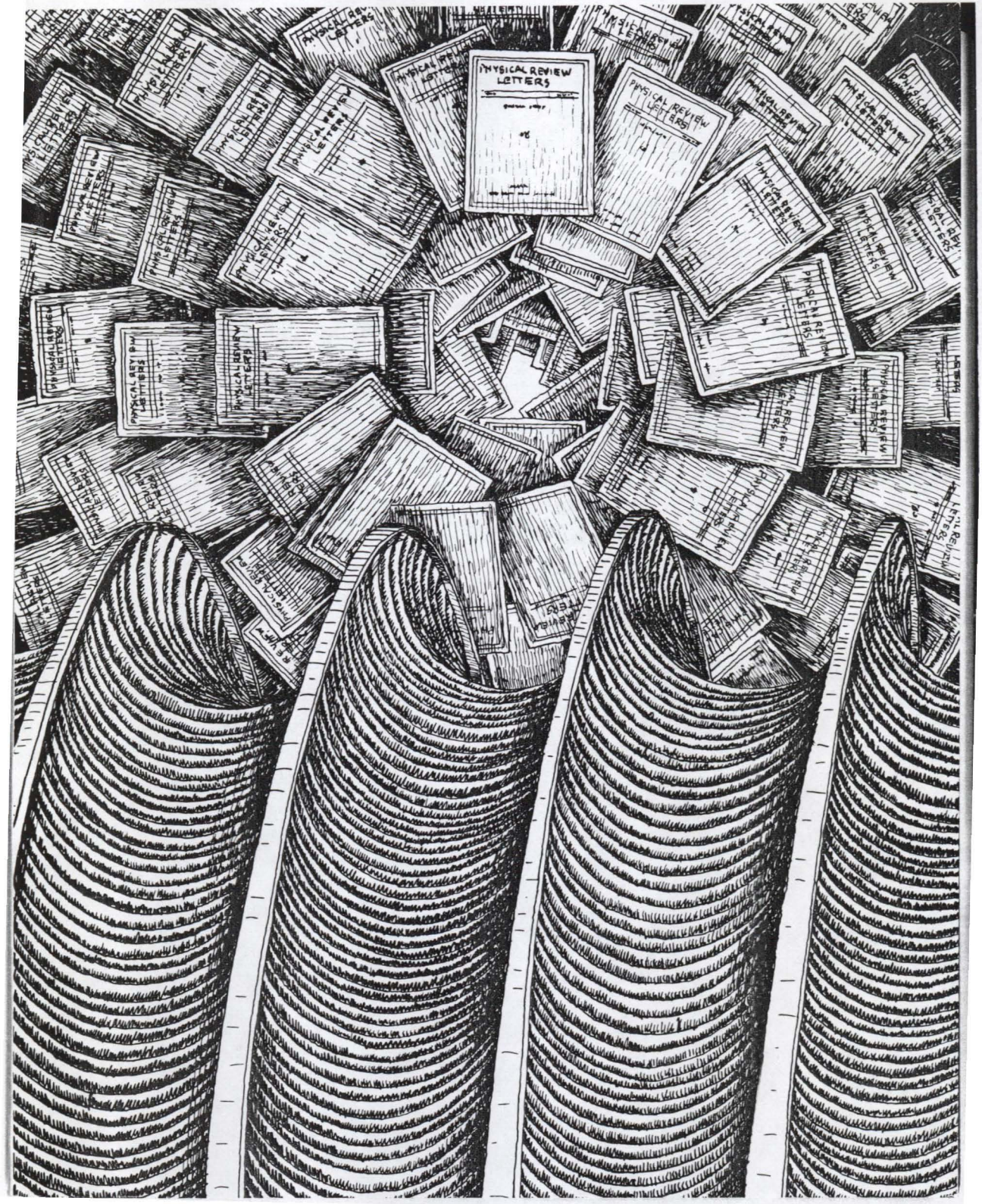
PHYSICAL REVIEW LETTERS

A Summary of Research Activities in the Meson Lab (1972-1977)

June, 1977

A. L. Read

Fermi National Accelerator Laboratory
Batavia, Illinois

Operated by Universities Research Association Inc.
under contract with the United States Department of Energy

TABLE OF CONTENTS

		Page
I.	Introduction	2
II.	Physics Results Published to Date	3
	A. Low Momentum Transfer Hadron Physics	
	Introduction	3
	Total Cross Sections of Hadrons on Hadrons	
	A.1 Experiment #104: Measurements of Total Cross Sections on Hydrogen and Deuterium	9
	A.2 Experiment #4: Neutron Total Cross Sections Up To 300 GeV	11
	A.3 Experiment #27/305: Neutron-Nuclear Total Cross Sections	12
	Elastic Scattering of Hadrons by Hadrons	
	A.4 Experiment #96: Elastic Scattering of Hadrons on Hydrogen and Deuterium	13
	A.5 Experiment #7: $\pi^{\pm}p$ and p-p Differential Elastic Scattering Cross Sections from 20 to 200 GeV	15
	A.6 Experiment #61: Polarization in pp, $\pi^{-}p$ and $\pi^{+}p$ Elastic Scattering at 100 and 300 GeV/c	16
	Charge Exchange and K^0 Regeneration Experiments	
	A.7 Experiment #111: Study of $\pi^{-}p \rightarrow \pi^{0}n$ and $\pi^{-}p \rightarrow \eta n$ at High Energy	17
	A.8 Experiment #82/425: Regeneration of Neutral K Mesons at Very High Energies	22
	A.9 Experiment #12: A Study of Neutron-Proton Charge-Exchange Scattering in the Momentum Range 50-300 GeV/c	26
	Inclusive Particle Production	
	A.10 Experiment #8: Λ^0 Polarization in Inclusive Production	28
	A.11 Experiment #96: Inclusive Particle Production	31

Page

A.12 Experiment #324: Single Particle Spectra in High-Energy Collisions of Charged Hadrons 34

Diffraction Dissociation

A.13 Experiment #27/305: Coherent Dissociation of Neutrons 36

Inelastic Collisions of Hadrons with Nuclei

A.14 Experiment #178: A Study of the Average Multiplicity and Multiplicity Distributions in Hadron-Nucleus Collisions at High Energies 41

B. Large Transverse Momentum Hadron Physics

Introduction 44

B.1 Experiment #268: Study of Meson Production at Large p_T with a γ-Ray Detector 45

B.2 Experiment #260: A Study of High-p_T Physics with a Multiparticle Spectrometer 47

C. Searches for New Particles

Introduction 50

Searches for Quarks

C.1 Experiment #72: Quark Search at Fermilab 51

C.2 Experiment #75: Search for Fractionally Charged Quarks 52

C.3 Experiment #330: Search for Massive Neutral Particles 53

Search for Charmed Particles

C.4 Experiment #357/472: Search for Charmed Particles 54

C.5 Experiment #305: Search for Narrow Resonances Produced by Neutron Dissociation 56

C.6 Experiment #366: Study of Heavy, Narrow Mesons Using a Mass Focusing Spectrometer 57

C.7 Experiment #416: Steamer Chamber Search for New States Which Decay Semi-Leptonically 58

Page

C.8 Experiment #365: Search for Forward Production of Massive States Which Decay with Muon Emission 59

D. Measurements of Fundamental Properties of Hadrons

D.1 Experiment #216: A Measurement of the Pion Form Factor by Direct Pion Electron Scattering 61

E. Other Experiments

E.1 Nuclear Emulsion, Nuclear Chemistry, and Applied Radiation Physics Experiments 63

E.2 Experiment #22: A Search for Multigamma Events from Magnetic Monopole Pairs 63

E.3 Experiment #230: A Search for "Schein Events" and Events with a High Multiplicity of γ's 64

III. Experiments with No Published Results to Date (June 1977) 66

F. Recently Completed Experiments; Data Presently Being Analyzed

Low Momentum Transfer Hadron Physics

F.1 Experiment #248: Neutron-Proton Diffraction Scattering 66

F.2 Experiment #486: Study of the Atomic Number Dependence of the Difference Between Particle and Anti-Particle Cross Sections 66

F.3 Experiment #397: Search for High Mass Particles Produced In Association With Prompt Muons 67

F.4 Experiment #415: Measurement of $\pi^- Cu \rightarrow K_s^0$, Λ^0, and Neutron Inclusive Cross Sections 68

Large Transverse Momentum Hadron Physics

F.5 Experiment #350: Study of π^0 and η Inclusive Production with Incident π^- in the Triple-Regge Region 69

Page

Measurements of Fundamental Properties of Hadrons

F.6 Experiment #456: Measurement of the Kaon Form Factor 70

F.7 Experiment #226: Coherent K_s^0 Regeneration by Electrons 71

F.8 Experiment #440: A New Measurement of the Magnetic Moment of the Λ^0 Hyperon 71

Other Experiments

F.9 Experiment #507: Study of Channeling at Fermilab 72

G. Experiments Presently in Progress

Low Momentum Transfer Hadron Physics

G.1 Experiment #110: Study of Multiparticle Peripheral Physics at NAL 73

G.2 Experiment #396: Elastic Scattering and Diffraction Dissociation at Small Momentum Transfer for $\pi^{\pm}$, $K^{\pm}$, $p^{\pm}$ on p and n 73

G.3 Experiment #383: Study of the Inclusive Production of K_s^0 by K^- on Hydrogen 74

G.4 Experiment #290: Backward Pion-Proton Elastic Scattering 75

G.5 Experiment #404: Inclusive Neutron Production by Protons on Protons and Nuclei 75

G.6 Experiment #441: Polarization in the Reaction $pp \rightarrow \Lambda^0$ + Anything, with a Liquid Hydrogen Target 76

G.7 Experiment #118: Hadron Spectra from High Energy Interactions 76

Large Transverse Momentum Hadron Physics

G.8 Experiment #236: Exploration of the Large p_T Domain -- Inclusive Cross Sections and Possible Jet Structures 77

G.9 Experiment #439: High Sensitivity Search for New States Which Decay Into Muons 78

Page

G.10 Experiment #395: Calorimeter-Array Study of High p_T Events 79

H. Approved Experiments Which Have Not Yet Been Installed

Low Momentum Transfer Hadron Physics

H.1 Experiment #99: Study of $\pi^+p \to K^+\Sigma^+$ and $\pi^+p \to K^+Y^{*+}$ using the Focusing Spectrometer Facility 80

H.2 Experiment #272: Study of the Coherent Dissociation of π, K and p into Strange Particles at NAL Energies 80

H.3 Experiment #451: Study of the A-Dependence of Inclusive Processes and Associated Multiplicity 81

H.4 Experiment #495: Study of Ξ^0 and $\bar{\Lambda}^0$ Production and Polarization 82

Search for New Particles

H.5 Experiment #490: Search for Short-Lived Particles Using a High Resolution Streamer Chamber 83

H.6 Experiment #515: Study of Charmed Particles Produced in Hadronic Interactions 84

H.7 Experiment #468: Search for Penetrating Massive Neutral Particles Produced in High Energy Proton Collisions 85

H.8 Experiment #354: Survey for Exotic Particles in the M1 Beam 85

Measurement of Fundamental Properties of Hadrons

H.9 Experiment #533: Measurement of the Rate of Formation of π-μ Atoms in $K_L^0 \to \pi\mu\nu$ Decay 86

I. Experiments Completed More Than a Year Ago, and With No Published Results Yet

I.1 Experiment #51: Mass spectrum and Decay Modes for Bosons with Masses Up to 15 GeV 87

Page

I.2 Experiment #86: Study of Inelastic Diffractive Processes by Observing Coherent Production of Multi-Pion Final States from He Nuclei 87

I.3 Experiment #69: Elastic Scattering of the Long-Lived Hadrons 88

IV. Summary and Conclusions 89

Acknowledgments 92 ~~93~~

Bibliography 93 ~~94~~

References 99 ~~100~~

Tables 105 ~~106~~

Figures 109 ~~110~~

Abstract

In this paper we summarize the results of the experiments done in the Meson Lab during the first five years of its operation. We also give a brief discussion of experiments which are presently in progress and for which results are not yet available.

I. Introduction

In this paper we summarize the results of the physics research program in the Meson Lab during the first five years of operation, 1972-77.

A beam of 200 GeV protons was first delivered to the Meson Lab target in September, 1972. The proton beam transport to the Meson Lab was subsequently upgraded to 300 GeV, in the winter of 1973. A 300 GeV beam was regularly delivered from spring 1973 onwards to the Meson target for experiments. The proton transport was upgraded (again!) to 400 GeV in the summer of 1975. From that time a 400 GeV proton beam has been routinely delivered to the Meson Area.

There are six secondary beams (denoted M1, M2, M3, M4, M5 and M6) in the Meson Area. The layout of these beams, as originally designed, was described in our Meson Laboratory Preliminary Design Report, [1] in 1971. Like the primary proton transport to the Meson Area, the secondary beams have also been steadily upgraded over the years. An up-to-date summary of the principal parameters of the beams is given in Table I.

A large number of experiments has been undertaken in the Meson Lab during its first five years. Approximately forty electronics experiments will have been run by the end of 1977. The principal object of this paper is to summarize the results of those experiments for which results have appeared in print. We shall summarize the goals of the completed experiments for which no results have yet been submitted for publication and also the goals of those experiments for which data-taking has not yet been completed.

II. Physics Results Published to Date

A. Low Momentum Transfer Hadron Physics

Introduction

The careful and precise total cross section measurements of Experiment #104--shortly to be extended to higher momenta $\sim$ 400 GeV/c--have confirmed and extended the evidence of rising total cross sections previously observed at Serpukhov and the CERN-ISR. The experiment has also shown the cross sections of π^+d and π^-d at high energies to be equal, at the 1% level of precision, as required by charge-symmetry. Differences between particle and antiparticle cross sections in the same target have been fitted by expressions of the form $A.s^{\alpha-1}$. The values found for α are consistent with the predictions of current Regge-pole models. Relations between cross sections which are related by SU(3) symmetry are found to agree with current theoretical models. No clearcut explanation yet exists for what pieces of the total cross section are responsible for the slow rise at high energies.

A very comprehensive and precise set of measurements of $\pi^{\pm}p$, $K^{\pm}p$, and $p^{\pm}p$ elastic scattering has been made by the Single Arm Spectrometer Group (Experiment #96), over the -t range from 0.03 to 0.8 GeV^2, for energies up to 175 GeV/c. The crossover points where particle-proton and antiparticle-proton differential cross sections are equal, are found to be approximately energy independent for both K^+/K^- and p^+/p^-. In impact parameter space, the data indicate that the interaction radii for C = +1 and C = -1 exchange amplitudes are equal, to within $\pm$ 10%, for both Kp and pp scattering. An impact parameter representation analysis of the

Experiment #96 data has revealed a number of interesting results, among them that the baryon-baryon interaction has a very large opacity at high energies (opacity $\sim$ 94%), that the meson-baryon interaction radius is about 6% smaller than the baryon-baryon interaction radius, and also that the increase in the pp total cross section as a function of energy is peripheral, while in the K^+p case it could also be central.

At larger momentum transfers, Experiment #7 has observed the diffractive dip previously established at CERN-ISR energies for a proton energy of 200 GeV. At 100 GeV, this dip is not seen.

The polarization parameters in π^+p and π^-p elastic scattering have been measured in Experiment #61 at an incident momentum of 100 GeV/c. The results analyzed to date cover the range $0.18 \lesssim -t \leq 1.4$ GeV^2 and are in good agreement with Regge-exchange absorption models.

The excellent charge-exchange studies made by Experiment #111 have yielded several results of interest. First and foremost, their measurements of $\pi^-p \to \pi^0n$ charge-exchange, over the energy range 20-200 GeV and over the -t range 0-1.5 GeV^2, have established that a single-Regge pole (the ρ-pole) analysis fits their data extremely well. The ρ trajectory $\alpha(t)$ obtained from the overall fit to the data is a linear function of -t at small -t (between 0 and 0.3 GeV^2); this line falls very close indeed to a straight line drawn through the points corresponding to the ρ and g mesons.

The $\pi^-p \to \eta n$ measurements, like $\pi\ p \to \pi^0n$, can be fitted very well by a single-Regge-pole (A_2-pole) analysis from which the experimenters determine a trajectory $\alpha(t)$. According

to the idea of exchange degeneracy, the ρ and A_2 trajectories should be equal; but the results of Experiment #111 demonstrate conclusively that they are not the same.

Experiment #111 also measured the reaction $\pi^- p \to \omega n$, $\omega \to \pi^0 \gamma$, $\pi^0 \to \gamma\gamma$. The measurements of the ω production spin density matrix show that in the 20-150 GeV energy range almost the entire cross section $\pi^- p \to \omega n$ comes from natural parity exchange (ρ exchange). The change, from low ($\sim$ 10 GeV) to high ($\sim$ 100 GeV) energies, of the rate of fall of σ_{tot} ($\pi^- p \to \omega n$) with increasing energy, is also consistent with natural-parity exchange dominance at high energies.

The $\pi^- p \to \omega^0 n$ differential cross sections can be fit very well by a simple single-Regge-pole analysis. The resulting Regge trajectory $\alpha(t)$ lies almost on top of the ρ trajectory obtained from the $\pi^- p \to \pi^0 n$ data. This provides further evidence that natural-parity (ρ) exchange dominates the reaction $\pi^- p \to \omega n$.

The charge-exchange reaction $np \to pn$ was studied by Experiment #12. Like the data at lower energies, the n-p charge exchange cross section, from 50 to 300 GeV/c, is characterized by a sharp peak at $u = 0$, with a width $\sim (m_\pi)^2$. A single-Regge-pole analysis of the np charge exchange data yields an inconclusive result; the value of $\alpha(u \sim 0)$ appears to vary with neutron energy. The dilemma is: π exchange would have $\alpha(0) \approx 0$, while ρ-A_2 exchange would have $\alpha(0) \approx 0.5$; how can one then reconcile the large value of $\alpha(0) = 0.5$ measured by Experiment #12 with the persisting very sharp ("pion exchange") forward peak?

An extensive program of $K_L^0 \to K_S^0$ regeneration experiments

has been undertaken by Experiment #82/425. So far, only their measurements of regeneration of K_S by carbon have been published; the modulus and phase of the regeneration amplitude have been measured over the energy range 30-130 GeV. The results are clearly consistent with the constant regeneration phase predicted for the ω-exchange Regge-amplitude which should be dominant for coherent regeneration by I = 0 nuclei. The result obtained for $\alpha_\omega(0)$ from the average regeneration phase can be compared with two other determinations of $\alpha_\omega(0)$, from an extrapolation to $M^2 = 0$ of the line connecting the ω-meson and its 3^- Regge recurrence, and from the momentum dependence of the $K^\pm d$ total cross section difference; the agreement between the three values of $\alpha_\omega(0)$ is excellent.

A major result is the discovery, by the Experiment #8 group, that there is a substantial polarization in the inclusive production of Λ^0's at 300 GeV, and "large" $p_T \sim 1$-2 GeV/c. This was the first result to be published from a series of experiments--which is continuing--which utilize the neutral hyperon facility which has been built at the end of the M2 beam line.

The observed Λ^0 polarization P_Λ, for Λ^0's produced in the reaction $p + A \rightarrow \Lambda^0 + X$, at 300 GeV, was found to have the following characteristics:

i) P_Λ is consistent with parity conservation in the Λ^0 production reaction;

ii) P_Λ increases monotonically with increasing p_T, independently of x;

iii) $P_\Lambda = 0.28 \pm 0.08$ at $p_T = 1.5$ GeV/c.

The above facts are consistent with the hypothesis that the polarization arises in the inclusive channel through the strong interaction.

The Experiment #8 group have also found that the inclusive production of $V^0 = \Lambda^0$, $\bar{\Lambda}^0$, and K^0_S are all consistent with single-term triple-Regge behavior for large values of Feynman x (near to 1). The fits to their data, from which they obtained $\alpha(t)$ trajectories, were consistent for Λ^0 production with K^* and K^{**} exchange. Interference between K^* and K^{**} exchanges is consistent with the polarization data discussed above.

The diffraction dissociation studies of Experiment #27/305 concentrated on the reaction

$$n + p \rightarrow (p\pi^-) + p$$

The $(p\pi^-)$ mass spectra have structures near 1.5 and 1.68 GeV. At large (t), the t spectra appear to be consistent with an exp(4.5t) dependence, for all $(p\pi^-)$ masses. Below $(-t) = 0.4\ \mathrm{GeV}^2$, the dependence of the slope parameter on mass is similar to that observed at lower energies. For low masses (< 1.5 GeV) the data are essentially energy independent--inconsistent with earlier experimental data which favored an $s^{-0.4}$ energy dependence. The decay angular distributions for the $(p\pi^-)$ system are found to agree rather well with a one-particle-exchange Deck mechanism calculation. It is found also that the t-spectra are reasonably consistent with the model calculations both in the region of low-mass $p\pi^-$ and for higher $p\pi^-$ masses in the region where pion-exchange dominates, namely $\cos\theta > 0.9$; in other angular regions, $-1 < \cos\theta < 0.9$, the model fails to reproduce the observed spectra.

There is a highly peripheral interference minimum in the t distribution, which moves out to larger values of -t as M increases, and eventually disappears, and which shows very little energy dependence between 50 GeV and 1,100 GeV; these features suggest strongly that the mechanism for this phenomenon must be basic to diffractive dissociation.

The studies by Experiment #178 of multiplicities and multiplicity distributions in hadron-nucleus collisions at Fermilab energies, using a very simple experimental set-up, have produced a number of interesting results. From a comparison of the multiplicity distributions produced by pions and by protons incident on various nuclei, it is found that in the forward region of rapidity, the distributions are the same when described in terms of the quantity $\bar{\nu}$, the average number of absorption mean free paths encountered by the incident particle in traversing the nucleus, thereby suggesting that the relevant parameter which describes the multiplication process is the absorption cross section of the incident particle, and not that of the secondaries.

A most striking result is that there is no increase, with increasing $\bar{\nu}$, in the number of particles produced in the forward region of rapidity, while at large angles the multiplicity is approximately proportional to thickness.

The data for Experiment #178 strongly support a description of multiparticle production of the energy-flux type, à la Gottfried.

Total Cross Sections of Hadrons on Hadrons

A.1 Experiment #104 - Measurements of Total Cross Sections on Hydrogen and Deuterium; by a Rockefeller, BNL, Fermilab, Washington, Munich, Padua collaboration

The principal objective of the experiment was to measure the energy dependence of a given cross section over the range of energies available with a relative accuracy of about 0.1%. The experiment was designed to achieve an absolute accuracy of about 0.4% which required the absolute density of liquid hydrogen and of liquid deuterium to be known to better than 0.1%.

In addition to precise measurements of the energy dependence of the cross sections, achievement of the accuracy discussed above would make possible comparisons of cross sections which are related by SU(3) symmetry, and stringent tests of various high energy limiting theorems for the total cross sections. Measurements at Serpukhov,[2] which indicated that the K^+p and π^+p total cross sections increase with energy at high energies, and the more recent results from the CERN-ISR [3] which showed that the pp total cross section increases with energy at very high energies, served to emphasize the importance of accurate total cross section measurements at Fermilab energies for all of the available strongly interacting particles.

The apparatus consisted of three Cerenkov counters (two differential and one threshold), three targets (one hydrogen, one deuterium, and one dummy), and a proportional wire chamber telescope, all in the incident beam, also a set of transmission counters (scintillation counters) and proportional wire chambers downstream

of the target. The experiment was performed in the M1 beam.

The results of Experiment #104[4] for p and $\bar{p}$ cross sections are shown in Figs. 1 and 2, together with data from previously published results of other experiments. Agreement with most of the other experiments in the momentum range of Experiment #104 is quite satisfactory. In particular, the increase of the pp cross section from 50 to 200 GeV/c -- about 2% -- is consistent with data on the rising pp total cross section obtained at the CERN-ISR.[3]

The particle-antiparticle differences $\sigma_{\bar{p}p}-\sigma_{pp}$, $\sigma_{\bar{p}d}-\sigma_{pd}$, and $\sigma_{\bar{p}n}-\sigma_{pn}$, which are dominated by ω exchange, are shown in Fig. 3. They can all be fitted by expressions of the form $A\cdot s^{\alpha-1}$. The data from Experiment #104 yield the following results:

$$\alpha = 0.39 \pm 0.04 \text{ for } \bar{p}p\text{-}pp$$

$$0.43 \pm 0.05 \text{ for } \bar{p}d\text{-}pd\ .$$

For scattering on neutrons, the authors of Experiment #104 use the Glauber-Wilkin formula[5] to take into account the shadowing in the deuteron. They find that the behavior of $\sigma_{\bar{p}n} - \sigma_{pn}$ is consistent with being the same as the behavior of $\sigma_{\bar{p}p} - \sigma_{pp}$.

The relative accuracy achieved in Experiment #104 was $\pm$ 0.15% for those cross sections where the statistical error was smaller than this. The absolute accuracies achieved were $\pm$ 0.5% for protons, $\pm$ 0.6% for deuterons, and $\pm$ 1.5% for neutrons.

The results of Experiment #104,[4] for $\pi^{\pm}$ and $K^{\pm}$ total cross sections on protons and deuterons, are shown in Figs. 1 and 2. The cross sections for $\pi^{\pm}$ and $K^{\pm}$ all show a slight rise with increasing momentum in the momentum range of Experiment #104 (50 to 200 GeV/c). The cross sections for $\pi^{\pm}d$ shown in Fig. 1 are equal

within the experimental errors as required by charge symmetry :

$$\frac{\sigma(\pi^- d)_{Exp}}{\sigma(\pi^+ d)_{Exp}} = 1.0014 \pm 0.0009 \ .$$

Antiparticle-particle cross section differences are shown in Fig. 3 . In all cases, the differences can be fitted by the form $As^{\alpha-1}$; the Experiment #104 data yield the following results:

$$\alpha = 0.60 \pm 0.10 \text{ for } \pi^- p - \pi^+ p$$
$$\alpha = 0.45 \pm 0.07 \text{ for } K^- p - K^+ p$$
$$\alpha = 0.39 \pm 0.08 \text{ for } K^- d - K^+ d \ .$$

A number of predictions of relations between total cross sections are made by quark and Regge-pole models [6]; these predictions, which had previously been found to be in agreement with data obtained at Serpukhov on total cross sections up to 50 GeV, are also consistent with the Experiment #104 data.

A.2 Experiment #4 - Neutron Total Cross Sections up to 300 GeV; by a Michigan, LBL collaboration

The principal objective of the experiment was to survey the energy dependence, from 40 to 300 GeV, of the total cross section of neutrons on protons and on heavier nuclei, to an accuracy of about 2%.

The experiment used a small-angle neutron beam (the M3 beam), and a standard good geometry transmission technique. The neutron detector was a total absorption spectrometer.

The n-p total cross sections measured by Experiment #4 [7] have a quoted accuracy of about 1% over the energy range 40-280 GeV/c.

The data from Experiment #4 (see Fig. 4) connect smoothly to lower energy n-p total cross section data, and they indicate a smooth rise of about 1.5mb in $\sigma_T(np)$ between 50 and 280 GeV/c. The pp and np total cross sections appear to be approximately equal over the entire range 30-300 GeV/c.

The Experiment #4 group also measured the total cross sections of neutrons on a wide variety of nuclei from deuterium to uranium, over the momentum range 30 to 270 GeV/c. The results of Experiment #4 on neutron-nucleus total cross sections,[8] together with the data of Experiment #27/305,[9] are presented in Fig. 5. In comparing the measured cross sections with the predictions of Glauber theory, it was found that a correction for inelastic screening is required. The cross sections were found to vary as $A^{0.77}$ over the entire energy range.

A.3 Experiment #27/305 - Neutron-Nuclear Total Cross Sections; by a Fermilab, Northwestern, Rochester, Massachusetts collaboration.

This experiment, carried out in the M3 beam line, was performed with the use of the standard good geometry transmission technique. However, a novel feature of the experiment was the method employed for neutron detection. A 0.25 in.-thick lead "neutron-converter" was placed in front of a high resolution forward-Vee spectrometer. The spectrometer was triggered on the coherent dissociation of a neutron into a $p\pi^-$ system (Vee) produced in the reaction $n + Pb \rightarrow (p\pi^-) + Pb$; this technique provided excellent position and energy measuring capability for neutrons transmitted through a target.

As mentioned earlier, the results of Experiment #27/305 [9] on neutron-nucleus total cross sections, together with the data of Experiment #4, [8] are presented in Fig. 5. The results of the two experiments are in good agreement at all energies for the heavier nuclei (Pb, Cu); for lighter nuclei (Al, C), there is some discrepancy between the two experiments.

Elastic Scattering of Hadrons by Hadrons

A.4 Experiment #96 - Elastic Scattering of Hadrons on Hydrogen and Deuterium; by an ANL, Bari, Brown, CERN, Cornell, MIT, Fermilab, Northeastern, Stanford collaboration.

The principal objective of Experiment #96 was to measure pp, $\bar{p}p$, $\pi^{\pm}p$ and $K^{\pm}p$ elastic scattering in the region $0 \leq -t \leq 1.5$ $(GeV/c)^2$, over the momentum interval $50 < p < 200$ GeV/c. The measurements would be repeated with a deuterium target, in order to study hardon-neutron elastic scattering. From these data one would obtain Regge coefficients, crossovers, and the overall behavior of the cross sections to a few per cent.

The Experiment #96 group has constructed a focusing magnetic spectrometer at the end of the M6E beam line. Changes in scattering angle are effected by magnetic steering of the incoming beam, while the spectrometer arm is kept fixed. Particle identification is achieved by the use of differential and threshold counters in both the beam and the spectrometer. Proportional wire planes placed at suitable locations enable the experimenters to determine outgoing particle variables such as momentum and production angle.

The hadron-proton elastic scattering data[10] are shown in Fig. 6. Over the range $0.03 \leq -t \leq 0.8$ $(GeV/c)^2$, the data can be parameterized in the form $\frac{d\sigma}{dt} = A \exp(Bt + Ct^2)$. The measurements are in good agreement with data obtained at Serpukhov[11] and with the optical points (at t = 0) derived from the total cross section measurements of Experiment #104.[4]

The "crossover" points where particle-proton and antiparticle proton cross sections are equal, are found to be energy independent; the results for both K^+/K^- and p^+/p^-, namely $-t$ = 0.17 and 0.12 GeV^2, respectively, are similar to the values previously measured in the 3-16 GeV/c range.

An analysis of the elastic scattering data in terms of Regge poles has shown that the cross sections for all the reactions are clearly dominated by the Pomeron pole as expected. The similar shrinkage patterns seen for the K^+p and pp diffraction peaks certainly encourages the belief that the Pomeron is the principal contributor to these channels, but the energy independence of $\pi^{\pm}p$ K^-p, together with the slow anti-shrinkage of $\bar{p}p$, indicates that the lower neutral meson trajectories are still important, also as expected.

The predictions of the Geometric Scaling Hypothesis -- similar energy dependences for the total cross section, total elastic cross section, and forward elastic logarithmic slope parameter $\frac{d}{dt}(\ln \frac{d\sigma}{dt})$ -- are satisfied by $\pi^{\pm}p$ and $K^{\pm}p$ across the whole energy range but by pp only above 100 GeV/c.

The Experiment #96 group have also analyzed their data in terms of the impact parameter representation of elastic scattering. They draw the following conclusions from this analysis:

a) Meson-baryon interactions are $\sim$ 20% more transparent

than baryon-baryon interactions, which approach on opacity of 94% for $s > 200\ GeV^2$.

b) Meson-baryon processes have an interaction radius $\sim$ 6% smaller than baryon-baryon processes.

c) The decrease with energy of the $\bar{p}p$ elastic cross section at large b values ($b \sim 1$ Fermi) is correlated with the decrease of $C = -1$ (non-flip ω) Regge exchanges, while the decrease at small b values is common to both pp and $\bar{p}p$ elastic cross sections and is produced by a different mechanism.

d) The increase in the pp total cross section as a function of energy is peripheral while in the K^+p case this increase could also be central.

e) The Fourier transform of the π hadronic density is found to be in excellent agreement with the π form factor measurements.

A.5 Experiment #7 - $\pi^{\pm}p$ and p-p Differential Elastic Scattering Cross Sections from 20 to 200 GeV; by a Michigan, ANL, Fermilab, Indiana collaboration.

The objective of this experiment was an exploratory survey of hadron-proton elastic scattering at Fermilab energies, in the momentum transfer range $0.1 < -t < 2\ GeV^2$.

The apparatus for the experiment consisted of three Cerenkov counters in the incident beam, a liquid hydrogen target, wire spark chambers, and two Cerenkov counters in the forward arm spectrometer.

Figure 7 shows the data of Experiment #7.[12] At 50 and 100 GeV/c, a fit of the form exp $(bt + ct^2)$ can describe all the measured differential cross sections. However, at 200 GeV/c there is a sharp break in the πp and pp cross sections near $-t = 0.4$ GeV^2; the two-term exponential fit no longer applies. A comparison of the energy dependence of the $\pi^- p$ and pp cross sections is given in Fig. 7b. For both reactions the slope $\frac{-1}{\sigma} \cdot \frac{d\sigma}{dt}$ increases with increasing momentum below $-t = 0.4$ GeV^2. However, at momentum transfers greater than $-t = 0.4$ GeV^2 the slopes of the differential cross sections change very rapidly and they are energy-independent within the accuracy of the data above $-t = 0.8$ GeV^2. At large $-t (\gtrsim 1.0$ GeV$^2)$ the $\pi^+ p$ and $\pi^- p$ elastic cross sections are equal, and independent of energy.

The pp elastic scattering measurements at 200 GeV/c show a diffractive dip (see Fig. 7c) at $-t = 1.5$ GeV^2 while no such dip is seen in the data at 100 GeV/c . This diffractive dip is well established at all CERN-ISR energies.[13]

A.6 Experiment #61 - Polarization in pp, $\pi^- p$ and $\pi^+ p$ Elastic Scattering at 100 and 300 GeV/c; by an ANL, Harvard, LBL,Fermilab,Yale collaboration.

The apparatus for Experiment #61 consists of a polarized proton target and a two-arm spectrometer for the scattered and recoil particles. Both arms of the spectrometer utilize proportional chambers; the forward arm uses Cerenkov counters for particle identification, the recoil arm identifies the detected particle as a proton by time of flight. The anticipated precision of the polarization measurements was $0.005 \leq \Delta P \leq 0.010$, over the t range

$0.15 \leq -t \leq 1.6$ GeV^2.

The Experiment #61 group have published the results of their measurements of the π^+p and π^-p polarization parameters at 100 GeV/c.[14] The data are shown in Fig. 8.

At small $|t|$, $\lesssim 0.6$ GeV^2, measured polarizations are small but non-zero, consistent with an $s^{-1/2}$ energy dependence. This $s^{-1/2}$ dependence is predicted by a model in which Pomeron and ρ exchange contributions to $P(t)$ are dominant.[15] The $s^{-1/2}$ dependence is further illustrated by the dashed curves in Fig. 8 which represent the π^+p and π^-p results of Borghini, et al.,[16] scaled from 10 to 100 GeV/c by $s^{[\alpha_\rho(t)-\alpha_P(t)]}$, where $\alpha_\rho(t)$ and $\alpha_P(t)$ are the effective trajectories for the ρ and Pomeron exchange contributions respectively.

The data also show that P_{π^+p} and P_{π^-p} are mirror symmetric, $P_{\pi^+p} = -P_{\pi^-p}$. At larger values of $|t|$ both the π^+p and π^-p polarizations remain small, in agreement with Regge-exchange absorption models.[17]

Charge Exchange and K^0 Regeneration Experiments

A.7 Experiment #111 - Study of $\pi^-p \to \pi^0n$ and $\pi^-p \to \eta n$ at High Energy; by a Caltech, LBL collaboration

The principal objective of Experiment #111 was to explore the asymptotic behavior of π^-p charge exchange scattering up to the highest energies available at Fermilab. By using isotopic spin conservation and the optical theorem, an upper limit on the difference between the π^-p and π^+p total cross sections would also be established.

The $\pi^- p$ charge exchange cross section measurements were also expected to provide an excellent test of Regge theory since only the ρ meson is exchanged. Finally, when the results of Experiment #111 and Experiment #104 on $\pi^- p$ and $\pi^+ p$ total cross sections were combined, they would make it possible to separate the charge-exchange scattering amplitude in the forward direction into its real and imaginary parts, thus enabling the consistency of the results of the experiment with the predictions of dispersion relations to be checked.

The Experiment #111 plan was to obtain data at six momenta over the range 20-250 GeV/c.

Experiment #111 utilized an elegant new detector [18] composed of 140 narrow finger counters which locate a photon shower position to about 1 mm and which integrate the total energy of the shower. This information made it possible to determine unambiguously the direction of a particle which decays into γ-rays and to determine the mass of the particle. The decays $\pi^0 \to 2\gamma$, $\eta^0 \to 2\gamma$, $\eta^0 \to 3\pi^0$, $\omega^0 \to \pi^0\gamma$, have all been clearly identified by the detector. The experiment was carried out in the M2 beam line.

i) <u>$\pi^- p \to \pi^0 n$ Measurements</u> [19]

Results for the reaction $\pi^- p \to \pi^0 n$ are presented in Fig. 9. According to Regge theory, if the $\pi^- p \to \pi^0 n$ amplitude is dominated by the ρ pole, it is expected to have a simple power-law energy dependence at fixed t, giving a differential cross section of the form:

$$\frac{d\sigma}{dt}(s,t) = \beta(t)\nu^{2\alpha(t)-2}$$

where $\nu \cong (s-u)/4M$ is the approximate π^- laboratory energy, M the proton mass, and s, t and u the usual energy and momentum transfer

variables. It was found from previous data at lower energies[20] that the ρ trajectory, $\alpha(t)$, is approximately linear in t, and that the extrapolation of $\alpha(t)$ as measured in the charge-exchange scattering experiments passes very nearly through the points which correspond to the observed spins and masses of the ρ and g mesons, namely $\alpha(m_\rho^2) = 1$ and $\alpha(m_g^2) = 3$.

Some deviation from the above simple power-law behavior of the cross section might be expected because of possible Regge cuts and because the observation of asymmetry in charge exchange scattering from polarized targets indicates that the scattering amplitudes must have other components besides the dominant ρ-pole at least in the energy region below 10 GeV.[21] Nevertheless, an excellent phenomenological description of the entire set of data obtained by Experiment #111 over the momentum range 20-200 GeV/c is provided by the simple expression $\frac{d\sigma}{dt} = \beta(t)\nu^{2\alpha(t)-2}$, where

$$\alpha(t) = \alpha_0 + \alpha_1 t + \alpha_2 t^2 , \qquad -1 \leq t \leq 0 \text{ GeV}^2$$

and

$$\beta(t) = \beta_1 \exp(b_1 t) + t(t-t_0)^2(\beta_2+\beta_3 t+\beta_4 t^2)\exp(b_2 t).$$

A fit to the Experiment #111 data has been found for the parameters α_0, α_1, ... b_2. The fit gives $\chi^2 = 107$ for 128 degrees of freedom. Differential cross section curves computed with this fit are shown in Fig. 9 .

The trajectory $\alpha(t)$ obtained from the overall fit to the data is shown by the solid curve in Fig. 10 , together with individual data points, $\alpha^*(t)$, obtained by fitting to the data at each value of t separately using the form $\beta(t)\nu^{2\alpha^*(t)-2}$. One

can see from Fig. 10 that the observed values of $\alpha^*(t)$ in the t range from -0.3 to 0.0 GeV^2 fall very close to a straight line drawn through the points corresponding to the ρ and g mesons.

Let us compare the charge exchange cross section data of Experiment #111 at t = 0 with the difference in π^-p and π^+p total cross sections, $\Delta\sigma = \sigma_{tot}(\pi^-p)-\sigma_{tot}(\pi^+p)$, as measured by Experiment #104. The relation between these quantities is $(\frac{d\sigma}{dt})_{t=0} = (\pi/P^2_{lab})(1+R^2)[\mathrm{Im}A(0)]^2$, where R is the ratio of real to imaginary parts of the forward charge exchange amplitude A(0), and P_{lab} is the incident laboratory momentum. In addition, if we assume that the observed power-law dependence of $(\frac{d\sigma}{dt})_{t=0}$ extends to higher energies, dispersion relations give a relation between R and $\alpha(0)$; namely, $R = \tan\frac{1}{2}\pi\alpha(0)$. Thus, one can predict the difference $\Delta\sigma$ from the charge exchange data. The predictions agree very well with the results of Experiment #104[4] obtained at Fermilab in the energy range 23 to 240 GeV .

ii) <u>$\pi^-p \to \eta n$ Measurements[18]</u>

Experiment #111 also recorded some 21000 events for the reaction $\pi^-p \to \eta n$ $(\eta \to 2\gamma)$. Data are shown in Fig. 11, for π^- energies of 20, 65 and 200 GeV; data of comparable quality were also recorded at 40, 100 and 150 GeV.

According to Regge theory, the A_2 Regge pole is expected to dominate the η reaction so that an analysis of these data should give information about the A_2 trajectory. Indeed, just as in the case of pion charge exchange, the data on $\pi^-p \to \eta n$ can be described extremely well by the simplest Regge-pole model with a power-law energy dependence and a nearly linear trajectory, $\alpha(t)$.

The trajectory $\alpha(t)$ obtained from the fit to the data is shown by the solid curve in Fig. 12, along with individual "data-points", $\alpha^*(t)$, obtained by fitting to the data at each value of t separately using the form $\beta(t)\nu^{2\alpha(t)-2}$. According to the idea of exchange degeneracy, the A_2 and ρ trajectories should be the same; however, the results of Experiment #111 demonstrate convincingly that they are not the same -- in agreement with the conclusion already reached from previous experiments at lower energies.[22]

iii) <u>$\pi^- p \to \omega n$ Measurements</u>[23]

Experiment #111 also recorded some 2100 events for the reaction $\pi^- p \to \omega n(\omega \to \pi^0\gamma)$. In this experiment, only a portion of the phase space for ω decay was observed. Thus, the determination of the production spin density matrix was crucial for extrapolating into the unobserved regions. The measured values of spin density matrix elements indicate that in the 20-150 GeV energy range almost the entire cross section $\pi^- p \to \omega n$ comes from natural parity exchange.

The change in the variation with energy of the total cross section as a function of energy, from lower energies[24] to the energy region measured by Experiment #111, is consistent with Regge theory. The unnatural-parity exchange part of the total cross section, sizable below 10 GeV/c, is mediated by the B-trajectory exchange, and is expected to decrease faster with energy than the natural-parity part, which is mediated by ρ-trajectory exchange.

The differential cross sections for ω production, shown in Fig. 13, exhibit a dip in the forward direction which is

characteristic of ρ-exchange interactions, and a structureless exponential fall beyond $t = -0.15$ GeV^2. Regge-model predictions based on earlier 6 GeV/c data[25] are also shown in Fig. 13. The qualitative agreement between the predictions based on the low energy fit and the high-energy data is quite striking.

The energy dependence of the $\pi^- p \to \omega n$ differential cross sections has been fitted to the simple Regge-form:

$$\frac{d\sigma}{dt} = A(t) p_{beam}^{2\alpha(t)-2}$$

The values of $\alpha(t)$ thus obtained are shown in Fig. 14; they lie almost on top of the ρ trajectory, obtained from the pion charge exchange measurements discussed earlier -- except in the forward direction where the ρ residue function goes to zero. The agreement between the measured values of $\alpha(t)$ with the ρ trajectory is further evidence that the natural-parity exchange dominates the high-energy ω production cross section.

A.8 Experiment #82/425 - Regeneration of Neutral K Mesons at Very High Energies; by a Chicago, SLAC, UCSD, ETH/Zurich, Wisconsin collaboration.

The original motivation for Experiment #82/425 arose in the following way. The regeneration amplitude for K_S mesons is proportional to $f(0) - \bar{f}(0)$ where f, $\bar{f}$ are the forward scattering amplitudes on the target used for regeneration. The Pomeranchuk Theorem says that $\mathrm{Im}\, f \to \mathrm{Im}\, \bar{f}$ as the laboratory energy tends to infinity; thus K_S regeneration should vanish asymptotically if that theorem holds and regardless of the

target material used. The regeneration phenomenon depends on the magnitude and the phase of $f - \bar{f}$, and thus supplies more information than the comparison of the total cross sections which depend only on the imaginary parts of f and $\bar{f}$.

The plan of operation of the experiment was as follows:

a) "Vacuum regeneration" run: as a test of the operation of their spectrometer, the Experiment #82/425 Group planned a preliminary run with no regenerator. The CP-violating $K_L \to \pi^+\pi^-$ mode would be used to check the apparatus acceptance for 2π decays; the $K_{\ell 3}$ modes which would be used as monitors in later stages of the experiment, would also be calibrated in this low-background run. The results from this run indicate a good understanding of the apparatus acceptance.

b) $|\rho|^2$ Measurement in Carbon: They planned to use a fairly thick regenerator (1.3m, or 2 collision lengths) and a short decay region ,26m or 4.8Λ at 100 GeV/c) to measure the intensity of regenerated $K_S \to \pi^+\pi^-$ decays relative to semi-leptonic K-decays at an early proper time downstream of the regenerator. Some phase (Φ_r) information was obtainable from this run.

c) $|\rho|, \Phi_r$ Measurements in Carbon: In order to obtain complete information on regeneration in carbon, they would next proceed to a more complete determination of the momentum dependence of $(f-\bar{f})/k$ and of the phase Φ_r by observing the interference between $K_S \to \pi^+\pi^-$ and $K_L \to \pi^+\pi^-$ behind the regenerator. This would involve the use of a 66 cm carbon regenerator, and 48m decay region.

d) Regeneration in Methane: They would next replace the carbon regenerator with one of CH_4. From these data and the earlier carbon data, they would extract the first measurement of regeneration from protons. (CH_2 was used, not CH_4, when the data were taken.)

e) Regeneration in liquid hydrogen: the experience gained in the previous steps plus the value of $\rho_{hydrogen}$ deduced from the earlier results with carbon and hydrocarbon regenerators, would serve to specify an optimal experimental arrangement for this part of the experiment.

The apparatus for the experiment, which was located in the M4 beam line, consisted principally of wire spark chambers and a spectrometer magnet; the spectrometer was essentially a longitudinally stretched version of the one used previously at ANL by Telegdi and collaborators.[26]

Cabibbo[27] had suggested several years ago that coherent regeneration of K_S's by I = 0 nuclei could be interpreted in terms of a single Regge trajectory, the ω. Experiment #82/425 has been carried out in an energy range (P_{K^0} = 30-130 GeV) where the Regge formulation should work well.

The analytical form of the ω exchange Regge amplitude implies two facts for f(0), $\bar{f}(0)$:

$$|f(0) - \bar{f}(0)|/k = C(0)P_K^{\alpha_\omega(0)-1} \sim P_K^{-n} \qquad (1)$$

-- power law dependence of the modulus of the regeneration amplitude on momentum; and

$$\arg[f(0)-\bar{f}(0)] = -\pi/2[\alpha_\omega(0)+1] = -\pi/2(2-n) \qquad (2)$$

a constant regeneration phase, determined by the Regge exponent n.

The modulus and phase of the regeneration amplitude in Carbon were measured by Experiment #82/425 over the energy range 30-130 GeV.

Figure 15a shows $|f-\bar{f}|/k$ vs. P_K, extracted from measurements of ρ in carbon.[28] Figure 15b shows $\arg(f-\bar{f})$ vs. P_K. Both the Experiment #82/425 data alone and also all data taken together[29] are well fit by a power law P_K^{-n}, yielding the results listed in Table II.

The results are clearly consistent with the predicted constant phase, and strongly support the hypothesis of ω-exchange dominance. From the Experiment #82/425 data alone, a fit for the parameter $\alpha_\omega(0)$ gives $\alpha_\omega(0) = 0.390 \pm 0.014$. This result from Experiment #82/425 may be compared with other measurements of the intercept of the ω-trajectory:

i) An extrapolation to $M^2 = 0$ of the line connecting the ω-meson and its 3^- recurrence gives

$$\alpha_\omega(0) = 0.43 \pm 0.02$$

ii) The momentum dependence of the $K^\pm d$ total cross section differences[4] -- also dominated by ω-exchange -- gives $\alpha_\omega(0) = 0.41 \pm 0.03$.

The overall agreement between the results is impressive and most convincing.

A.9 Experiment #12 - A Study of Neutron-Proton Charge-Exchange Scattering in the Momentum Range 50-300 GeV/c; by an Ohio State, Michigan State, Carleton collaboration

The neutron-proton charge exchange differential cross section has been measured in the momentum interval 50 to 300 GeV/c, with squared four-momentum transfers 0.002 to 0.8 $(\mathrm{GeV/c})^2$.

The experiment was performed in a continuous spectrum of 5×10^6 neutrons/pulse in the M3 beam line. Charge exchange reactions occurring in a liquid hydrogen target were observed using a magnetic spectrometer for the forward proton and banks of thick plastic scintillators with time of flight electronics for the recoil neutron.

The final sample of about 25,000 events[30] is shown in Fig. 16. The data are characterized by a sharp peak of width $\sim m_\pi^2$ at small momentum transfers, followed by a gentler falloff at larger momentum transfers.

Fits of the form

$$\frac{d\sigma}{dt} = A \frac{m_\pi^4}{(|t|+m_\pi^2)^2} + B$$

may be used to characterize the size of the forward peak, and though discrepancies arise between different experiments, the ratio A/B shrinks from ~ 2 at low energies[31] to ~ 1 at the energies of this experiment.

The energy dependence of the data may be examined by fitting the data to the Regge form

$$\frac{d\sigma}{dt} = \eta(t)\, s^{2\alpha(t)-2} \quad .$$

For $|t|$ less than 0.25 GeV^2, the value of α is approximately 0.5 for incident momenta 50 to 300 GeV/c. Comparisons with the value $\alpha < 0.1$ for momenta less than 27 GeV/c, and $\alpha = 0.25$ for momenta 23-62 GeV/c indicate the high energy data vary less rapidly with incident energy.

The pion exchange contribution to n-p charge exchange is expected to have a variation with energy corresponding to $\alpha(\rho) \cong 0$, while ρ-A_2 exchange should vary with energy corresponding to $\alpha(0) \cong 0.5$. It is not clear how one can reconcile the large value of $\alpha(0) = 0.5$ measured in this experiment, a value which is compatible with ρ-A_2 exchange, with the persistence of the very sharp ("pion exchange") forward peak at high energies.

The u = 0 differential cross sections may be used to place bounds on the difference between the np and pp total interaction cross sections. The limits obtained in Experiment #12 are comparable in accuracy to those found from subtraction of the measured np and pp total cross sections.[4,7]

Inclusive Particle Production

A.10 Experiment #8 - Λ^0 Polarization in Inclusive Production; by a Wisconsin, Rutgers, Michigan collaboration

The principal objectives of Experiment #8 were as follows:

1. Neutral hyperon beam survey to measure the production of Λ^0, $\bar{\Lambda}^0$, Ξ^0, K_1^0, and K_2^0 at 0, 5 and 10 mrad, by 300 GeV protons on various solid targets.

2. Search for hyperon and anti-hyperon polarization.

3. Measurement of ΛN total and diffraction elastic scatterin cross sections between 100 and 250 GeV/c.

A schematic representation of the neutral hyperon beam [32] is shown in Fig. 17 . The incident protons in the M2 diffracted proton beam are deflected vertically by a magnet placed 150m upstream of the Λ^0 production target, and then restored to the targets with magnets (M1) placed just upstream, to obtain production angles between 0 and 9.5 mrad in a vertical plane. The neutral beam is defined by a fixed collimator with its axis in the horizontal plane. A vertical magnetic field of 21 kG is applied to the collimator by the sweeping magnet. A multiwire proportional chamber system and spectrometer magnet of conventional design are used to reconstruct the decays $\Lambda \rightarrow p + \pi^-$.

The first results published by the Experiment #8 group describe their measurement of Λ^0 polarization in inclusive production by 300 GeV protons incident on a beryllium target.[32] A total of 1.2×10^6 Λ^0 decays were recorded at a number of fixed lab

angles between 0 and 9.5 mrad, covering a range of kinematic variables $0.3 \leq x \leq 0.7$ and $0 \leq p_T \leq 1.5$ GeV/c. The observed Λ^0 polarization was consistent with parity conservation in the Λ^0 production reaction; the polarization increased monotonically with increasing p_T independently of x, to reach a value of $P_\Lambda = 0.28 \pm 0.08$ at $p_T = 1.5$ GeV/c. The measured values of Λ^0 polarization are plotted in Fig. 18. This experiment has reported the first observation of substantial polarization effects at high energies. The inclusive Λ^0 production reaction is, of course, particularly well suited to polarization measurements because the Λ^0 serves as its own spin analyzer through the decay $p + \pi^-$.

The orientation of the spin vector P_Λ (normal to the production plane) and the linear dependence of P_Λ on p_T are both consistent with the hypothesis that the polarization arises in the inclusive channel through the strong interaction. Thus, any model of this high energy inclusive reaction should accommodate a monotonic rise of P_Λ with increasing p_T, and a weak dependence of P_Λ on the scaling variable x; the observed x range in this experiment corresponds to a missing mass M_X of the recoil system X of $13 \leq M_X \leq 20$ GeV/c^2. The polarization is produced by interference of two amplitudes f_1 and f_2, $P_\Lambda = 2\mathrm{Im} f_1 f_2^* / (|f_1|^2 + |f_2|^2)$, so it will have a weak x dependence if f_1 and f_2 depend on x in about the same way.

In a second paper, the Experiment #8 group describe their measurements of the process p + nucleon → V^0 + anything, for $V^0 = \Lambda^0, \bar{\Lambda}^0$, and K_s, at an incident proton energy of 300 GeV. Data were obtained for production angles of 0 to 9 mrad.[33] The measured inclusive production cross sections are shown in Fig. 19.

In the higher range of Feynman x, the invariant inclusive

production cross sections converge to a single-term triple-Regge behavior. Fits to the data yield values of $\alpha(t)$ consistent with K^* (K^{**}) exchange, with Σ exchange, and with Regge-like behavior of a strange di-baryon system for Λ^0, K_s^0 and Λ^0, respectively. Interference between K^* and K^{**} exchange is consistent with the Feynman-x dependence of the Λ^0 polarization which was discussed earlier. In order for the triple-Regge representation of the K^*-K^{**} interference to have a non-zero contribution to the inclusive cross section, the Pomeron cannot be a pure SU(3) singlet. Absorptive corrections may also play a role in the Λ^0 polarization.

Other experiments which are part of the program of neutral hyperon experiments have recently been run or will be run soon by the same group. These include Experiment #415, (see page 68), an experiment to study inclusive reactions $\pi^- Cu \rightarrow K_s^0$, Λ, and neutron; Experiment #440, (see page 71), a measurement of the magnetic moment of the Λ^0 hyperon; Experiment #441, (see page 76), a study of Λ^0 polarization in the inclusive reaction $p + p \rightarrow \Lambda^0$ + anything, with a liquid hydrogen target; and Experiment #495, (see page 82), a study of Ξ^0 and $\bar{\Lambda}^0$ inclusive production and polarization.

In the course of studying the Λ^0 polarization mentioned earlier, the production spectra of Λ^0's by 300 GeV protons was measured for three different neuclear targets: beryllium, copper, and lead. The kinematic region was dominated by fragmentation of the incident proton: $0.2 < x < 1$, $0 < p_\perp < 1.5$ GeV/c. When the invariant inclusive cross section was expressed as a power law in the atomic weight, $Ed^3\sigma/dp^3 = A^{\alpha(x, p_\perp)} \cdot Ed^3\sigma(A=1)/$

the power α was found to be less than 0.67 over the whole kinematic region except at small x. This behavior is consistent with a simple collision model in which the incident proton becomes an excited system which loses energy and gains transverse momentum in collisions with target nucleons as it leaves the nucleus.

A.11 Experiment #96 - Inclusive Particle Production; by an ANL, Bari, Brown, CERN, Cornell, MIT, Fermilab, Northeastern, Stanford collaboration

Experiment #96 was principally devoted to hadron-hadron elastic scattering measurements. In this section we discuss some inclusive particle production measurements which were also made with the same apparatus.

The Experiment #96 group have reported their measurements of inclusive hadron processes of the type $a + p \rightarrow b + \ldots$ at energies of 50 to 175 GeV for Feynman x in the range 0.75 to 0.95 and -t up to 0.65 GeV.[34] In the context of Regge theory, inclusive reactions of the type $a + p \rightarrow b + \ldots$ are of particular interest since they involve quantum-number exchange and cannot proceed via Pomeron exchange. The data were fitted to a semi-empirical form suggested by the Regge theory for $\frac{d^2\sigma}{dt \cdot dx}$.

The results of these fits are shown in Table III.

The cross sections should "scale", that is they should show no additional s-dependence except for the part implicit in σ_{tot}^{cp}. The measured data were consistent with less than 15% departures from scaling resulting from additional s dependences, except for the "$\pi^+p \to p$" cross section which showed departures from scaling of about 30% from 50 to 175 GeV. Because of this, only the data at 140 and 175 GeV were included in the Regge fits for this channel.

The values obtained for "α_{eff}" are consistent with those from Regge exchange theory: for $\pi^\pm p \to K^\pm + \ldots$ the observed values of α_{eff} are small and positive, 0.25 and 0.20 respectively, while for reactions involving nucleon or antinucleon exchange, "$\pi^- p \to \bar{p}$", and "$pp \to \pi^+$", the α_{eff} are all approximately -0.6.

The second set of results on inclusive scattering to be presented by the Experiment #96 group were for reactions of the type $a + p \to a + X$, for large values of Feynman $x \geq 0.975$.[35] Differential inclusive cross sections have been measured for $\pi^\pm p$, $K^\pm p$ and $p^\pm p$ at incident momenta of 140 and 175 GeV/c, over a $|t|$ range from 0.05 to 0.6 GeV^2, and covering a missing-mass-squared (M_X^2) region from 2.4 to 9 GeV^2.

The principal results of these measurements were as follows:

i) The differential cross section $M_X^2 \frac{d^2\sigma}{dt\, dM_X^2}$ is a function of t only, above the resonance missing-mass region (see Fig. 20); and

ii) A pronounced enhancement centered at M_X^2 of (1660 MeV)^2 is observed for all projectile particles (see Fig. 20).

The Experiment #96 group have also reported their measurements of the inclusive processes $a + p \rightarrow a + X$, where a is $\pi^{\pm}$, $K^{\pm}$, $p^{\pm}$, over a range of Feynman x from 0.7 to 0.965, and over the energy range 50 to 175 GeV.[36] The t range covered by these measurements was from 0.03 to 0.7 GeV^2.

The authors have compared the absolute rates for their proton cross sections at 175 GeV/c to the results of other experiments[37] in this energy region. Their results are consistently higher than the USA-USSR and Imperial College-Rutgers results from the Fermilab Internal Target Area by between 1 and 2 standard deviations. The Experiment #96 results above $-t = 0.01$ GeV^2 are higher than but within 1 standard deviation of the Fermilab Bubble Chamber results at 205 GeV/c. Finally, the Experiment #96 results extrapolate quite well to ISR data.

The data from this experiment have been fitted by the following empirical form for the cross section:

$$\frac{s d^2\sigma}{dt\, dM_X^2} = A_1(s,t)(1-x) + \frac{A_2(s,t)}{(1-x)} \quad .$$

There is no theoretical basis for this simple expression. The data at 70 GeV/c and the results of the fits described above, are shown in Fig. 21.

If the Pomeron trajectory were to dominate both the elastic and inelastic cross sections measured in this experiment, the ratio of the inelastic to the elastic cross section at the same value of t should be independent of the beam particle. This would be correct at high energy for x values close to 1,

but it may fail for lower x values where various Reggeon exchanges are possible. The data from this experiment show that this statement of factorization is valid for π^+ and proton to about $\pm$ 5-10% for x near 1 and for $-t \lesssim 0.4$ GeV^2.

At smaller x, the K^+ and π^+ inelastic-to-elastic cross section ratios also follow one another to about $\pm$ 20% over the entire s and t range of Experiment #96; data for K^- and π^- exhibit qualitatively similar behavior. However, the p and $\bar{p}$ inelastic cross sections increase relative to the π and K inelastic cross sections as x decreases, breaking the factorization relation.

The departure from factorization associated with protons as x decreases suggests the presence of an additional effect which is not present in π or K reactions. Two possibilities are: the π-π-Pomeron term in the triple Regge formalism, which is allowed only in p (and $\bar{p}$) reactions; the increase in the proton cross section in the region $x \sim 0.75$ relative to that for π and K may also be partly attributed to decay products of nucleon isobars produced near x = 1.

A.12 Experiment #324 - Single Particle Spectra in High-Energy Collisions of Charged Hadrons; by a BNL-Pennsylvania collaboration

The objective of Experiment #324 is to measure the differential cross sections for the inclusive reactions $a + p \rightarrow c$ + anything, where a, c = p, $\bar{p}$, $\pi^\pm$ and $K^\pm$, at incident momenta between 30 and 250 GeV/c. The experiment covers secondary momenta

$0.3 < p^c_{lab} < 1.25$ GeV/c, corresponding to the "target fragmentation" region of particle production.

The apparatus for Experiment #324 is a magnetic spectrometer, which uses proportional chambers and pivots mechanically about the target position. Cerenkov counters in the incident M1 beam and in the spectrometer are used for particle identification.

The first results to be published by the Experiment #324 group constitute a set of experimental tests of Pomeron factorization in single-particle-inclusive hadron scattering. The incident momenta were 4-24 GeV/c (BNL data):[38] also 150 and 250 GeV/c (Fermilab data).[38] The data have been studied in terms of the Mueller-Regge theory,[39] which suggests that the differential cross sections at high energy should depend on s according to $A + B.s^{-1/2}$. Fits of the s dependence of the measured cross sections are extrapolated to $s^{-1/2} = 0$ and the ratios of the resulting "asymptotic" cross sections are compared with appropriate total cross section ratios to test the prediction of Pomeron factorization:

$$\frac{Ed^3\sigma/d^3p(ab \to c)}{Ed^3\sigma/d^3p(a'b \to c)} = \lim_{s\to\infty} \frac{\sigma_{tot}^{(ab)}}{\sigma_{tot}^{(a'b)}}$$

All of the measurements were made in a small, fixed region of the phase space of particle c, corresponding approximately to $p_T = 0.3$ GeV/c and $y_L = 0.6$, 0.4 and 0.2 for produced π, K, and p respectively.

The measured cross sections, integrated over the fixed kinematic region, are shown as a function of $s^{-1/2}$ in Fig. 22 . One can see from Fig. 22 that the cross section for the production of particle c by particle a and by its antiparticle $\bar{a}$, approach

each other as $s^{-1/2} \rightarrow 0$, in agreement with the expectation from Pomeron exchange.

The pion production cross sections are not well described by the parameterization $A + B.s^{-1/2}$; a better fit is obtained if we use the form $A + B.s^{-1/2} + C.s^{-1}$. However, if all the fits shown in Fig. 22 are extrapolated to $s^{-1/2} = 0$, one can make asymptotic tests which are independent of assumptions about the low-energy behavior of the cross sections. The results agree well with Pomeron factorization.

These comprehensive measurements set the scale of the non-asymptotic contributions to inclusive scattering, for a particular region of the target fragmentation phase space. It appears that, at least in this region, the large size of the non-asymptotic contributions will make difficult any detailed test of Regge-Mueller predictions beyond Pomeron factorization.

Further measurements, as yet unpublished, were made at incident momenta of 30 and 75 GeV/c to augment the data set of Fig. 22. In addition measurements were made in angle sweeps over the range $8 \leq \theta_{lab} \leq 160$ degrees at 75 and 175 GeV/c.

Diffraction Dissociation

A.13 Experiment #27/305 - Coherent Dissociation of Neutrons; by a Rochester, Fermilab, Northwestern, Massachusetts collaboration

At Fermilab energies, neutrons can be coherently excited by nuclei with an appreciable cross section. By coherent it is meant that the target nucleus recoils as a single entity without nuclear excitation. This neutron excitation can occur

either by γ absorption in the nuclear Coulomb field ("Coulomb dissociation") or by Pomeron exchange with the nucleus ("diffractive dissociation"). Both channels can result in the formation of Vees ("n" $\rightarrow p\pi^-$) which Experiment #27/305 is able to study by using a Vee spectrometer which consists of wire spark chambers, counters and an analyzing magnet; the experiment was located in the M3 beam line.

In designing their experiment, the authors of Experiment #27/305 planned to identify and distinguish the two coherent processes mentioned above by utilizing their quite different characteristic variation with neutron energy and momentum transfer, their effective-mass dependence and A dependence, and the angular correlation between the decay particles. While Coulomb dissociation is dominated by Δ^0 (1236) production, diffractive dissociation is dominated by a low mass enhancement at m $\approx$ 1300 MeV. Also, Coulomb dissociation is expected to be an order of magnitude more copious in high-Z materials.

The principal objective of the experiment was to carry out a comprehensive survey and study of Coulomb and diffractive dissociation. Variations in momentum transfer, angular correlations and invariant mass (up to $\sim$ 3 GeV) were to be investigated as a function of target material and of neutron energy (50-300 GeV) using complex nuclear targets and hydrogen. The experimenters also planned to observe Coulomb and diffractive dissociation of the anti-neutron and of partially-polarized neutrons.

The apparatus for Experiment #27/305 consisted essentially of a target (for n-p collisions, a high-pressure hydrogen gas target was used), veto and trigger counters, a Vee spectrometer

which consisted of a dipole analysis magnet and an array of wire spark chambers.

We now discuss the various results which have been published to date.

1. General features of neutron diffractive dissociation.[40] Figure 23 shows the mass distributions for neutron momenta between 50 and 300 GeV/c, which were obtained for the momentum-analyzed $(p\pi^-)$ Vees which were produced in the reaction $n + p \rightarrow (p\pi^-) + p$. The mass spectra are observed to have structure near 1.5 and 1.68 GeV, particularly at the largest values of t. Because the experimental mass resolution is small ($\sigma \lesssim 15$ MeV), the absence of narrow peaks suggests that the mass spectrum consists of an overlap of intrinsically broad states.

Distributions in t for various regions of $(p\pi^-)$ mass are shown in Fig. 24 . The characteristically rapid variation of the t distributions with mass is clearly evident in the data. It is interesting to note that all of the t spectra appear to be consistent with an exp(4.5t) dependence for $|t| \gtrsim 0.4$ GeV^2. Table IV presents the results of a simple exponential parameterization of the t spectrum as a function of the $(p\pi^-)$ mass. The dependence of the slope parameter on mass is similar to that observed at lower energies.

For the reaction $n + p \rightarrow (p\pi^-) + p$ integrated over the t range from 0.02 to 1.0 GeV^2, for the production of small $(p\pi^-)$ masses, the data in the mass region $1.25 < M < 1.45$ GeV are essentially energy independent; this is inconsistent with earlier data, which favored an $s^{-0.4}$ energy dependence.[41] The authors note however that their measured cross sections are approximately

a factor of 1.5-2.0 smaller than those previously measured in the 10-30 GeV/c momentum band.

2. Decay properties of the $(p\pi^-)$ systems.[42] (The decay angular distributions discussed below will be described in terms of the decay angular variables θ and ϕ of the proton in the Gottfried-Jackson (GJ) t-channel frame.)

The distributions in ϕ of the data in two regions of θ, (a) $\cos\theta > 0.8$ and (b) $\cos\theta < -0.8$, are shown in Fig. 25 . The Deck diagrams which are expected to dominate in these regions of $\cos\theta$ are also shown in Fig. 25 . A pion-exchange Deck calculation[43] is seen to fit the measured data for $\cos\theta > 0.8$ rather well. Also, a proton-exchange Deck calculation[43] fits the data well for $\cos\theta < -0.8$. In addition to these comparisons of Deck-mechanism predictions with the data, one can also compare Deck model predictions of the M and t characteristics of the data with the actual measurements; there is reasonable qualitative agreement between theory and experiment.

3. Study of structure in the t distributions for the $(p\pi^-)$ systems [44]

Experiment #27/305 finds that the four-momentum distribution of $(p\pi^-)$ systems produced in the neutron dissociation reaction, $n + p \rightarrow (p\pi^-) + p$, has substantial structure which depends strongly on the mass and on the angular decay properties of the produced $(p\pi^-)$ system. No significant energy dependence is observed in the data for incident neutrons in the momentum range 50-300 GeV/c.

For a series of small ranges of M, the t-spectra can be approximated at low t by simple exponentials of the form exp(Bt),

where B is a function of M. The slope parameters obtained from the Experiment #27/305 data are shown in Fig. 26; the correlation between B and M is seen to be energy independent over the energy range covered by the experiment.

We next consider the correlation between the t-distribution and the GJ polar angle (θ) of the decay proton in the rest frame of the ($p\pi^-$) system. Momentum transfer distributions as a function of the GJ polar angle for different regions of M, are shown in Fig. 27. We note that, especially for small M, the character of the t distribution is strongly dependent on θ. There is no significant dependence of the displayed data on the incident neutron momentum. All of these results are in close agreement with a similar experiment previously performed at the CERN-ISR to study the reaction $p + p \rightarrow p + (n\pi^+)$.[45]

The theoretical curves are based on pion-exchange and baryon-exchange Deck calculations.[46] In the region of phase-space where pion-exchange dominates, namely $\cos\theta > 0.9$, the model is in excellent agreement with the data shown in Fig. 27; as well as with the azimuthal decay angular distributions. Also, at low mass values, where resonance production is unimportant, the t-spectra are again reasonably consistent with the model calculations. However, in the "baryon exchange region", $\cos\theta < -0.9$, the model predicts decay angular distributions which completely fail to reproduce the data. Finally, for central regions of $\cos\theta$, the model fails to reproduce both the mass dependence as well as the dramatic structure observed in the data at small t.

The highly peripheral interference minimum in the t distribution (see Fig. 27), which moves out to larger values as M

increases, and eventually disappears, is a result very similar to that found by the ISR group. The fact that such an interference pattern has very little energy dependence between 50 GeV/c and 1100 GeV/c suggests strongly that the mechanism responsible for this phenomenon must be basic to diffraction dissociation.

Inelastic Collisions of Hadrons with Nuclei

A.14 Experiment #178 - A Study of the Average Multiplicity and Multiplicity Distribution in Hadron-Nucleus Collisions at High Energies; by a MIT, Carleton, Fermilab collaboration

The objective of Experiment #178 was to study the average charged particle multiplicities $\langle n_A \rangle$ and the pseudo-rapidity distributions $\Delta N/\Delta\eta$, with pions, kaons, and protons incident on nuclear targets, in order to obtain data that could discriminate between the several classes of theoretical models for multiparticle production at high energies. The data would also throw light on the currently not understood mechanisms of particle multiplication inside nuclear matter.

The experiment was located in the M6W beam line. Threshold and differential Cerenkov counters in the beam line were used to identify the incident particles. The M6W beam was incident on a nuclear target surrounded by a hodoscope array of lucite Cerenkov counters. The pulse height in a downstream lucite Cerenkov counter, together with information from the array of Cerenkov counters surrounding the target, determined the angular distribution and the charged multiplicity of the interaction. The use of lucite imposed a velocity selection of $\beta > 0.85$.

In an early run of the experiment, the average charged multiplicities of π^--nucleus interactions were measured at 100 and 175 GeV/c. The pseudorapidity distributions for incident π^+, K^+ and p at 50 and 100 GeV/c, and $\pi^\pm$ and $p^\pm$ at 200 GeV/c were obtained in a subsequent run. Targets ranging from carbon to uranium were used. Data on a hydrogen target were obtained by a polyethylene (CH_2)-carbon subtraction.

The total absorption cross sections[47] are in good agreement with the data previously obtained at Serpukhov[48]. they follow approximately an $A^{0.75}$ power law which is predicted by a simple optical model calculation in which a Woods-Saxon distribution of nucleons is assumed.

The measured values of $\langle n_H \rangle$, the average charged multiplicity of relativistic ($\beta > 0.85$) particles in inelastic hadron-proton collisions, were in agreement with hydrogen bubble chamber results.[49]

Measured values of the scaled multiplicity $R_A = \langle n_A \rangle / \langle n_H \rangle$ are shown in Fig. 28, as a function of $\bar{\nu}$; $\bar{\nu}$ is defined as the average number of mean free paths encountered by the incident hadron in going through a nucleus. Figure 28 shows that the average multiplicity grows slowly with the atomic weight of the target, and considered as a function of $\bar{\nu}$, is only weakly dependent on the beam energy and the identity of the beam particle.

For the same value of $\bar{\nu}$, the shapes of the pseudorapidity distributions are similar for the different incident beams. There are slight differences, which are compatible with the differences in multiplicities for the different beam particles on hydrogen.

Figure 29 shows how at 200 GeV/c the pseudorapidity distribution changes as the average thickness of the nucleus changes from one to four mean free paths. The data at 50 and 100 GeV/c have similar features. In the target-fragmentation region, there is a clear indication of cascading with increasing $\bar{\nu}$, showing that the slowest particles are created well inside the nucleus. On the other hand, the almost complete target-independence of the forward-going particles suggests that the asymptotic final state of the fast particles is reached in distances $\gtrsim$ 10 fm.

The energy dependence of the pseudorapidity distribution is illustrated in Fig. 30. If a comparison is made between these data and the 3 TeV emulsion data obtained with cosmic rays,[51] it appears that at all energies it is only the forwardmost two units of the pseudorapidity distribution that are approximately A independent. Since R_A does not decrease with energy and the region of rapidity where $N(\Delta z)/\Delta z$ is target-dependent moves out in η as energy increases, the data are incompatible with all models which have only short-range order.

The results of Experiment #178 clearly indicate that $\bar{\nu}$, which depends on the absorption cross section of the incident particle and not that of the secondaries, is the relevant parameter in the description of the multiplication process. The data rule out all cascade models where the asymptotic states are formed in distances short compared to the mean free path of hadrons in nuclear matter; instead, they support a description of "forward" multiparticle production of the hydrodynamic (or energy-flux) type.[52] However, more definitive comparisons with models must await more detailed theoretical calculations.

B. Large Transverse Momentum Hadron Physics

Introduction

The Experiment #268 group has studied π^0 production at high p_T by both pions and protons, in an attempt to probe the structure of the nucleon, and in particular to investigate its possible constituents. The principal objective of the experiment was to measure the ratio of π^0 inclusive production at large p_T by protons, to production by $\pi^{\pm}$ mesons.

It was found that the ratio of π^0 production cross sections from π^+ and from π^- was close to unity, over the entire p_T region covered by the experiment. However, the ratio of p to π^- cross sections falls from 1.6 at $p_T \sim 1.6$ GeV/c (a result which can be predicted by factorization arguments in the Mueller-Regge theory) to well below 1, at $p_T \sim 4$ GeV/c. The results of this experiment are in reasonable agreement with the quark-quark hard scattering model of Field and Feynman.

Preliminary results from one of the two experiments that are studying hadron jets in the Meson Lab (#236 and #260) are now available from Experiment #260. For the trigger conditions of Experiment #260, the most striking feature of their results is the very large ratio of "jets" to single-particle cross sections, (for $p_T \sim 3$-5 GeV/c). The jet events also appear to be "coplanar" -- the particles in the "jet" have a sharp exponential dependence, with a mean of 200 MeV/c, for the component of momentum out of the plane formed by the "jet" and the initial hadron. The distribution of (fractional) momentum for the charged particles in the jet is similar to that for lepton-induced processes.

B.1 Experiment #268 - Study of Meson Production at Large p_T with a γ-Ray Detector; by a Caltech, LBL Collaboration

Experiment #268 used the γ-ray detector, the incident beam Cerenkov counters and hydrogen target previously used by Experiment #111 in the M2 beam line, to study the production of π^0, η^0 and other mesons at large p_T from $\pi^{\pm}p$ and pp interactions for c.m. angles from 8° to 110°.

The motivation and principal objectives of this experiment were quite straightforward. High transverse momentum (p_T) phenomena have for a long time been associated with interactions at small distances, and for the case of hadron-nucleon collisions they provide a tool to probe the structure of the nucleon, in particular to investigate its possible constituents. However, most of the experimental studies which had been performed at the time Experiment #268 was proposed, were confined to the proton-nucleon interaction; very little data existed for meson-nucleon interactions. From the simple quark model of hadrons, only qq interactions are probed by producing high p_T events in proton-nucleon collisions. On the other hand, in the case of meson-nucleon collisions, one probes $\bar{q}q$ interactions, also. There was a strong suggestion from the constituent picture of hadrons that inclusive meson production could be qualitatively different and considerably more copious for incident mesons than for incident baryons.

The principal objective of this experiment was to measure the ratios $R(A/B) = \frac{Ed\sigma(Ap \to \pi^0 X)/d^3p}{Ed\sigma(Bp \to \pi^0 X)/d^3p}$, where A and B are p, π^+, or π^-.

The ratios $R(\pi^+/\pi^-)$ and $R(p/\pi^-)$ are shown in Fig. 31[53] as a functi of p_T. At both 100 and 200 GeV/c, $R(\pi^+/\pi^-)$ is close to unity over the entire p_T region which was investigated. In contrast, $R(p/\pi^-)$ changes markedly between $p_T \sim 1$, and $p_T \sim 4$ GeV/c. At $p_T \sim 1.6$ GeV/c the ratio is about 1.6, which is equal to the ratio of the total pp and πp cross sections; this can be understood by factorization arguments in the Mueller-Regge theory.[54] However, the ratio $R(p/\pi^-)$ decreases with increasing p_T; the πp cross section significantly exceeds the pp cross section at the largest measured values of p_T.

Although the value of $R(p/\pi^-)$ at a fixed p_T is different at 100 and 200 GeV/c, $R(p/\pi^-)$ is independent of energy when expressed as a function of $x_T = p_T/p_{max}$ as shown in Fig. 32 . The pp and πp cross sections can be parameterized by a factorized function:

$$E \frac{d\sigma}{d^3p} \alpha(p_T^2 + M^2)^N \cdot (1-x_T)^F .$$

In the context of this parameterization both the πp and pp reactions have the same p_T dependence, and so the fall of $R(p/\pi)$ versus x_T shown in Fig. 32 can be interpreted as a difference in the power of $(1-x_T)$. The quark-quark hard scattering model of Field and Feynman[55] is in good agreement with the results of this experiment.

B.2 Experiment #260 - A Study of High-p_T Physics with a Multiparticle Spectrometer; by a Caltech, UCLA, UICC, Indiana, Fermilab Collaboration.

The objective of Experiment #260 was to use the Multiparticle Spectrometer located at the end of the M6W beam line to gain a global view of interactions in which one or more particles carry off high values of p_T. In particular, it was decided to study the momentum transfer region $2 < p_T < 6$ GeV/c.

The arrangement of the multiparticle spectrometer for Experiment #260 is shown in Fig. 33.[56] The p_T for charged particles is determined by the spectrometer; for photons and neutrons, the calorimeters provide the p_T determination. The calorimeters are also used to generate a high-p_T trigger.

Two classes of events were studied: (i) "single particle" triggers, where the p_T detected by at least one of the calorimeter modules exceeded a preset trigger bias, 3 GeV/c; and (ii) "jet" triggers, where the total p_T detected by all four modules of either the left or the right calorimeter exceeded the jet trigger preset bias; data were taken with biases of 3, 4 and 4.5 GeV/c. Figure 33 shows a typical event recorded with a high-p_T "jet" trigger.

The single-particle inclusive cross sections have been compared with the results of the Chicago-Princeton group[57]; there is good agreement between the two sets of data, for p_T above the calorimeter trigger threshold of 3 GeV/c.

For the "jet trigger" events, the transverse momentum of a jet was defined by summing the p_T of all particles observed in the trigger calorimeter. These particles divide into three separate

categories:

i) Charged particles (typical multiplicity is 3), measured by track chambers. On the average, charged particles carry about 57% of the jet momentum.

ii) Photons (from π^0, η, etc.), measured in the electron part of the calorimeter. Photons carry 30% of the momentum of the jet, on the average.

iii) Neutral hadrons (K_s^0, Λ, etc.). This component, measured in the hadron part of the calorimeter after the energies of charged tracks have been subtracted, is typically about 13% of the total jet momentum.

The jet cross sections presented in Fig. 34 come from jets which lie in the same fiducial region as that used for the single particle data. No correction has been applied for the trigger bias of the calorimeter for the "jet trigger" events; however, comparison of the data for three trigger bias thresholds allows one to extract an unbiased jet cross section, shown as the broad solid line in the Figure.

The most striking feature of Fig. 34 is the very large (over two orders of magnitude) ratio of jet to single-particle cross sectior The data on jet events also show evidence for the generally coplanar structure of the events. For example, it is found that there is a sharp exponential dependence, with a mean of 200 MeV/c, for the component of momentum out of plane formed by jet and initial hadron, for the particles in the jet. Also, the two-dimensional momentum perpendicular to the jet axis is strongly cut off, for the members of the jet. The above observations are both suggested by the constituent models.[58]

Figure 35 shows the distribution of (fractional) momenta (z) for charged particles in the jet. There is a striking similarity between the z distributions of Experiment #260 and those for lepton-induced processes.[59]

Figure 36 plots the momentum distribution on the "away" side (see Fig. 34, these are the particles that balance the p_T of the trigger). We see that single-particle and jet triggers balance transverse momentum in similar ways. We note further the "away" and "towards" z distributions have similar shapes but differ by a factor $\sim$ 2.5 at large z. In constituent models,[58] this is a direct reflection of the transverse momenta of quarks/partons inside hadrons.

The conclusion reached by Experiment #260 is that their data give strong support to the idea that the same constituents of hadrons are responsible for both high p_T hadrons and high p_T lepton-induced processes.

The analysis of the data from Experiment #260 is continuing.

C. Searches for New Particles

Introduction

The experiments to search for free quarks and the experiments to search for charmed particles would be very important and merit lengthy discussion -- if any of the new particles were discovered. No quarks and no charmed particles have been detected in any Meson Lab experiments performed to date, so this summary can be brief.

Three experiments (C1, C2, C3) all have searched unsuccessfully for quarks. The limits they have established are as follows:

Experiment #72: $|Q| = 1/3,\ 2/3$: $m_Q \lesssim 12\ \mathrm{GeV}/c^2$;
cross section limit $\sim 10^{-35}\mathrm{cm}^2$.

Experiment #72: $|Q| = 4/3$: $m_Q \lesssim 12\ \mathrm{GeV}/c^2$;
cross section limit $\sim 10^{-32}\mathrm{cm}^2$

Experiment #75: $|Q| = 1/3,\ 2/3$: $m_Q \lesssim 9\ \mathrm{GeV}/c^2$;
cross section limit $\sim 10^{-36}\mathrm{cm}^2$

Experiment #330: $|Q| = 1$: $m_Q \lesssim 12\ \mathrm{GeV}/c^2$;
cross section limit $\sim 10^{-33}\mathrm{cm}^2$.

Following the discovery in November, 1974 of the J/ψ and ψ' particles, which were widely interpreted as low-lying states of charmonium, a concerted effort was begun to observe directly the charmed mesons and baryons. Charmed particles have since been detected in e^+e^- annihilation experiments, in high energy neutrino interactions, and in photoproduction. However, observation of the hadronic production of charm still eludes us.

Five experiments performed in the Meson Lab, which are described in the sections C.4-C.8 following, were all of them

attempts to observe the hadronic production of charm. While they were not successful in producing charmed particles, they were able to establish upper limits for specific production and decay modes. The upper limits established by these experiments (#305, #357/472, #365, #366 and #416) for σ.B [(production cross section) x (branching ratio to the decay mode searched for by the experiment), at $m_c \sim 2$ GeV/c^2] are all in the range 100-500 nb. Apparatus for experiments with higher sensitivity (Experiments #490 and #515, see pages 83 and 84) is now being built, as the search for the hadronic production of charm continues.

Searches for Quarks

C.1 Experiment #72 - Quark Search at Fermilab; by a Yale, BNL collaboration.

This experiment was installed in the M4 secondary beam line shortly after the Meson Lab first came into operation. The detector of "free" quarks was a series of eight scintillation counters in which the ionization energy loss of beam particles was measured. The pulse heights from the eight counters were examined separately to minimize the effects of statistical fluctuations and of the Landau tail.

This quark search was intended to be sensitive not only to particles of charge e/3 and 2e/3 but also to particles of charge 4e/3, 5e/3 and greater. With a primary proton energy of 300 GeV,

quarks as heavy as 12 GeV/c^2 could be produced.

No quarks were detected by Experiment #72.[60] The authors of this experiment have observed that while all accelerator quark searches to date have resulted in limits on differential production cross sections for quarks, nevertheless, it is useful to attempt to estimate a limit in terms of the total production cross section. To do this in a meaningful fashion, one must have recourse to a model of quark production which is not tied too closely to a particular view of the production process. The Experiment #72 group therefore chose a method of measurement, at 6.5 mrad production angle but using no magnetic fields, which is sensitive to a very wide range of production models. The conclusion was reached by Experiment #72 that it is unlikely that the cross section for the production of either charge e/3 quarks or charge 2e/3 quarks is greater than 10^{-35} cm^2; the kinematic mass limit was about 12 GeV/c^2.

The Experiment #72 group conducted a separate search for charge 4e/3 quarks. This search was done with the 6.5 mrad beam deflected by about 8 cm at their apparatus, and with the magnetic field adjusted so that they accepted particles with charge +e in the momentum interval 60 $\pm$ 20 GeV/c -- slow protons, with their large energy losses, were thereby eliminated from the beam. No charge 4/3 quarks were detected -- an upper limit for the production cross section of charge 4/3 quarks was set at 5×10^{-31} cm^2.

C.2 Experiment #75 - Search for Fractionally Charged Quarks; by a NYU, Fermilab collaboration.

Experiment #75 used the M2 secondary beam channel. By tuning the elements of the beam line to a momentum (for singly

charged particles) which was higher than the primary proton beam momentum, no particle with $|Q| \geq 1$ could pass through the entire length of the beam channel, unless it were scattered several times by collimator walls, magnet poles or other elements in the beam channel. On the other hand, quarks with charge $|Q| = 2/3$ and momentum $\sim 2P_0/3$ or charge $|Q| = 1/3$ and momentum $\sim P_0/3$ (where P_0 is the tuned momentum value of the beam channel), would pass through.

An array of scintillation counters followed by an ionization calorimeter measured the ionization loss and total energy of those particles transmitted by the beam channel. Further rejection of highly relativistic background particles was obtained by the use of threshold Cerenkov counters.

The experiment was sensitive for detection of quarks up to a kinematic mass limit of 9 GeV/c^2.

No fractionally-charged quarks were seen in the experiment. Upper limits on the quark production cross section,[61] up to the kinematic mass limits of 9 GeV/c^2, are shown in Fig. 37 . Also shown for comparison are the upper limits on production cross sections which had previously been measured at the CERN-ISR.[62]

C.3 Experiment #330 - Search for Massive Neutral Particles; by a Michigan collaboration

The search by Experiment #330 for new massive neutral particles of long lifetime $\gtrsim 10^{-7}$ sec was carried out by measuring the time-of-flight of neutral particles along the M4 beam line, relative to the accelerator r.f.; their energies were determined by a total absorption calorimeter.

The result of the experiment was that no evidence was seen for the production of long-lived neutral particles with masses $\gtrsim 2$ GeV/c^2.[63] The cross section limits obtained are $\sim 10^{-1}$ of the cross sections for the production of ψ's at comparable values of p_T. The authors of Experiment #330 argue that their result constitutes the strongest experimental evidence to date against the existence of quasi-stable integrally charged quarks.

Search for Charmed Particles

C.4 Experiment #357/472 - Search for Charmed Particles; by a Fermilab, Michigan, Purdue collaboration.

The principal objective of Experiments #357/472 was to search for charmed mesons produced in the reaction:

$$\text{hadron} + \text{hadron} \rightarrow \underset{\hookrightarrow \pi K}{C} + \text{anything}$$

where C is a charmed meson. The C meson would be identified as a narrow spike in the πK effective mass spectrum as recorded by the two-arm spectrometer. As a byproduct, the experiment would also obtain data on inclusive two-particle production as a function of the two-particle momenta and types.

Experiment #357/472 utilized the M2 beam operating at an intensity of 10^8 protons per pulse. The detection system consisted of two identical spectrometers; they were aimed at $\pm$ 100 mrad with a respect to the incident beam direction. Each spectrometer employed an analysis magnet, three gas threshold Cerenkov counters and 16 planes of drift chambers. The set-up covered the mass

range $2 < m_c < 10$ GeV/c, with a mass resolution of approximately $\Delta m_c = 0.005 M_c$ and a detection efficiency on the order of 10^{-3}.

Experiment #357/472 group has published the results of their search for new mesons in the mass range 1.5 to 4.0 GeV/c;[64] no evidence for narrow resonances was seen. Experimental checks of the operation of the two-arm spectrometer were provided by the observation of a clean $J/\psi \rightarrow \mu^+\mu^-$ signal.

Representative di-hadron spectra are shown in Fig. 38 . The rapidity distribution of these hadron pairs is concentrated in the region y = -0.4 in the center-of-mass system. The (4σ) limits for the production of new particles decaying to πK, at the D° mass of 1.87 GeV/c^2, were $B_{\pi^- K^+} \cdot \frac{d\sigma}{dy} < 415$ nb and $B_{\pi^+ K} \cdot \frac{d\sigma}{dy} < 330$ nb. These limits decrease to 33 nb and 25 nb respectively, at effective mass 4.0 GeV/c^2.

An important conclusion drawn by the authors of this experiment was that for charmed particles with masses near 2 GeV/c^2, if they are produced with cross sections similar to that for J/ψ, then they will not be observable in a hadron experiment such as Experiment #357/472 unless a more sophisticated trigger can be devised to reduce the large physical hadron background.

Motivated by the fact that data from many other experiments -- hadron interactions, neutrino interactions, and e^+e^- annihilation, each with prompt leptons in the final state -- give rather compelling evidence for the production of new particles, the Experiment #357/472 group have also searched for narrow resonances in two-body hadron mass spectra for events containing a prompt muon. In addition, they have searched for the existence of long-lived states ($\tau \geq 10^{-13}$

sec), by vetoing particles which come to their detectors directly from the proton-beam target.

The πK mass spectra obtained with the di-hadron-plus-muon trigger requirement showed no enhancements in the data[65]; the (4σ) upper limits on the cross section for associated C-μ production, $B_{\pi K} B_{\mu+X} \frac{d\sigma}{dy}$, are 0.67 times the upper limits on simple πK production of a new particle. No enhancements were seen in the πK spectra, in the "long-lived" search.[65] The sensitivity of this search is shown in Fig. 39.

C.5 Experiment #305 - Search for Narrow Resonances Produced by Neutron Dissociation; by a Fermilab, Massachusetts, Northwestern, Rochester collaboration.

The apparatus in the M3 beam line which had been previously used for the neutron diffraction dissociation studies of Experiment #27/305, namely a downstream Vee spectrometer, consisting basically of a BM 109 analysis magnet and a number of wire spark chambers, were used to measure the angles and momenta of up to 4 charged particles produced in a high energy neutron-beryllium interaction. The acceptance of the spectrometer was $20 < |\theta| < 75$ mrad (horizontal) and $|\theta| < 25$ mrad (vertical).

The result of the experiment was that no significant enhancement was seen in the high-mass $K^{\pm}\pi^{\mp}$ or pK^{-} systems.[66] The limit obtained for production cross section times branching ratio was $\lesssim 150$ nb/nucleon for $K\pi$ masses ~ 2 GeV/c^2.

C.6 Experiment #366 - Study of Heavy, Narrow Mesons Using a Mass Focusing Spectrometer; by a Michigan State, Ohio State, Carleton, Fermilab collaboration.

The apparatus for Experiment #366 was a high resolution, mass focusing spectrometer capable of focusing two-body masses up to $\sim$ 3 GeV/c^2 with a resolution of 15-30 MeV/c^2 FWHM. The spectrometer consisted of a proportional chamber-spark chamber array constructed around a dipole analysis magnet. A two-cell, 10m long Cerenkov counter made possible the identification of decay particles. The experiment was located in the M3 beam line.

The apparatus was especially sensitive to peripherally or diffractively produced objects and was thus complementary to those which searched in the central region. The experiment design was optimized for a particle mass of 2.5 GeV/c^2, produced with $p_T \leq 0.6$ GeV/c and $0.2 \leq x \leq 1$.

Invariant mass distributions for the two-body hadronic channels $\pi^+\pi^-$, π^+K^-, pK^- and $\bar{p}p$ are shown in Fig. 40.[67] No significant enhancements are seen in the data -- except for a 4σ enhancement at $M = 2.29$ GeV/c^2 in the $K^-\pi^+$ mass spectrum; more statistics would be needed to confirm this possible mass peak. A second run of the experiment was carried out in mid-1976; however, no results have yet been published from this run.

In the absence of significant enhancements, upper limits on cross section times branching ratio for production of a particle which decays by a two-body hadronic channel, were estimated for $x \geq 0.2$, and corresponding to a 4σ limit. The conclusion of the Experiment #366 group is that they observe no narrow resonances with a $\sigma.B > 1\mu b$.

C.7 Experiment #416 - Steamer Chamber Search for New States Which Decay Semi-Leptonically; by a Washington, Orsay, UC/Davis collaboration.

A 225-GeV π^- beam struck a 5 cm lucite target at the entrance to a streamer chamber (1x.5x.3 m^3), which was placed in a large magnet whose field in the visible volume was approximately 8 kG. Immediately downstream of the streamer chamber was a magnetized-iron muon filter. Wire spark chambers located downstream from the muon filter made possible the determination of the muon momentum and production angle. The experiment was carried out in the M1 beam line.

The specific objective of the experiment was to determine if there is an enhancement in the production of neutral strange particles observed in the streamer chamber when the chamber is triggered on prompt muon pairs.

The data have been analyzed to give a measurement of the cross section for hadronic production of ψ/J mesons.[68] The result is consistent with that obtained by K.J. Anderson, et al.[69] Only a small fraction ($\sim$ 15%) of the low-mass dimuons could be accounted for by vector meson production. At the level of 22 events/nb, the hadrons produced in association with muon pairs appear to be the same as hadrons produced in any inelastic interaction. The absence of correlated μ-V^0 production leads to an upper limit of $\sim$ 10 μb cross section for production of new states which decay semi-leptonically.

C.8 Experiment #365 - Search for Forward Production of Massive States Which Decay with Muon Emission; by a Northeastern collaboration.

The object of this experiment was to search for the production of charmed mesons, D, produced in such reactions as

$$\pi^- p \rightarrow D\bar{D}p$$

and

$$\pi^- p \rightarrow D\bar{D}(n\pi)p.$$

For each event, the final state proton as well as one or more of the muons from the D or $\bar{D}$ decays would be measured. The experiment would look for D's in the mass range $1 < M_D < 4.5$ GeV.

The apparatus for this experiment consisted of beam defining counters in the M2 beam, a hydrogen target, a spectrometer (scintillation counters and wire spark chambers) which measured the recoil proton, and a magnetized iron spectrometer (also including scintillation counters and wire spark chambers) which measured forward muons. A coincidence between a beam particle, a recoil proton and a forward muon was required for an event to be recorded. Data were obtained at π^- and proton energies of 200 and 240 GeV.

The distribution of events as a function of M^2 (where M^2 is the square of the effective mass of the forward system as determined ~~for~~ by the incident beam and recoil proton 4-momentum vectors) showed no unusual enhancements and no qualitative change in shape, whether the muon ~~required event~~ requirement was ~~incident~~ included in the trigger, or not.[70]

The conclusion reached by the authors was that the measured upper limit on the total charm production cross section times muonic decay branching ratio was

$$\sigma_{tot} \cdot B_{\mu} < 380 \text{ nb} \quad \text{(2 standard deviations).}$$

D. Measurements of Fundamental Properties of Hadrons

D.1 Experiment #216 -- A Measurement of the Pion Form Factor by Direct Pion Electron Scattering; by a Dubna, UCLA, Pittsburgh, Notre Dame, Fermilab collaboration.

The primary objective of Experiment #216 was to measure the pion electromagnetic form factor in the space-like region of momentum transfer by direct observation of pions and electrons from a pion beam scattered from stationary electrons in a hydrogen target. A previous experiment at Serpukhov [71] had measured a pion radius squared of $(0.61 \pm 0.15)F^2$. It was planned to take the first set of data in Experiment #216 at 100 GeV -- twice the pion energy used at Serpukhov. The momentum transfer range would thus be extended to 0.08 GeV^2, and thus the effect of pion size would be significantly increased and several systematic errors in the measurement would be reduced.

In the experiment, the trajectories of the incident pion and of the scattered pion and electron were measured by an arrangement of magnetostrictive and proportional chambers. The momenta of the recoil π-e pairs were determined with the use of two analyzing magnets. Electrons, and hence the q^2 label for each event, were identified through the kinematic analysis of the recoiling particles using the excellent angular precision of the apparatus ($\pm$ 0.2 mrad). A redundancy check on the electron identification was provided by total-absorption lead-glass shower counters; any μ-e events were rejected with the use of a simple muon filter.

The experiment was carried out using 100 GeV π^- mesons in the M1 beam line. A sample of 10,000 elastic pion-electron events

was obtained in the momentum transfer range $0.03 \leq q^2 \leq 0.07$ GeV^2.[72] The form factor $|F_\pi|^2$ calculated from the data is plotted as a function of q^2 in Fig. 41 . With a 2% uncertainty in the integrated pion-electron elastic cross section, Experiment #216 obtains the following result:

$$\langle r^2 \rangle_\pi = 0.33 \pm 0.06 \text{ F}^2 .$$

For comparison, vector dominance predicts 0.40 F^2, the size of the proton is 0.66 F^2. The Serpukhov result for $\langle r^2 \rangle_\pi$ was 0.61 $\pm$ 0.15 F^2 -- the difference between the two experimental values for F_π^2 is 1.75 standard deviations.

E. Other Experiments

E.1 Nuclear Emulsion, Nuclear Chemistry, and Applied Radiation Physics Experiments

Many nuclear emulsion exposures have been made in the last few years at Fermilab. Several of the first exposures were in the 200 GeV proton beam in the Meson Target Hall in the fall of 1972. Since that time, emulsion exposures at Fermilab have been carried out almost exclusively in the Neutrino Lab. We do not discuss or describe the individual nuclear emulsion experiments in this report. The interested reader is referred to Reference 73 for a list of the nuclear emulsion experiments which have been carried out or are planned to be carried out at Fermilab.

A small number of detector development, nuclear chemistry and applied radiation physics experiments -- including some searches (none as yet successful) for the existence of super-heavy elements -- have been carried out at Fermilab; many of these experiments were done in the Meson Lab. We shall not discuss the individual experiments in this report, but the reader can find a list of them in Reference 73.

E.2 Experiment #22 - A Search for Multigamma Events from Magnetic Monopole Pairs; by a Virginia Polytechnic Institute, BNL collaboration.

The purpose of this experiment was to discover more events of the kind found by Schein, et al.,[74] in cosmic rays. If they could be detected at Fermilab, the next step would, of course, be to investigate the nature of their origin. Ruderman

and Zwanziger have suggested that the photons may originate from the production and annihilation of magnetic monopole pairs.

The apparatus for the experiment was designed to measure the multiplicity and angular distributions of simultaneous photons produced at small angles ($\sim$ 1 mrad). This was accomplished by recording the position and number of unresolved electromagnetic showers produced by the photons in a lead converter placed in front of a proportional chamber array. A veto counter array was placed in front of the converter to anti-out any charged particles. Slow neutrons were avoided by recording only those high multiplicity events with good time resolution ($\leq$ 100 nsec). Also included in the trigger logic for the experiment were a threshold gas Cerenkov counter set to be sensitive to a high multiplicity of electrons, and a lead glass counter with its threshold set at 100 GeV electromagnetic energy. The experiment was located in the M2 beam line.

Experiment #22 made measurements of the angular, energy and multiplicity distributions of multiphoton events produced in photon-beryllium interactions at 300 GeV/c.[75] The dominant features are well described by known processes; however, a few multiphoton events said to be inconsistent with known processes, but consistent with a monopole pair origin, were found at a level of $\sim 10^{-7}$ per proton interaction. Because of the small number of these events, the authors are unwilling to attest to their interpretation as monopole pair events.

E.3 Experiment #230 - A Search for "Schein Events" and Events with a High Multiplicity of γ's; by a Michigan collaboration.

Experiment #230, like Experiment #22, was designed to discover and study Schein-type events.[74] The apparatus consisted basically of an array of wide-gap chambers which were used to study the forward multigamma production by neutrons and photons in a CH_2 target. The trigger system selected events in which a neutral particle came to the target, no charged particles came out, and many charged particles were produced by the lead converter in front of the wide gap spark chambers. This experiment was performed in the M3 beam line.

No anomalous events were found in this experiment.[76] The authors of Experiment #230 place an upper limit of 2.7μb on the production cross section for Schein-type events--this is $\sim 10^{-2}$ of the production cross section deduced from the cosmic ray data.

III. Experiments with No Published Results to Date (June 1977)

F. Recently Completed Experiments; Data Presently Being Analyzed

Low Momentum Transfer Hadron Physics

F.1 Experiment #248 - Neutron-Proton Diffraction Scattering; by a Michigan collaboration.

The apparatus for this experiment which was located in the M3 beam line, consisted essentially of two detectors: forward going neutrons were detected in an array of wire spark chambers interspersed with steel plates, while recoil protons coming off near 90° in the lab were detected in a wire spark chamber magnetic spectrometer.

The objective of the experiment was to measure differential cross sections for np scattering in the energy and momentum transfer regions $50 < E < 400$ GeV, $0.1 < -t < 3.5$ GeV^2. The precision of the differential cross section data should permit determination of the slope of the diffraction peak to a few per cent, and should permit study of the development with increasing energy of a diffractic minimum and secondary maximum as seen in the ISR and Experiment #7 pp data. The np data should also be sensitive to changes in the slope of the diffraction peak as s and t vary, if these changes are comparable in magnitude to what has already been observed in pp elastic scattering.

F.2 Experiment #486 - Study of the Atomic Number Dependence of the Difference Between Particle and Anti-Particle Cross Sections; by a Chicago, ETH/Zurich, Wisconsin collaboration.

Experiment #486 was a high statistics, virtually systematics-free measurement of the A-dependence of the difference in particle/antiparticle total cross sections by use of coherent regeneration in a "double-beam" arrangement in the M4 neutral beam line. For a given accelerator pulse, one of the beams was used for monitoring, while the other beam contained the target. The roles of the beams were then interchanged on a pulse-by-pulse basis.

If the cross section difference goes like $A^{\beta(E)}$, then β as a function of energy should be determined to an absolute accuracy of better than $\pm$ 0.01 in several momentum bins from 30 to 150 GeV/c.

F.3 Experiment #397 - Search for High Mass Particles Produced in Association with Prompt Muons; by a Fermilab, Northwestern, Rochester, SLAC collaboration.

This experiment has investigated the possible existence of narrow, high mass states (e.g., charmed particles) which are produced in association with prompt muons.

Most theoretical estimates of the expected magnitude of direct muon production by hadrons, taking into account electromagnetic processes and the known vector mesons, fail to saturate the observed μ/π ratio of 10^{-4}. A significant fraction of these muons may result from weak decays of new hadrons. These new hadrons would necessarily be produced in pairs. The technique employed by Experiment #397 was to employ the muon resulting from the leptonic or semi-leptonic decay of one of the new hadron states to trigger their detector, and then to examine the characteristics of the associatively produced particles using a modified version of the Experiment #27/305 spectrometer

The muons were identified by their traversal of a steel and heavimet telescope which was instrumented with counters, proportional chambers, and wire spark chambers.

F.4 Experiment #415 - Measurement of $\pi^- Cu \rightarrow K_S^0$, Λ^0, and Neutron Inclusive Cross Sections; by a Colorado, Michigan, Rutgers, Wisconsin collaboration.

Experiment #415, a study of inclusive strange particle yields from a pion bombardment of a copper target, was motivated principally by the needs for the strange particle production data as an aid in the design of a K_L^0 beam in the Proton West area at Fermilab. The proposed K_L^0 beam would be produced by a high energy, high intensity pion beam; there would thus be a smaller fraction of background neutrons in the beam than in a proton-produced K_L^0 beam.

The experiment used the M2 beam, set for π^- at 200 GeV/c but with much lower intensity than is planned for the P-West pion beam. As a detector, the experimenters used the apparatus of Experiment #8 -- a neutral Vee spectrometer. In this apparatus, K^0's were identified through their decay to $\pi^+\pi^-$, Λ^0's through their $p\pi^-$ decay mode, while neutrons were detected by a technique previously utilized by the coherent neutron dissociation experiment (#305) -- the neutrons are scattered in a carbon target, producing N*'s which decay to $p\pi$.

Large Transverse Momentum Hadron Physics

F.5 Experiment #350 - Study of π^0 and η Inclusive Production with Incident π^- in the Triple-Regge Region; by a Caltech, BNL, LBL collaboration.

Experiment #350 measured the following reactions,

$$\pi^- p \rightarrow (\pi^0, \eta^0, \omega, \ldots.) + X^0$$

$$X^0 \rightarrow \text{charged} + \text{neutrals},$$

and

$$\pi^- p \rightarrow (\pi^0, \eta^0, \omega, \ldots.) + X^0$$

$$X^0 \rightarrow \text{neutral};$$

These measurements were made in the essentially unexplored kinematic region $0 \leq -t \leq 3$ GeV^2 and $0.8 \leq x \leq 1$. Experiment #350 is a further continuation of the work begun by the same group in Experiment #111 (study of exclusive π^- charge exchange) and Experiment #268 (inclusive production of π^0, η, etc., at p_T up to about 5 GeV/c). The experiment, like its predecessor, was located in the M2 beam line.

The objectives of Experiment #350 were as follows:

a) To measure the ρ and A_2 Regge trajectories to larger t-values than can be reached in exclusive π-charge exchange;

b) To obtain data in the triple-Regge region for comparison with theory for reactions involving relatively simple exchanges and where the theory makes unambiguous predictions.

c) To study the relation between high-p_T and low p_T phenomena.

Data were to be collected for π^- energies of 100, 150 and 200 GeV.

The apparatus for Experiment #350 consisted basically of the photon detector utilized for the two earlier experiments (#111 and #268) with the addition of a charged particle hodoscope.

Measurements of Fundamental Properties of Hadrons

F.6 Experiment #456 - Measurement of the Kaon Form Factor, by a UCLA, Dubna, Fermilab, Notre Dame, Pittsburgh collaboration.

The objective of the experiment was to measure the charged kaon electromagnetic form factor in the spacelike region of momentum transfer by direct observation of kaons scattered from a kaon beam by stationary electrons in a liquid hydrogen target.

The experiment was performed in the M1 beam, at a kaon momentum of 250 GeV/c; differential Cerenkov counters were used to select the kaons in the beam. The scattered kaons and recoil electrons were to be detected with nearly 100% efficiency over the momentum transfer range 0.03 to 0.13 GeV^2. The experimenters hoped to record $\sim$ 6,000 K-e scatters, and to measure the mean square radius of the kaons within a precision of 0.04 $(Fermi)^2$.

The apparatus used for Experiment #456 was an upgraded version of the apparatus used for Experiment #216 (the pion form factor experiment, see page 61). Drift chambers were used, for increased angular precision; proportional chambers were used in place of wire spark chambers.

F.7 Experiment #226 - Coherent K_S^0 Regeneration by Electrons; by a Chicago, ETH/Zurich, UCSD, Wisconsin collaboration.

Experiment #226 used the E-82/425 spectrometer in the M4 beam line to measure the amplitude for K_S regeneration by electrons. Since this amplitude is proportional to the rms neutral kaon charge radius, Fermilab is well suited to this kind of experiment, since the electron contribution to regeneration is $\Sigma \simeq 7\%$ at 100 GeV, and grows as the square root of the kaon momentum. Experiment #226 planned to measure the electron-induced regeneration to a precision $\Delta\Sigma \approx 1.8\%$.

Some ancillary measurements of interest were also included in the run plans of Experiment #226:

a) Measurement of the K^0-p elastic scattering cross section, by measuring the angular dependence of K_S^0 events, and determining the t = 0 point in absolute value from σ_{tot} via the optical theorem.

b) Measurement of K_S^0 diffractively regenerated from a moderately thin regenerator.

c) Measurement of inelastic regeneration.

F.8 Experiment #440 - A New Measurement of the Magnetic Moment of the Λ^0 Hyperon; by a Wisconsin, Michigan, Rutgers collaboration.

The design of Experiment #440 was based on the earlier measurement of Experiment #8 (see page 28) that the Λ^0's produced at 6 mrad by 400 GeV protons in the inclusive reaction

$$p + Be \rightarrow \Lambda^0 + X$$

have a significant average polarization:

$$[\alpha \underline{P}_{\Lambda}] = 0.1.$$

The experimenters exploit this relatively large polarization to measure the magnetic moment of the Λ^0 to better than 1%. The angle of precision of the Λ^0 spin, ω, is measured in a 10 foot long bending magnet placed in the neutral beam at the end of the M2 beam line. The bulk of the apparatus used for this experiment was inherited from Experiment #8.

Other Experiments

F.9 Experiment #507 - Study of Channeling at Fermilab; by a UCLA, Fermilab, Dubna, Lehigh, SUNY/Albany collaboration.

Channeling, the behavior of charged particles moving through the planes and rows of aligned single crystals, has been much studied in connection with many solid state and nuclear processes at low energies. Experiment #507 has studied channeling at Fermilab energies, where the de-channeling lengths are so long that thick single crystals may be used, and where many different particles, including negative particles other than electrons, are available. Both of these factors permit significant extensions of channeling experiments.

The apparatus for Experiment #507, which was located in the M1 beam line, consisted essentially of a germanium single crystal and its associated goniometer along with position detectors fore and aft of the goniometer (drift chamber planes from Experiment #456) to measure the trajectories of the particles.

G. Experiments Presently in Progress

Low Momentum Transfer Hadron Physics

G.1 Experiment #110 - Study of Multiparticle Peripheral Physics at NAL; by a Caltech, Fermilab, UCLA, UICC, Indiana collaboration.

This experiment is one of the two initial experiments being done with the recently-commissioned Multiparticle Spectrometer (MPS) located at the downstream end of the M6W beam line. (The other early experiment with the MPS is Experiment #260, see page 47).

The objective of Experiment #110 is to make an initial survey of those multiparticle processes which are easiest to measure (e.g., processes where no neutral pions are produced), which nevertheless span a wide range of strong interaction problems. It was planned to isolate specific reaction channels in order to study the s and t dependences of the cross sections for peripheral processes, search for new resonant states, measure π-π and K-π elastic and inelastic scattering, and study the properties of high multiplicity events.

G.2 Experiment #396 -- Elastic Scattering and Diffraction Dissociation at Small Momentum Transfer for $\pi^{\pm}$, $K^{\pm}$, $p^{\pm}$ on p and n; by a Rockefeller collaboration.

A simple apparatus is used in this experiment to measure the energy, angle and identity of the recoil p or d at small t from a gas target. The recoil detector labels each diffractively produced state with M_x, $|t|$, and $\hat{n}$, the normal to the production

plane, for study by downstream apparatus. The experiment is located in the M6W beam line.

In Phase I of the experiment, a simple downstream detector is used, to record the number and angles of the charged particles and γ-rays. In Phase II, the experimenters plan to add a magnet and lead glass (or calorimeter) detectors for energy determination in the downstream area.

In addition to the $\frac{d^2\sigma}{dm_X^2 \cdot dt}$ measurements, Experiment #396 also plans to measure $d\sigma/dt$ for elastic scattering in the range $0.01 \lesssim -t \lesssim 0.12$ GeV^2, thus giving a measurement of the ratio of the real to the imaginary amplitudes in the forward direction.

G.3 Experiment #383 - Study of the Inclusive Production of K_S^0 by K^- on Hydrogen; by an MSU, UCSD collaboration.

The objective of Experiment #383 is to measure the inclusive cross section $\frac{d^2\sigma}{dx \cdot dt}$ for the reaction $K^- p \rightarrow K_S^0 X$ with incident kaons of 20-150 GeV/c. The experiment will study the triple-Regge region of the x, t plane ($0.8 < x < 1$, $0 < -t < 3$ GeV^2), and the results will be compared with triple-Regge theory. Only ρ and A_2 exchange should be present in the reaction studied, so the analysis of results should be quite straightforward. By imposing additional constraints -- SU_3 symmetry, and factorization -- one can make direct comparison with the production of π^0 and η by π^-.

The experiment will use the newly installed charged-particle configuration of the M4 beam line. The K_S^0 will be detected by the $\pi^+\pi^-$ decay mode in a pair spectrometer similar to that used in the K_S^0 regeneration experiment #82/425.

G.4 Experiment #290 - Backward Pion-Proton Elastic Scattering; by a Fermilab, Arizona collaboration.

It is planned to measure the backward scattering of π^+ and π^- mesons on hydrogen at 10, 50 and 80 (or 100) GeV/c in the angular range $-0.8 < u < 0$ GeV^2. The experiment is located in the M6W beam line.

The principal objective of the experiment is to survey the energy and angular dependences of the elastic differential backward cross sections. Both the π^- and π^+ measurements will yield tests of Regge pole models in situations where only one or two specific trajectories may be exchanges -- Δ_δ in $\pi^- p \to p\pi^-$, Δ_δ and N_α in $\pi^+ p \to p\pi^+$. The previously available high energy data disagree with Regge pole model predictions.

G.5 Experiment #404 - Inclusive Neutron Production by Protons on Protons and Nuclei; by a Michigan collaboration.

Experiment #404 plans to study the inclusive production of neutrons in the reaction $p + p \to n + X$ at either 300 GeV or 400 GeV, or both energies, using the diffracted proton beam in the M2 beam line. The physics studied will be the character of the exchange processes at the projectile proton vertex.

An ionization calorimeter neutron detector will be used to detect the neutrons and to measure their energies. The neutron production angle relative to the incident proton direction can be varied over the range 0-10 mrad by appropriate aiming of the incident proton beam on the production target.

This experiment runs parasitically on the experiments which

utilize the Hyperon Facility at the end of the M2 beam line.

G.6 Experiment #441 - Polarization in the Reaction $pp \rightarrow \Lambda^0$ + Anything, with a Liquid Hydrogen Target; by a Wisconsin, Rutgers, Michigan collaboration

In Experiment #441, a 50 cm-long liquid hydrogen target will be installed as the hyperon production target at the end of the M2 beam line. The experiment will study Λ^0 polarization in pp collisions with 400 GeV protons. Measurements of $\underline{P}_\Lambda(x,p_T)$ have already been made in p + Be collisions by Experiment #8 (see page 28) with sufficient accuracy to establish firmly the polarization effect. In order to learn more about the physical process which causes the polarization, it is necessary to use a proton target, and to extend the range of p_T which is studied.

G.7 Experiment #118 - Hadron Spectra from High Energy Interactions; by a Bari, Brown, Fermilab, MIT collaboration

Experiment #118 is studying inclusive reactions of the type

$$a + p \text{ (or n)} \rightarrow b + X,$$

where a is p, $\bar{p}$, K^-, π^+, π^-, and b = any of the above particles and is the particle which is detected.

The overall objective of the experiment is to map out the general behavior of these reactions over as wide a range of the kinematical variables as possible, concentrating on those reactions which cannot be measured at the CERN-ISR.

The incident particle momenta will be $\pm$ 50, $\pm$ 100, and $\pm$ 175 GeV/c, and the range of transverse momentum covered will be $0 \lesssim p_T \lesssim 1.5$ GeV/c.

The experiment utilizes the Fermilab Focusing Spectrometer Facility in the M7E beam line. In addition, the target is surrounded by detectors, the purpose of which is to study the correlation of the inclusive cross sections with charged particle multiplicities.

A DISC Counter, a differential and a threshold Cerenkov counter are used in the incident beam, and three threshold Cerenkov counters and one differential Cerenkov counter in the spectrometer. These counters permit the simultaneous measurement of different reactions.

Large Transverse Momentum Hadron Physics

G.8 Experiment #236 - Exploration of the Large p_T Domain -- Inclusive Cross Sections and Possible Jet Structures; by a Washington, Fermilab collaboration.

Experiment #236 utilizes a large aperture magnetic spectrometer, followed by three segmented threshold Cerenkov counters. The spectrometer was designed to study the charged particle components of large p_T events; it covers the c.m. angular region from 45° to 110°, and is complemented by a segmented photon and hadron calorimeter on the recoil side. The calorimeter covers an angular region of 60° to 135° in the c.m. frame. The experiment is located in the M1 beam line.

The physics objectives of Experiment #236 are as follows:

a) High statistics measurements of the single particle inclusive cross sections above p_T = 2 GeV/c, using incident $\pi^{\pm}$, $K^{\pm}$, and $p^{\pm}$.

b) Search for hadron-jets associated with the large-p_T events.

c) Observe the recoil structure opposite the large-p_T particle (or jet) with the (large acceptance) photon and hadron calorimeter.

d) Observe the rapidity distribution of all charged particles accompanying the large-p_T events.

G.9 Experiment #439 - High Sensitivity Search for New States Which Decay Into Muons; by a Northeastern collaboration.

This is an experiment to measure the reaction p + Fe → muons + anything, in order to search for new states up to 25 GeV in mass which decay into two or more muons. A "beam dump" method is used with a beam of 400 GeV protons at an intensity of $\sim 10^{10} - 10^{1}$ protons/pulse in the M2 beam line. The experiment utilizes a pencil beam, magnetized iron and proportional chambers to determine muon angles and momenta and hence the effective mass of the muons detected in each event. Processes with cross sections as low as $\sigma.B \sim 10^{-40}$ cm^2 per nucleon will be studied.

G.10 Experiment #395 - Calorimeter-Array Study of High p_T Events; by a Fermilab, Lehigh, Penn, Wisconsin collaboration.

Experiment #395 is studying high-p_T events produced by pions and protons using a segmented pair of calorimeters; the experiment is located in the M2 beam line. In general, the objective is to study both single- and multiparticle high-p_T events. More specifically, Experiment #395 plans to measure the following quantities:

a) The frequency of high-p_T clusters of particles relative to single-particle high-p_T events.

b) Total-p_T dependence of the cross section, for such clusters.

c) Some angular correlation information from the two-arm calorimeter system.

H. Approved Experiments Which Have Not Yet Been Installed

Low Momentum Transfer Hadron Physics

H.1 Experiment #99 - Study of $\pi^+p \to K^+\Sigma^+$ and $\pi^+p \to K^+Y^{*+}$ Using the Focusing Spectrometer Facility; by an ANL, Fermilab, Stanford, SLAC, Wisconsin collaboration.

In Experiment #99 the Single Arm Spectrometer Facility in the M6E beam line will be used to detect K^+ mesons produced in association with Σ^+,Y^* (1385) and Y^*(1670) by π^+p interactions. The s and t depndences of these reactions will give information on K^* exchange as well as on the importance of Regge cuts at high energies.

These reactions will be studied at five incident momenta from 30 to 200 GeV/c and for momentum transfers up to -0.8 GeV^2. The recoil baryon will be identified by the missing mass technique; Cerenkov counters in the incident pion beam and in the spectrometer will be used to achieve the required particle identification.

The line-reversed reactions such as $K^-p \to \pi^-\Sigma^+$ will also be studied at one or two momenta.

H.2 Experiment #272 - Study of the Coherent Dissociation of π, K and p into Strange Particles at NAL Energies; by a Fermilab, Minnesota, Rochester collaboration.

The objective of this experiment, to be done in the M1 beam line, is to investigate with high statistics, the dependence of the cross sections on mass, momentum transfer, nuclear target and energy, for the following two-body dissociation reactions:

$$\pi^- \to \pi^-\pi^0$$

$$\pi^- \to K^-K_S^0$$

$$K^- \to K^-\pi^0$$

$$K^0 \to K_S^0\pi^-$$

$$K^- \to \Lambda\bar{p}$$

$$\bar{p} \to \bar{\Lambda}K^-$$

The decay angular distributions and the $\Lambda(\bar{\Lambda})$ polarization will also be measured. This experiment will provide new information on radiative widths (from the Coulomb dissociation events) and will probe in detail the nature of the Pomeron trajectory in the inelastic regime. The experiment will utilize a drift chamber spectrometer system in conjunction with a high-precision π^0 detector.

H.3 Experiment #451 - Study of the A-Dependence of Inclusive Processes and Associated Multiplicity; by a Bari, Brown Fermilab, MIT, Warsaw collaboration.

Experiment #451 will study the A-dependence of inclusive reactions over a wide range of kinematical variables, using the M6E Focusing Spectrometer Facility along with a detector of π^0's which are produced at large p_T. The multiplicity detector of Experiment #118 will be used to obtain the associated charged particle multiplicity and the pseudo-rapidity distribution associated with each event. The π^0 detector will consist of an array of lead-glass detectors, preceded by a shower hodoscope of lead-scintillator construction.

The principal objective of Experiment #451 is to explore

inclusive reactions over a wide range of A, x, and p_T. Cronin, et al., and Lederman, et al., have shown that the A-dependence of the inclusive π^0 cross section increases from $A^{2/3}$ to $A^{4/3}$ in going from $p_T \sim 0$ to $p_T \sim 4$ GeV/c, in clear disagreement with current theoretical models. Experiment #451 will be able to measure the correlation of this phenomenon with the associated multiplicity and incident particle type.

H.4 Experiment #495 - Study of Ξ^0 and $\bar{\Lambda}^0$ Production and Polarization; by a Michigan, Rutgers, Wisconsin collaboration.

Experiment #495 plans to measure the production spectrum and polarization of the Ξ^0 and $\bar{\Lambda}^0$ hyperons produced in the inclusive reactions $p + N \rightarrow \Xi^0 + X$ and $p + N \rightarrow \bar{\Lambda}^0 + X$, in the kinematic region $0 \leq p_T \leq 1.6$ GeV/c, $0.2 \leq x \leq 0.8$, for the produced hyperons. The experiment will be done at a proton energy of 400 GeV.

The discovery by Experiment #8 that 300 GeV protons can produce Λ^0's which are strongly polarized (see page 28),

$$[\underline{P}_\Lambda] = 0.15 \pm 0.01$$

for Λ's with $p_T > 0.8$ GeV/c, has motivated the experimenters to investigate the polarization of other accessible neutral hyperons produced by high energy protons. If a substantial polarization is found, then the magnetic moments of the Ξ^0 and $\bar{\Lambda}^0$, previously unmeasured, will be determined.

The experiment will be done by using the Hyperon Facility built by the Experiment #8 group at the end of the M2 beam line.

Search for New Particles

H.5 Experiment #490 - Search for Short-Lived Particles Using a High Resolution Streamer Chamber; by a Yale, Fermilab collaboration.

The object of Experiment #490 is to search for new short-lived particles produced in hadronic collisions in a manner which is independent of decay mode, with $\sim 4\pi$ geometry and with a sensitivity such that cross sections comparable to those for ψ/J production would be successfully detected.

Using a small triggered high resolution (< 10μm) high pressure streamer chamber, currently under construction at Yale, Experiment #490 expects to be able to observe directly particles with lifetimes as short as 2.5×10^{-14} sec. If such particles exist, the experimenters would expect to measure their lifetimes, decay multiplicities, semi-leptonic branching ratios and production cross sections. They would also observe phenomena associated with the production of these particles such as associated production or pair production, the topological and kinematical character of the events in which the new particles are produced, and any new "short time" phenomena associated with the new particles (such as decays of new heavy mesons into heavy leptons). If such particles do not exist, the experiment will set an upper limit on $\sigma.B$ for semi-leptonic decays of $\sim$ 10 to 50 nb for lifetimes from 2×10^{-14} sec to 5×10^{-13} sec.

The experiment will be located in the M6W beam line.

H.6 Experiment #515 - Study of Charmed Particles Produced In Hadronic Interactions; by a Carnegie-Mellon, Fermilab, Northwestern collaboration.

This experiment was proposed as a study of charmed particles produced in hadron-nucleon interactions, using a prompt muon trigger. The method capitalizes on the associated production of charmed particles and uses the semi-muonic decay of one member of the pair to trigger the detector.

A preliminary analysis (unpublished) of the recently completed Experiment #397 suggests that the charm search was sensitive to charm production at the 10μb level. However, the spectrometer of Experiment #515 will have a sensitivity to charm production at the 0.1μb level. Based on this, the experimenters hope that their new experiment will be sufficient not only to identify particular states, but also to provide detailed measurements of production and decay distributions.

The detector for Experiment #515 will employ a muon trigger arm of heavimet, steel, and magnetized iron, instrumented with counter hodoscopes and proportional chambers. The detector also includes a large-acceptance high-resolution spectrometer. The spectrometer includes analysis magnets, a trigger hodoscope, proportional chambers, a shower detector for electron and neutral particle detection, also a Cerenkov counter system capable of separating $\pi/K/p$ in the range 10-50 GeV/c. Final state Vees can be reconstructed in the spectrometer.

The detector will be placed in a charged-particle beam (M1) of intensity $\gtrsim 10^7$ per pulse.

H.7 Experiment #468 - Search for Penetrating Massive Neutral Particles Produced in High Energy Proton Collisions; by a Maryland collaboration.

Experiment #468 is a search for long-lived neutral heavy leptons produced in high energy proton interactions in a beam dump--the hyperon beam magnet used by Experiment #8 at the end of the M2 beam line. The strong magnetic field will sweep out most of the penetrating muons arising from the hadronic showers. The heavy leptons would be detected through their decays in a decay region downstream of the magnet.

With the M2 beam tuned to 400 GeV protons and with an intensity of 10^9 protons/pulse, the sensitivity of the experiment would be 10 events per hour per nanobarn of (cross sections x branching ratio x detection efficiency).

H.8 Experiment #354 - Survey for Exotic Particles in the M1 Beam; by a Rockefeller, Fermilab collaboration

Experiment #354 will study the production of $\bar{d}$, $\bar{t}$, $\overline{He}^3$, and will search for $\overline{He}^4$ and heavy mass particles with charges -1 and -2, and will also search for heavy, quasi-stable leptons. The apparatus consists of the equipment for Experiment #104, which will have a final run in the M1 beam line in the fall of 1977. Especially important to the successful operation of Experiment #354 will be the two BNL differential Cerenkov counters which will be used for the experiment.

Measurement of Fundamental Properties of Hadrons

H.9 Experiment #533 - Measurement of the Rate of Formation of π-μ Atoms in $K_L^0 \to \pi\mu\nu$ Decay; by a Chicago, Stanford, Wisconsin collaboration.

Experiment #533 will measure the branching ratio:

$$R = \frac{K_L^0 \to (\pi\mu)_{Atom}\nu}{K_L^0 \to \pi\mu\nu}$$

in a K_L^0 beam (M3). The previous measurement of R, at BNL, found R to be too low by a factor ≈ 5 relative to theoretical calculations. Clearly, a confirmation of this discrepancy would be suggestive of an anomalous interaction between π and μ.

The proposed apparatus set-up calls for modifications to the M3 beam line, to widen its aperture to $\approx$ 6" x 18" at the apparatus (a V-spectrometer with proportional chambers and 3 large analysis magnets). The experimenters will record π-μ events from ordinary $K_{\mu 3}$ decays and from atomic decays simultaneously, with atoms stripped in a thin foil located just outside of the neutral beam.

I. Experiments Completed More Than a Year Ago, And With No Published Results Yet

I.1 Experiment #51 - Mass Spectrum and Decay Modes for Bosons with Masses up to 15 GeV; by a Northeastern collaboration.

This was a "missing mass" spectrometer experiment to study the spectrum of hadrons produced in the reactions

$$\pi (K \text{ or } p) + N \rightarrow N + X$$

for momentum transfers $\sim 0.2 < -t < 0.4$ GeV^2, at beam momenta up to 200 GeV/c. Measurement of the missing mass "background" over the large range of s and M_X^2 should provide data to test some current ideas about inclusive reactions. The experiment was carried out in the M2 beam line.

I.2 Experiment #86 - Study of Inelastic Diffractive Processes by Observing Coherent Production of Multi-Pion Final States from He Nuclei; by a Washington, Orsay collaboration.

This experiment was designed to measure the quantities $\frac{d^2\sigma}{dtdm^2}$, the average multiplicity of charged particles, and the momentum spectrum of the secondaries below 20 GeV, in the diffractive dissociation reaction $\pi^- + He \rightarrow He + X^-$, using a helium-filled streamer chamber as the target as well as the detector of the recoiling helium nucleus. The object of this experiment is to provide data to check the predictions of various diffractive and triple-Regge models. The experiment was performed in the M1 beam line.

I.3 Experiment #69 - Elastic Scattering of the Long-Lived Hadrons; by a Yale, Fermilab collaboration.

The principal objective of Experiment #69 was to measure the elastic and near-elastic scattering of the charged long-lived hadrons on hydrogen and a number of selected heavy nuclei in the small-angle region (θ_{lab} = 0.2 to 24 milliradians is the range actually studied). About 10^5 elastic scattering events were obtained at each of several energies from 50 to 200 GeV, for pions of both signs and also for protons. This would make possible a determination of the ratio of the real part to the imaginary part of the forward scattering amplitude, by measurement of the nuclear-Coulomb interference, to an accuracy of about $\pm$ 0.01. Measurements with $K^{\pm}$ and $\bar{p}$ would be somewhat less precise since the number of events was about a factor of 2 less for these particles. The data on nuclei, made possible by the high angular resolution of the experimental set-up, would allow accurate measurement of the hadron-nuclear elastic scattering cross sections.

The detector system for Experiment #69 consisted of a high resolution ($\sim$ 70μm) proportional chamber system to determine the scattering angle and a high resolution proportional chamber magnetic spectrometer to provide a measurement of the elasticity of the events. Data from the high resolution chambers were immediately encoded and used in the trigger to define scattered particles. The experiment was located in the M6W beam line.

IV. Summary and Conclusions

A wide variety of experiments have been understaken in the Meson Lab in its brief history to date.

In the field of strong interactions at relatively small momentum transfers ($p_T \lesssim 1$ GeV/c), the "traditional" hadron physics of the kind which had been previously been done at the CERN-PS and at the BNL-AGS has been carried out fairly thoroughly at Fermilab--and largely in the Meson Laboratory. This includes several technically excellent experiments which have produced results of great interest, for example:

The measurements of Experiment #104, which have provided details of total cross sections rising with energy for a number of incident hadrons;

The comprehensive elastic scattering and single-particle inclusive production measurements of Experiment #96, providing a clear phenomenological picture -- mostly interpretable by Regge theory -- of those processes;

The charge exchange data of Experiment #111, which provided clearcut evidence for the validity of one-pole-exchange Regge theory in describing the reaction $\pi^- p \to \pi^0 n$.

The first results from Experiment #82 -- on $K_L^0 \to K_S^0$ regeneration by carbon, which showed similarly clearcut evidence for the validity of one-pole exchange Regge theory; and

Experiment #178, a simple but elegant experiment which has revealed a certain simplicity in the growth of a high energy particle cascade inside a nucleus which is consistent with the Energy Flux Cascade Model of Gottfried.

There are several connections between these results -- relating

the difference between $\pi^- p$ and $\pi^+ p$ total cross sections (Experiment #104) to the forward charge exchange cross sections (Experiment #111), relating the difference between $K^+ d$ and $K^- d$ total cross sections (Experiment #104) to coherent regeneration of K_L^0 into K_S^0 (Experiment #82); relating the forward differential elastic hadron-nucleon cross sections (Experiment #96) to the corresponding total cross sections (Experiment #104). The consistency between the results of all these experiments is excellent.

A number of interesting experiments have been undertaken to study phenomena at larget p_T ($\gtrsim$ 1 GeV/c):

A major result is the discovery, by the Experiment #8 group, that there is a substantial polarization in the inclusive production of Λ^0's at large $p_T \sim$ 1-2 GeV/c. The mechanism whereby the polarization is produced is not yet understood--perhaps it is due to interference between K* and K** exchanges as in the triple Regge theory--and continues to be studied. Also, the large polarization is being exploited, to make a precision measurement of the Λ^0 magnetic moment;

The Experiment #268 group has measured π^0 production at large p_T up to 4 GeV/c, and has obtained data which are consistent with naïve ideas of quark-parton constituents of hadrons, and which are in agreement with the quark-quark hard scattering model of Field and Feynman;

Data are just beginning to become available from two experiments which are studying hadron jet phenomena (#236 and #260). The study of hadron jets promises to be a vigorous activity in the next year or two.

Searches for direct evidence of new particles, such as quarks,

charmed particles, and maybe others, can be summarized very briefly -- nothing has yet been found. However, the search for the hadronic production of charm continues in the Meson Lab (major efforts will be undertaken by Experiments #490 and #515).

Finally a number of measurements have been made of fundamental properties of hadrons. A precision measurement of the Λ^0 magnetic moment has been undertaken by the Experiment #8 group. Also, the pion and kaon electromagnetic radii have been measured (Experiments #216 and #456) by direct scattering off electron targets -- these measurements are the most precise yet made anywhere.

The Meson Lab research program has been rich in variety. No spectacular discoveries have been made -- but many important results have been obtained. The emphasis has been shifting -- from "traditional" hadron physics at the beginning, five years ago, to such current topics as fundamental properties of hadrons, hadron jets and hadronic production of new particles. In another five years or so, with 1,000 GeV protons expected to be available, the emphasis of the program will surely shift once again.

Acknowledgments

Many physicists, too numerous to mention, have helped with comments and suggestions on my brief summaries of the results of their own experiments; my thanks go to them all. I would like to thank C. Quigg and J.R. Orr for reading the entire manuscript, and making a number of helpful suggestions. Most of all, it is a pleasure to thank J. Peoples and H. Miettinen for their careful reading of the manuscript and for providing many detailed, critica comments on the text. I wish also to thank Nancy Patterson and Shirley Rittierodt for their assistance in the preparation of this paper.

BIBLIOGRAPHY

Below is a list of all papers published to date or submitted for publication on the results of the experiments discussed in this report.

A. Low Momentum Transfer Hadron Physics

Total Cross Sections of Hadrons on Hadrons

A.1. Experiment #104: Measurements of Total Cross Sections on Hydrogen and Deuterium; by a Rockefeller-BNL-Fermilab-Washington-Munich-Padua collaboration.

A. S. Carroll, et al., "Total Cross Sections of p and $\bar{p}$ on Protons and Deuterons Between 50 and 200 GeV/c", Phys. Rev. Letters 33, 928(1974).

A. S. Carroll, et al., "Total Cross Sections of $\pi^{\pm}$ and $K^{\pm}$ on Protons and Deuterons Between 50 and 200 GeV/c", Phys. Rev. Letters 33, 932(1974).

A. S. Carroll, et al., "Total Cross Sections of $\pi^{\pm}$, $K^{\pm}$, p and $\bar{p}$ on Protons and Deuterons Between 23 and 280 GeV/c", Phys. Rev. Letters 61B, 303(1976).

A.2. Experiment #4: Neutron Total Cross Sections up to 300 GeV; by a Michigan-LBL collaboration.

M. J. Longo, et al., "Neutron-Proton Total Cross Sections from 30 to 280 GeV/c", Phys. Rev. Letters 33, 725(1974).

L. W. Jones, et al., "Neutron Total Cross Sections on Nuclei from 30 to 270 GeV/c", Phys. Rev. Letters 33, 1440(1974).

P. V. R. Murthy, et al., "Neutron Total Cross Sections on Nuclei at Fermilab Energies", Nuclear Physics B92, 269(1975).

A.3. Experiment #27/305: Neutron-Nuclear Total Cross Sections; by a Fermilab-Northwestern-Rochester-Massachusetts collaboration.

J. Biel, et al., "Neutron-Nuclear Total Cross Sections Between 30 and 300 GeV/c", Phys. Rev. Letters 36, 1004(1976).

Elastic Scattering of Hadrons by Hadrons

A.4. Experiment #96: Elastic Scattering of Hadrons on Hydrogen and Deuterium; by an ANL-Bari-Brown-CERN-Cornell-MIT-Fermilab-Northeastern-Stanford collaboration.

D. S. Ayres, et al., "Measurement of Elastic Scattering of Hadrons on Protons from 50 to 175 GeV/c", Phys. Rev. Letters 35, 1195(1975).

D. S. Ayres, et al., "Comparison of the Shapes of π^+p and pp Diffraction Peaks from 50 to 175 GeV/c", Phys. Rev. Letters 37, 548(1976).

R. L. Anderson, et al., "Elastic Scattering Crossovers from 50 to 175 GeV/c", Phys. Rev. Letters 37, 1025(1976).

D. S. Ayres, et al., "Impact Parameter Analysis of Elastic Scattering from 50 to 175 GeV/c", Phys. Review 14D, 3092(1976).

D. S. Ayres, et al., "$\pi^{\pm}p$, $K^{\pm}p$, pp and $\bar{p}p$ Elastic Scattering from 50 to 175 GeV/c", Phys. Review 15D, 3105(1977).

A.5. Experiment #7: $\pi^{\pm}p$ and p-p Differential Elastic Scattering Cross Sections from 20 to 200 GeV; by a Michigan-ANL-Fermilab-Purdue collaboration.

C. W. Akerlof, et al., "Observation of Structure in Elastic pp Scattering at 100 and 200 GeV/c", Phys. Letters 59B, 197(1975)

C. W. Akerlof, et al., "Elastic Scattering of Hadrons at 50 to 200 GeV/c", Phys. Rev. Letters 35, 1406(1975).

C. W. Akerlof, et al., "Hadron-Proton Elastic Scattering at 50, 100, and 200 GeV/c Momentum", Phys. Review 14D, 2864(1976)

A.6. Experiment #61: Polarization in pp, π^-p, and π^+p Elastic Scattering at 100 and 300 GeV/c; by an ANL-Harvard-LBL-Fermilab-Yale collaboration.

I. P. Auer, et al., "Measurement of the π^+p and π^-p Polarization Parameters at 100 GeV/c", Phys. Rev. Letters 39, 313(1977).

Charge Exchange and K^0 Regeneration Experiments

A.7. Experiment #111: Study of $\pi^-p \to \pi^0n$ and $\pi^-p \to \eta n$ at High Energy; by a Caltech-LBL collaboration.

A. V. Barnes, et al., "Pion Charge-Exchange Scattering at High Energies", Phys. Rev. Letters 37, 76(1976).

O. I. Dahl, et al., "Reaction $\pi^-p \to \eta n$ at High Energies", Phys. Rev. Letters 37, 80(1976).

O. I. Dahl, et al., "Reaction $\pi^-p \to \omega n$ at the Momenta from 20 to 200 GeV/c", Phys. Rev. Letters 38, 54(1977).

A.8. Experiment #82/425: Regeneration of Neutral K Mesons at Very High Energies; by a Chicago-SLAC-UCSD-ETH/Zurich-Wisconsin collaboration.

J. Roehrig, et al., "Coherent Regeneration of K_s's by Carbon as a Test of Regge-Pole-Exchange Theory", Phys. Rev. Letters 38, 1116(1977).

A.9 Experiment #12: A Study of Neutron-Proton Charge-Exchange Scattering in the Momentum Range 50-300 GeV/c; by an Ohio State-Michigan State-Carleton collaboration;

H.R. Barton, Jr., et al., "n-p Charge Exchange Scattering from 60 to 300 GeV/c", Phys. Rev. Letters 37, 1656(1976)

Inclusive Particle Production

A.10 Experiment #8: Λ^0 Polarization in Inclusive Production; by a Wisconsin-Rutgers-Michigan collaboration.

G. Bunce, et al., "Λ^0 Hyperon Polarization in Inclusive Production by 300 GeV Protons on Beryllium", Phys. Rev. Letters 36, 1113(1976).

T. Devlin, et al., "Inclusive Production of Neutral Strange Particles at 300 GeV: Triple-Regge Behavior", Nucl. Physics 123B, 1(1977).

K. Heller, et al., "Inclusive Polarization of Λ^0 Hyperons by 300 GeV Protons: A-Dependence", (submitted to Physical Review).

A.11 Experiment #96: Inclusive Particle Production; by an ANL-Bari-Brown-CERN-Cornell-MIT-Fermilab-Northeastern-Stanford collaboration.

R.L. Anderson, et al., "Inclusive Hadron Scattering at 50-175 GeV/c", Phys. Rev. Letters 37, 1111(1976).

D.S. Ayres, et al., "Inclusive Diffractive Scattering at Energies of 140 to 175 GeV/c", Phys. Rev. Letters 37, 1724(1976).

R.L. Anderson, et al., "Inclusive Hadron Scattering from 50-175 GeV/c", Phys. Rev. Letters 38, 880 (1977).

A.12 Experiment #324: Single-Particle Spectra in High-Energy Collisions of Charged Hadrons; by a Pennsylvania collaboration.

E.W. Beier, et al., "Experimental Tests of Pomeron Factorization in Single-Particle Inclusive Hadron Scattering", Phys. Rev. Letters 37, 1120(1976).

Diffraction Dissociation

A.13 Experiment #27/305: Coherent Dissociation of Neutrons;by a Rochester-Fermilab-Northwestern-Massachusetts collaboration.

J. Biel, et al., "Features of Diffraction Dissociation of Neutrons in np Collisions at 50-300 GeV/c", Phys. Rev. Letters 36, 504(1976).

J. Biel, et al., "Decay Properties of $p\pi^-$ Systems Produced in Neutron Dissociation at 50-300 GeV/c", Phys. Rev. Letters 36, 507(1976).

J. Biel, et al., "Structure in Momentum Transfer for ($p\pi^-$) Systems Produced in Diffractive Dissociation of Neutrons on Protons", Phys. Letters 65B, 291(1976).

Inelastic Collisions of Hadrons with Nuclei

A.14 Experiment #178: A Study of the Average Multiplicity and Multiplicity Distribution in Hadron-Nucleus Collisions at High Energies; by a MIT-Carleton-Fermilab collaboration.

W. Busza, et al., "Charged-Particle Multiplicity in π^--Nucleus Interactions at 100 and 175 GeV/c", Phys. Rev. Letters 34, 836(1975).

C. Halliwell, et al., "Energy Dependence of Pseudorapidity Distributions in Proton-Nucleus Collisions Between 50 and 200 GeV/c", Phys. Rev. Letters 39, 1499(1977).

C. Halliwell, et al., "Comparison of Pseudorapidity Distributions in Proton-, Antiproton-, Kaon- and Pion-Nucleus Collisions Between 50 and 200 GeV/c", (submitted to Phys. Rev. Letters).

B. Large Transverse Momentum Hadron Physics

B.1 Experiment #268: Study of Meson Production at Large p_T with a γ-Ray Detector; by a Caltech-LBL collaboration.

G. Donaldson, et al., "Inclusive π^0 Production at Large Transverse Momentum from $\pi^{\pm}p$ and pp Interactions at 100 and 200 GeV/c", Phys. Rev. Letters 36, 1110(1976).

B.2 Experiment #260: A Study of High-p_T Physics with a Multiparticle Spectrometer; by a Caltech-UCLA-UICC-Indiana-Fermilab collaboration.

B. Bromberg, et al., "Observation of the Production of Jets of Particles at High Transverse Momentum and Comparison with Inclusive Single Particle Reactions", Phys. Rev. Letters 38, 1447(1977).

C. Searches for New Particles

Searches for Quarks

C.1 Experiment #72: Quark Search at Fermilab; by a Yale-BNL collaboration.

L.B. Leipuner, et al., "Search for Quarks and Heavy Stable Particles Produced at 300 GeV", Phys. Rev. Letters 31, 1226(1973).

C.2 Experiment #75: Search for Fractionally Charged Quarks; by a NTY-Fermilab collaboration.

T. Nash, et al., "Search for Fractionally Charged Quarks Produced by 200- and 300-GeV Proton-Nuclear Interactions", Phys. Rev. Letters 32, 858(1974).

C.3 Experiment #330: Search for Massive Neutral Particles; by a Michigan collaboration.

H. R. Gustafson, et al., "Search for New Massive Long-Lived Neutral Particles", Phys. Rev. Letters 37, 474(1976).

Search for Charmed Particles

C.4 Experiment #357/472: Search for Charmed Particles; by a Fermilab-Michigan-Purdue collaboration.

D. Bintinger, et al., "Limits on Charmed-Particle Production in Proton-Nucleus Collisions at 400 GeV/c", Phys. Rev. Letters 37, 732(1976).

W.R. Ditzler, et al., "New Limits on D^0(1.865) Production in Proton-Nucleus Collisions at 400 GeV/c", Phys. Letters 71B, 451(1977).

C.5 Experiment #305: Search for Narrow Resonances Produced by Neutron Dissociation; by a Fermilab-Massachusetts-Northwestern-Rochester collaboration.

E. J. Bleser, et al., "Search for Narrow Resonances Produced by Neutron Dissociation", Phys. Rev. Letters 35, 76(1975).

C.6 Experiment #366: Study of Heavy, Narrow Mesons Using a Mass Focusing Spectrometer; by a Michigan State-Ohio State-Carleton-Fermilab collaboration.

M. A. Abolins, et al., "Search for Narrow Two-Body Enhancements at Fermilab", Phys. Rev. Letters 37, 417(1976).

C.7 Experiment #416: Streamer Chamber Search for New States Which Decay Semi-Leptonically; by a Washington-Orsay-UC/Davis collaboration.

V. Cook, et al., "Search for Correlated Neutral Strange Particles and Muon Production in $\pi^- p$ Interactions at 225 GeV", Phys. Letters 64B, 221(1976).

A.M. Jonckherre, et al., "Study of Final States in $\pi^- N \rightarrow \mu^+\mu^-$ + Hadrons at 225 GeV", (Physical Review, to be published).

C.8 Experiment #365: Search for Forward Production of Massive States Which Decay with Muon Emission; by a Northeastern collaboration.

G.J. Blanar, et al., "Search for Forward Production of Massive States Which Decay with Muon Emission", Phys. Rev. Letters 38, 192(1977).

D. Measurements of Fundamental Properties of Hadrons

D.1 Experiment #216: A Measurement of the Pion-Form Factor by Direct Pion Electron Scattering; by a UCLA-Pittsburgh-Notre Dame-Fermilab collaboration.

E. Dally, et al., "Measurement of the Pion Form Factor," Phys. Rev. Letters 39, 1176(1977).

E. Other Experiments

E.1 Nuclear Emulsion, Nuclear Chemistry, and Applied Radiation Physics Experiments.

(Since these experiments were not discussed individually in this Report, we do not give a list of references to publications of their results in this bibliography. See Ref. #73 for a list of these experiments.)

E.2 Experiment #22: A Search for Multigamma Events from Magnetic Monopole Pairs; by a Virginia Polytechnic Institute-BNL collaboration.

D.M. Stevens, et al., "Search for Multi-Photon Events from Proton-Nuclei Interactions at 300 GeV/c", Phys. Rev. 14D, 2267(1976).

E.3 Experiment #230: A Search for "Schein Events" and Events with a High Multiplicity of γ's; by a Michigan collaboration.

D.L. Burke, et al., "Search for Anomalous Multi-Photon Production at 100-300 GeV", Phys. Letters 60B, 113(1975).

REFERENCES

1. J.R. Orr and A.L. Read, "Meson Laboratory Preliminary Design Report", Fermilab Report, March (1971).
2. S.P. Denisov, et al., Phys. Lett. 36B, 415(1971); Phys. Lett. 36B, 528(1971); Nucl. Phys. B65, 1(1973); V.D. Apokhin, et al., paper 7-86, Proc. XVII International Conference on High Energy Physics, London (1974), ed. J.R. Smith.
3. U. Amaldi, et al., Phys. Lett. 44B, 112(1973); S.R. Amendolia, et al., Phys. Lett. 44B, 119(1973).
4. A.S. Carroll, et al., Phys. Rev. Lett. 33, 928(1974); Phys. Rev. Lett. 33, 932(1974); Phys. Lett. 61B, 303(1976).
5. R.J. Glauber, Phys. Rev. 100, 242(1955); C. Wilkin, Phys. Rev. Lett. 17, 561(1966).
6. R.E. Hendrick, et al., Phys. Rev. D11, 536(1975), and references therein.
7. M.J. Longo, et al., Phys. Rev. Lett. 33, 725(1974).
8. L.W. Jones, et al., Phys. Rev. Lett. 33, 1440(1974); P.V.R. Murthy, et al., Nucl. Phys. B92, 269(1975).
9. J. Biel, et al., Phys. Rev. Lett. 36, 1004(1976).
10. D.S. Ayres, et al., Phys. Rev. Lett. 35, 1195(1975); D.S. Ayres, et al., Phys. Rev. Lett. 37, 548(1976). R.L. Anderson, et al., Phys. Rev. Lett. 37, 1025(1976); D.S. Ayres, et al., Phys. Rev. Lett. 14D, 3092(1976); D.S. Ayres, et al., Phys. Rev. Lett. 15D, 3105(1977).

11. Yu. M. Antipov, et al., Nucl. Phys. B57, 333(1973);
A. Dererchekov, et al., Phys. Lett. 48B, 367(1974).

12. C.W. Akerlof, et al., Phys. Rev. Lett. 59B, 197(1975);
C.W. Akerlof, et al., Phys. Rev. Lett. 35, 1406(1975);
C.W. Akerlof, et al., Phys. Rev. 14D, 2864(1976).

13. A. Böhm, et al., Phys. Lett. 49B, 491(1974).

14. I.P. Auer, et al., Phys. Rev. Lett. 39, 313(1977).

15. T. Chin, Ann. Rev. Nucl. Sci. 22, 255(1972).

16. M. Borghini, et al., Phys. Lett. 36B, 493(1971).

17. G.L. Kane and A. Seidl, Rev. Mod. Phys. 48, 309(1976);
G.L. Kane, AIP Conf. Proc. No. 35, Particles and Fields Subseries No. 12, 43(1976).

18. O.I. Dahl, et al., Phys. Rev. Lett. 37, 80(1976);
A.V. Barnes, A.V. Tollestrup, and R.L. Walker to be published.

19. A.V. Barnes, et al., Phys. Rev. Lett. 37, 76(1976).

20. A.V. Stirling, et al., Phys. Rev. Lett. 14, 763(1965);
P. Sonderegger, et al., Phys. Rev. Lett. 20, 75(1966).

21. P. Bonamy, et al., Nucl. Phys. B52, 392(1973).
D. Hill, et al., Phys. Rev. Lett. 30, 239(1973).

22. O. Guisan, et al., Phys. Lett. 18, 200(1965).
M.A. Wahlig and I. Mannelli, Phys. Rev. 168, 1515(1968);
V.N. Bolotov, et al., Nucl. Phys. B73, 387(1974).

23. O.I. Dahl, et al., Phys. Rev. Lett. 38, 54(1977).

24. V.N. Bolotov, et al., Phys. Lett. 53B, 217(1968);
E. Shibata and M.A. Wahlig, Phys. Lett. 22, 354(1966);
L.E. Holloway, et al., Phys. Rev. D8, 2814(1973);
W.D. Apel, et al., Phys. Lett. 55B, 111(1975).

25. A.C. Irving and C. Michael, Nucl. Phys. B82, 282(1974).

26. D.A. Jensen, et al., Phys. Rev. Lett. 23, 615(1969);
S.H. Aronson, et al., Phys. Rev. Lett. 25, 1057(1970);
S.H. Aronson, et al., Nuovo Cim. 32A, 236(1976).

27. N. Cabibbo, Phys. Lett. 22, 212(1966).

28. J. Roehrig, et al., Phys. Rev. Lett. 38, 1116(1977).

29. W.C. Carithers, et al., Phys. Rev. Lett. 34, 1240(1975);
W.C. Carithers, et al., (to be published).
M. Bott-Bodenhausen, et al., Phys. Lett. 23, 277(1966);
K.-F. Albrecht, et al., Nucl. Phys. B93, 237(1975).

30. H.R. Barton, Jr., et al., Phys. Rev. Lett. 37, 1656(1976).

31. E.L. Miller, et al., Phys. Rev. Lett. 26, 984(1971);
J. Engler, et al., Phys. Lett. 34B, 528(1971);
M.N. Kreisler, et al., Nucl. Phys. B84, 3(1975);
V. Bohmer, et al., Nucl. Phys. B110, 205(1976);
A. Babaev, et al., Nucl. Phys. B110, 189(1976).

32. G. Bunce, et al., Phys. Rev. Lett. 36, 1113(1976).

33. T. Devlin, et al., Nucl. Phys. 123B, 1(1977).

34. R.L. Anderson, et al., Phys. Rev. Lett. 37, 1111(1976).

35. D.S. Ayres, et al., Phys. Rev. Lett. 37, 1724(1976).

36. R.L. Anderson, et al., Phys. Rev. Lett. 38, 880(1977).

37. Y. Akimov, et al., Phys. Rev. Lett. 35, 766(1975);
K. Abe, et al., Phys. Rev. Lett. 31, 1527(1973);
J. Whitmore, et al., Phys. Rev. D11, 3124(1975);
M.G. Albrow, et al., Nucl. Phys. B108, 1(1976).

38. E.W. Beier, et al., Phys. Rev. Lett. 37, 1120(1976).

39. A.H. Mueller, Phys. Rev. D2, 2963(1970). Representative reviews are: H. Boggild and T. Ferbel, Ann. Rev. Nucl. Sci. 24, 451(1974); R.G. Roberts in "Phenomenology of Particles at High Energies", edited by R.L. Crawford and R. Jennings (Academic, London and New York, 1974); and T. Ferbel, SLAC Report No. 179, 1974 (unpublished).

40. J. Biel, et al., Phys. Rev. Lett. 36, 504(1976).

41. E. Nagy, et al., in Proceedings of the Seventeenth International Conference on High Energy Physics, London, 1974 (unpublished). The relevant information from the CERN intersecting storage ring is contained in the report of A. Diddens which appears in the Proceedings of the Seventeenth International Conference on High Energy Physics, London, England, 1974, edited by J. R. Smith (Rutherford High Energy Laboratory, Didcot, Berkshire, England, 1975). For data at low energies see J. Hanlon et al., Vanderbilt University Report No. VAND-HEP 74(2), 1974 (unpublished).

42. J. Biel, et al., Phys. Rev. Lett. 36, 507(1976).

43. R.T. Deck, Phys. Rev. Lett. 13, 169(1974). For a recent comprehensive review, see E. L. Berger in Proceedings of the Daresbury Conference on Analysis of Three-Particle Decays and Meson Resonance Production, 1975, edited by J.B. Dainton and A.J.G. Hey (Daresbury Nuclear Physics Laboratory, Daresbury, Warrington, Lancashire, England, 1975).

44. J. Biel, et al., Phys. Lett. 65B, 291(1976).

45. H. DeKerret, et al., Phys. Lett. 63B, 477 and 483(1976).

46. A. Babaev, et al., CERN Report (June 23, 1976); Nucl. Phys. B116, 28(1976).

47. W. Busza, et al., Phys. Rev. Lett. 34, 836(1975); C. Halliwell, et al., Phys. Rev. Lett. 39, 1499(1977).

48. S.P. Denisov, et al., Nucl. Phys. B61, 62(1974) .

49. J. Erwin, et al., Phys. Rev. Lett. 32, 254(1974). D. Bogert, et al., Phys. Rev. Lett. 31, 1271(1973).

50. J. Babecki, Acta Physica Polonica, B6, No. 3, 443(1975).

51. J. Babecki, et al., Phys. Lett. 52B, 247(1974).

52. K. Gottfried, Phys. Rev. Lett. 32, 957(1974).

53. G. Donaldson, et al., Phys. Rev. Lett. 36, 1110(1976).

54. A.H. Mueller, Phys. Rev. D2, 2963(1970).

55. T.D. Field and R.P. Feynman, Phys. Rev. D15, 2590(1977).

56. D. Bromberg, et al., Phys. Rev. Lett. 38, 1447(1977).

57. J.W. Cronin, et al., Phys. Rev. D11, 3105(1975); Phys. Rev. Lett. 38, 115(1977).

58. S.M. Berman, J.D. Bjorken and J.B. Kogut, Phys. Rev. D4, 3388(1971); S.D. Ellis and M.B. Kislinger, Phys. Rev. D9, 2027(1976); See also Reference 55.

59. J.C. Vander Velde, "Neutrino-Proton Interactions in the 15-Foot Bubble Chamber and Properties of Hadron Jets", Univ. of Michigan preprint (1976), (unpublished).

60. L.B. Leipuner, et al., Phys. Rev. Lett. 31, 1226(1973).

61. T. Nash, et al., Phys. Rev. Lett. 32, 858(1974).

62. M. Bott-Bodenhausen, et al., Phys. Lett. 40B, 693(1972).

63. H.R. Gustafson, et al., Phys. Rev. Lett. 37, 474(1976).

64. D. Bintinger, et al., Phys. Rev. Lett. 37, 732(1976).

65. W.R. Ditzler, et al., Phys. Letters 71B, 451(1977).

66. E.J. Bleser, et al., Phys. Rev. Lett. 35, 76(1975).

67. M.A. Abolins, et al., Phys. Rev. Lett. 37, 417(1976).

68. V. Cook, et al., Phys. Lett. 64B, 221(1976).

69. K.J. Anderson, et al., Phys. Rev. Lett. 36, 237(1976).

70. G.J. Blanar, et al., Phys. Rev. Lett. 38, 192(1977).

71. G.T. Adylov, et al., Phys. Lett. 51B, 402(1974).

72. E. Dally, et al., Phys. Rev. Lett. 39, 1176(1977).

73. A.F. Greene and T. Yamanouchi, Fermilab Research Program Workbook (May 1977); this workbook is updated annually.

74. M. Schein, D.M. Haskin and R.G. Glasser, Phys. Rev. 95, 855(1954); Phys. Rev. 99, 643(1955).

75. D.M. Stevens, et al., Phys. Rev. 14D, 2267(1976).

76. D.L. Burke, et al., Phys. Lett. 60B, 113(1975).

PARTICLE BEAMS IN THE MESON LAB (Circa 1978)

Beam	Beam Particles	Momentum Range (GeV/c)	Flux (Per 10^{13} 400 GeV Incident Protons)	Remarks
M1	Charged Hadrons	Tune A: 20-200 Tune B: 20-400	3×10^{7} π^- @ 175 GeV/c 4×10^{5} π^- @ 300 GeV/c	$(\Delta p/p)$ max = $\pm$ 2%; two differential Č counters
M2	Charged Hadrons	20-400	~5×10^{10} diffracted protons 3×10^{6} π^- @ 200 GeV/c	Two differential Č counters; neutral hyperon beam at end of M2
M3	Neutrons, K_L^0	50-350		
M4	Charged Hadrons	35-200	1.4×10^{6} K^- @ 50 GeV/c ~10^{5} K^- @ 200 GeV/c	$(\Delta p/p)$ ≈ $\pm$ 4%; emphasis on K^- production; one differential Č counter
M5	Charged Particle Test Beam	6-40	~5×10^{5} $\pi^{\pm}$ @ 20-30 GeV/c 15,000 electrons @ 10 GeV/c	Threshold Č counter available
M6	Charged Hadrons	20-200	4×10^{7} π^- @ 100 GeV/c	$(\Delta p/p)$ = $\pm$ 0.6; one DISC, one differential and one threshold Č counter

TABLE II

DETERMINATION OF $\alpha_\omega(0)$ FROM CARBON REGENERATION DATA

Quantity	This Experiment (30-130 GeV/c)	All Data (4-130 GeV/c)
$\alpha_\omega(0)$ from n and Eq. (1)	0.393 ± 0.020	0.379 ± 0.003
$\alpha_\omega(0)$ from measured phase and Eq. (2)	0.0389 ± 0.018	0.410 ± 0.015

TABLE III

BEST FIT VALUES TO THE INVARIANT/INCLUSIVE CROSS SECTION PARAMETERIZED IN THE FORM $d^2\sigma/dtdx = (|\beta|^2/16\pi_0^2)(1-x)^{1-2\alpha_{eff}}\sigma_{tot}^{cp}(M_m^2)e^{b_{eff}t}$

Channel	Effective -t Range (GeV^2)	Laboratory Energy Range (GeV)	$\|\beta\|^2/16\pi s_0^2$ (GeV^{-2})	α_{eff}	b_{eff} (GeV^{-2})
$\pi^+ + p \to K^+ + \ldots$	0.1-0.65	50-140	0.155 ± 0.015	0.20 ± 0.05	3.7 ± 0.3
$\pi^- + p \to K^- + \ldots$	0.1-0.65	50-140	0.135 ± 0.014	0.25 ± 0.05	3.7 ± 0.3
$\pi^- + p \to \bar{p} + \ldots$	0.2-0.65	50-175	0.128 ± 0.012	-0.55 ± 0.15	2.0 ± 0.3
$\pi^+ + p \to p + \ldots$	0.2-0.65	140-175	0.240 ± 0.022	-0.50 ± 0.10	3.1 ± 0.5
$p + p \to \pi^+ + \ldots$	-0.2-0.20	50-175	0.270 ± 0.025	-0.65 ± 0.15	4.4 ± 0.5
$p + p \to K^+ + \ldots$	-0.2-0.20	50-175	0.108 ± 0.015	-0.65 ± 0.20	3.0 ± 1.0

TABLE IV

DEPENDENCE OF EXPONENTIAL SLOPE PARAMETER b ON ($p\pi^-$) MASS.

Mass Interval (GeV)	Slope (GeV^{-2})
< 1.25	19.1 ± 0.9
1.25-1.35	15.0 ± 0.7
1.35-1.45	12.8 ± 0.6
1.45-1.55	6.8 ± 0.7
1.55-1.65	4.9 ± 0.6
1.65-1.75	4.2 ± 0.6
1.75-2.00	4.2 ± 0.8

The value of b is obtained from a fit of the data to the form exp(bt). The range of $|t|$ in the fit was 0.04 to 0.16 GeV^2 for the first four mass bands and 0.04 to 0.5 GeV^2 for the last three mass regions.

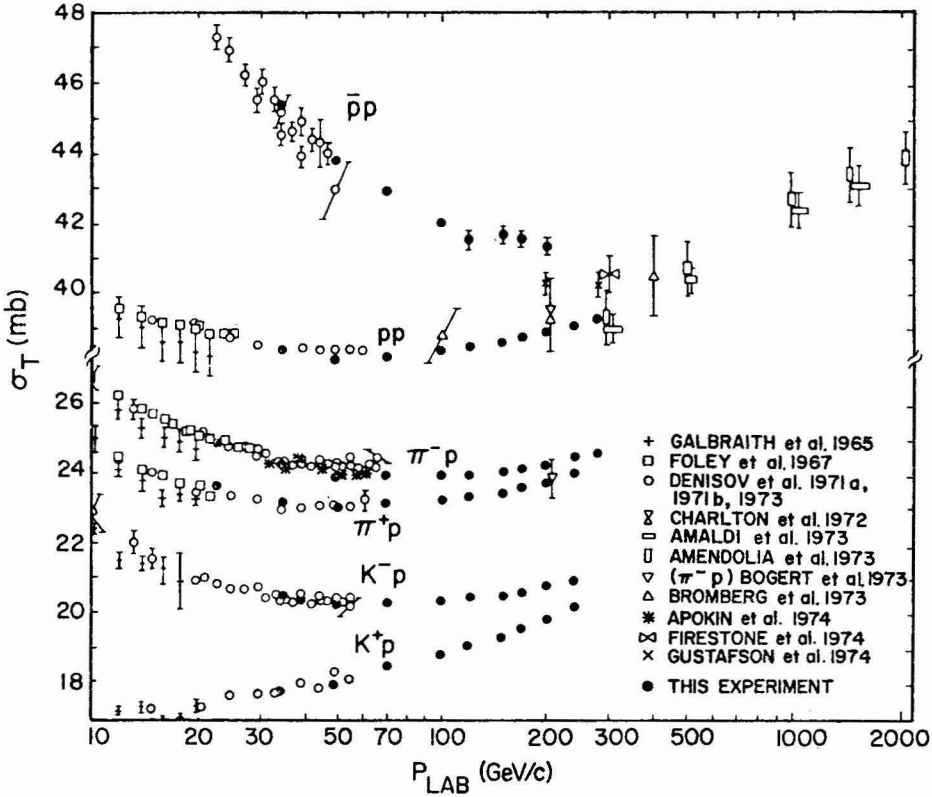

Figure 1. Total cross sections on protons. Only momentum dependent errors are shown.

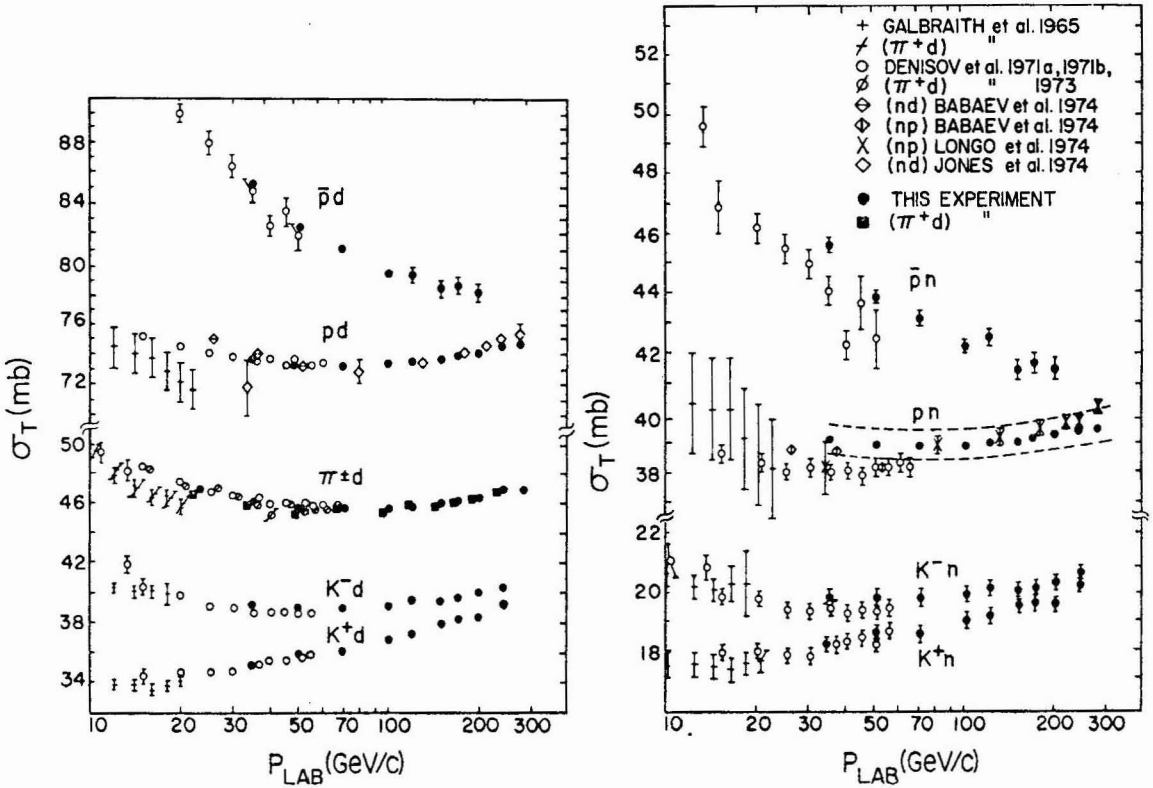

Figure 2. Total cross sections on deuterons and neutrons. Only momentum dependent errors are shown. The upper and lower dashed curves represent the p-n cross sections obtained assuming $\langle r^{-2} \rangle = 0.039$ and $0.031\ mb^{-1}$ respectively.

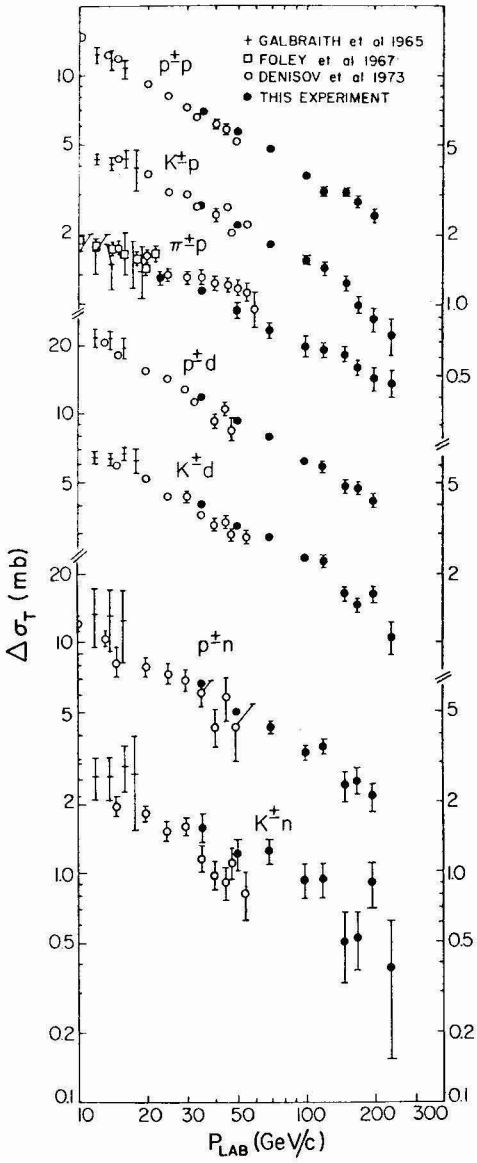

Figure 3. Antiparticle-particle total cross section differences.

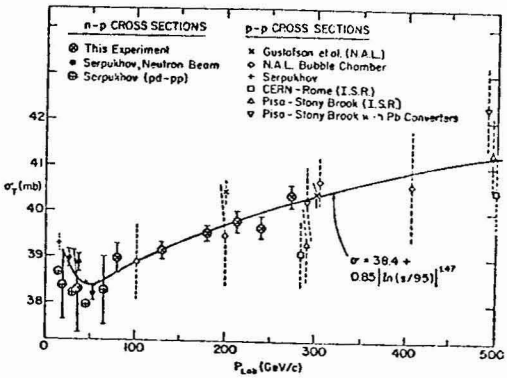

Figure 4. n-p and p-p total cross sections. Not all the data below 60 GeV/c are shown.

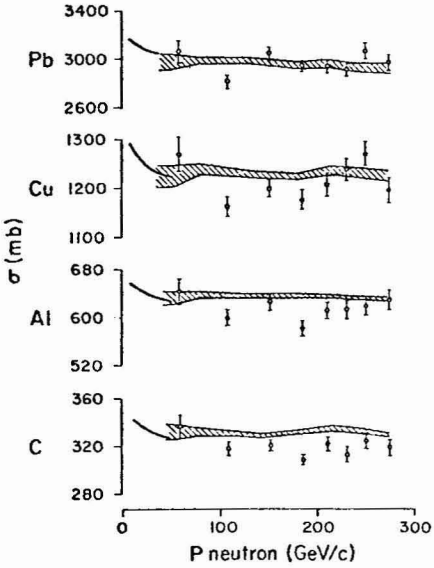

Figure 5. Neutron-nuclear total cross sections measured in Experiment #305. The cross-hatched region represents the data from Fermilab Experiment #4; the curves summarize lower energy results.

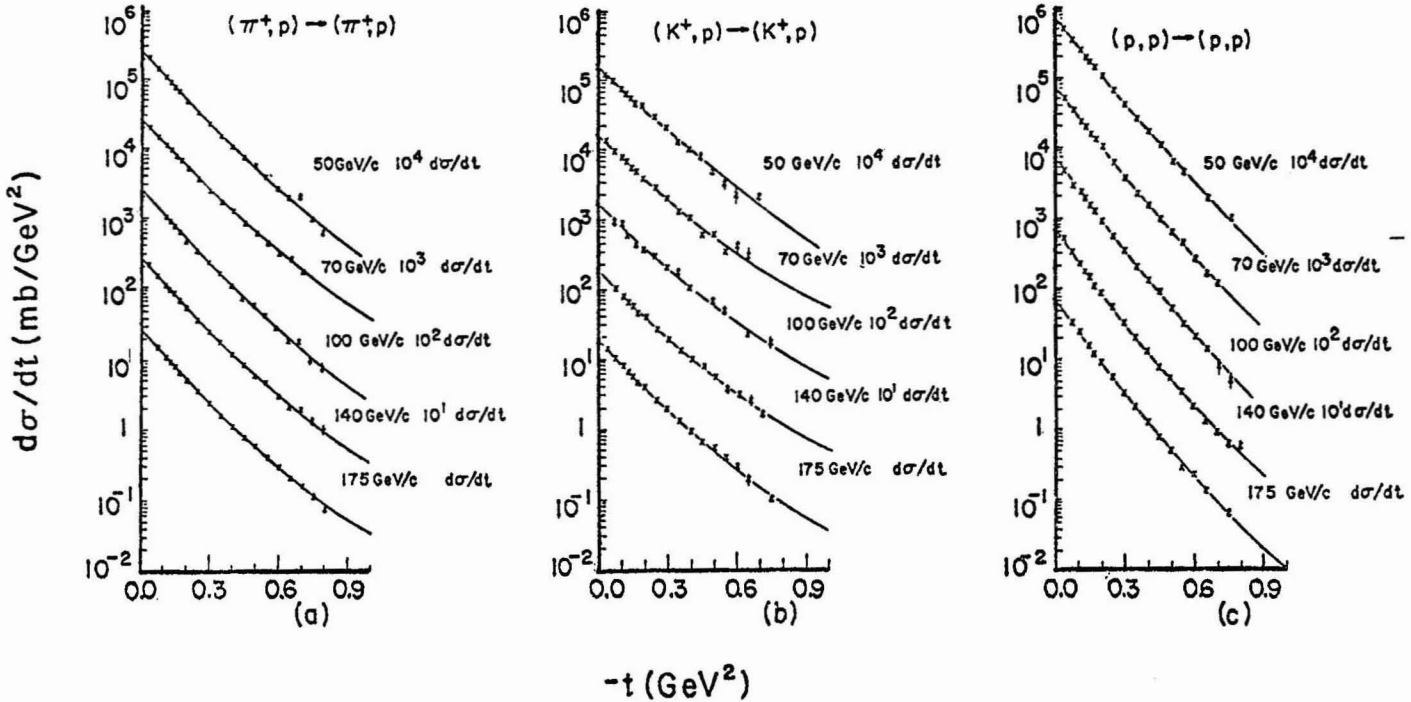

Figure 6a. Elastic scattering differential cross-sections for π^+, K^+ and p on protons.

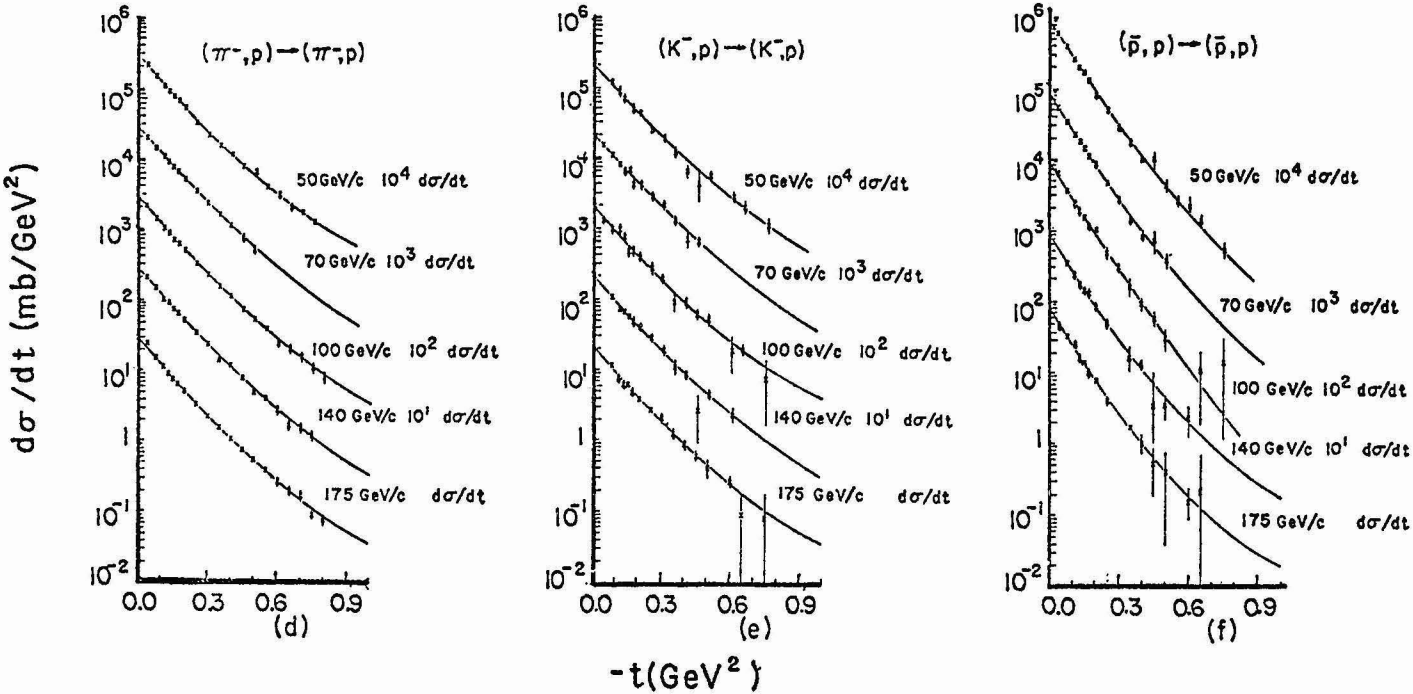

Figure 6b. Elastic scattering differential cross-sections for π^-, K^- and $\bar{p}$ on protons.

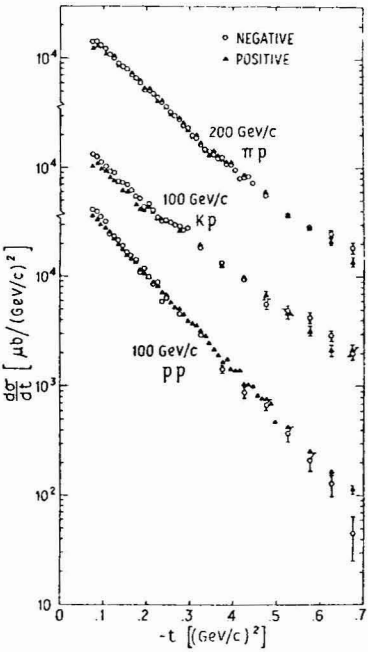

Figure 7a. Comparison of particle and antiparticle elastic scattering.

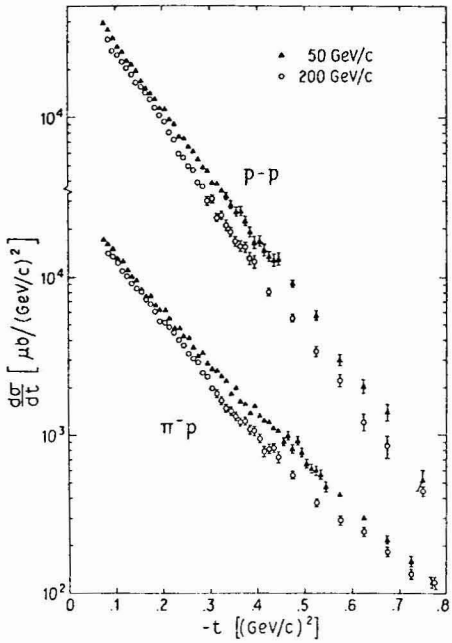

Figure 7b. Energy dependence of pp and π^-p differential elastic cross sections.

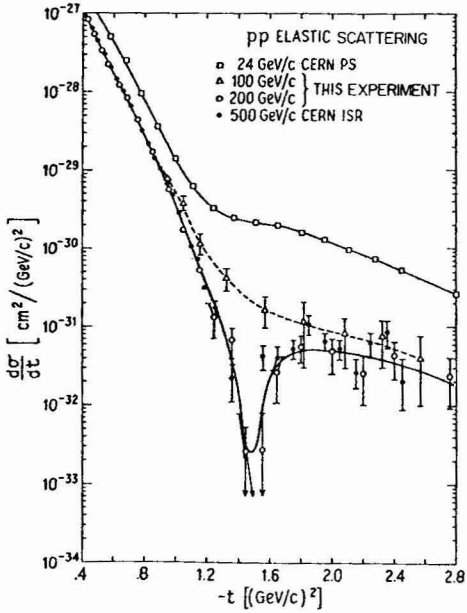

Figure 7c. Energy and t dependence of pp elastic scattering. The data at 100 GeV/c, because of limited statistical accuracy, do not preclude a moderate dip. The two lowest points at 200 GeV/c are consistent with $d\sigma/dt = 0$. The 90% confidence limit is approximately twice the upper error bar.

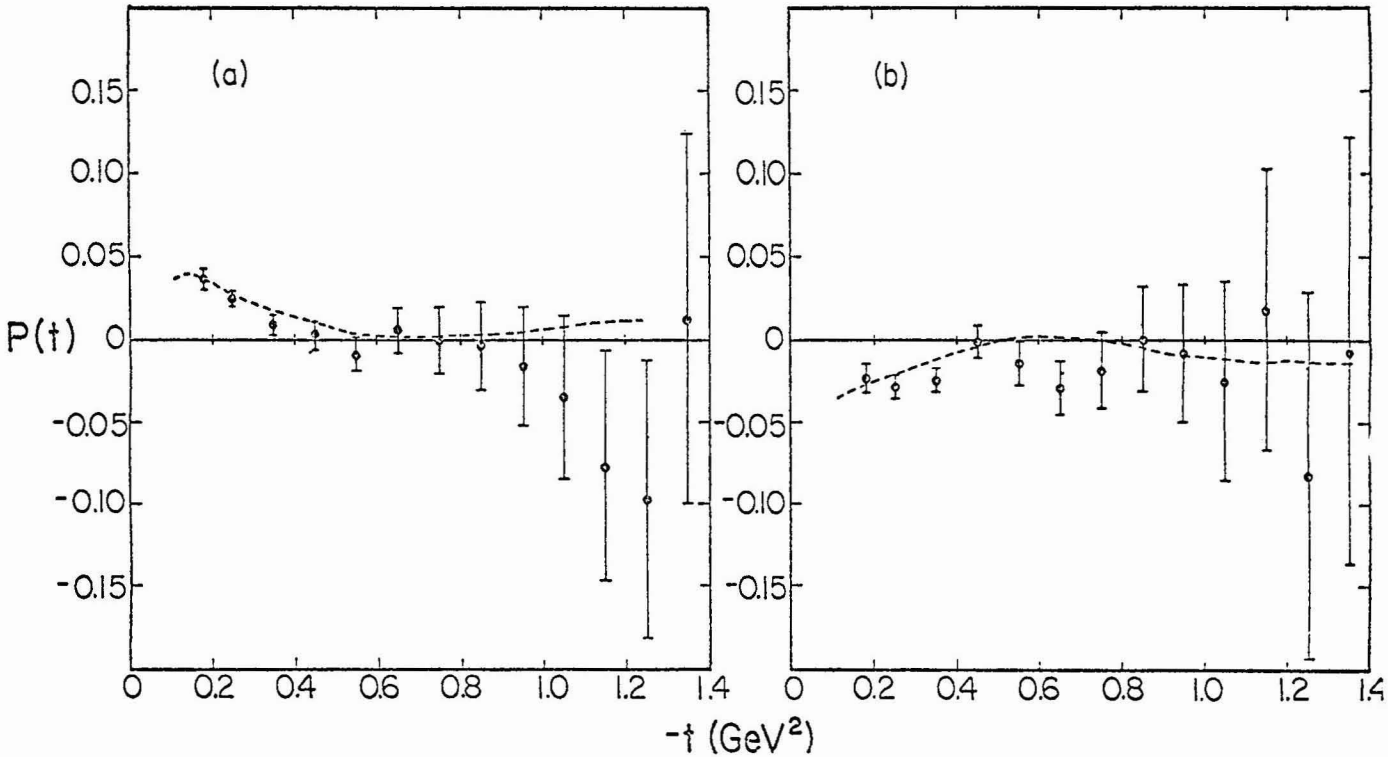

Figure 8. Polarization parameter P(t) for (a) π^+p and (b) π^-p elastic scattering. Only statistical errors are shown. The dashed curves represent the results of Reference 16 scaled from 10 to 100 GeV/c as described in the text.

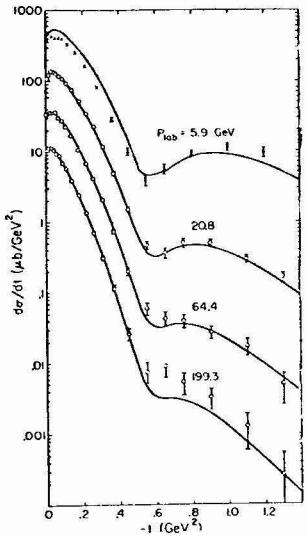

Figure 9a. Differential cross sections at 20.8, 64.4, and 199.3 GeV from this experiment, and at 5.9 GeV from Ref.20 . The curves are the result of a fit described in the text.

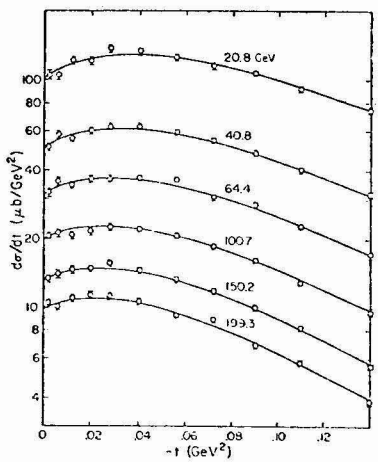

Figure 9b. Differential cross sections in the region of small t. The curves are the result of a fit described in the text.

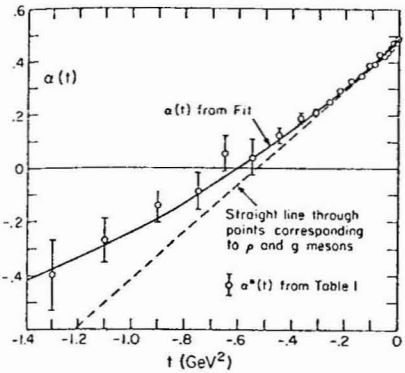

Figure 10. The effective trajectory $\alpha(t)$.

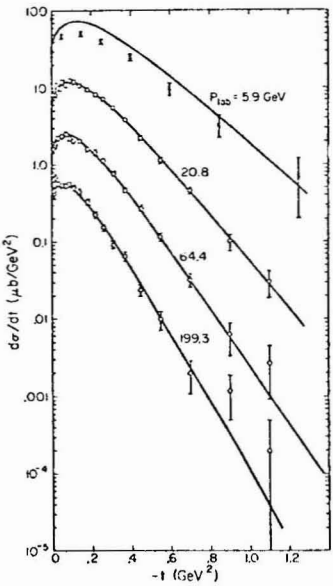

Figure 11. Differential cross sections for the reaction $\pi^- p \to \eta n$ with $\eta \to 2\gamma$ at 20.8, 64.4, and 199.3 GeV from this experiment and 5.9 GeV from the experiment of O. Guisan, et al., Reference 22. The curves are the result of a fit described in the text.

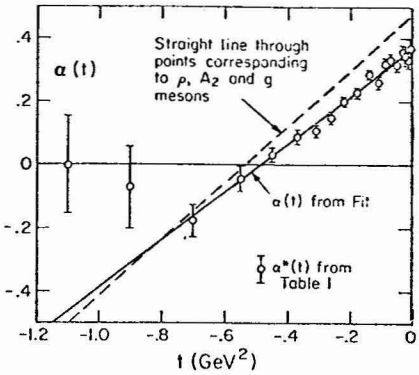

Figure 12. The effective trajectory α(t).

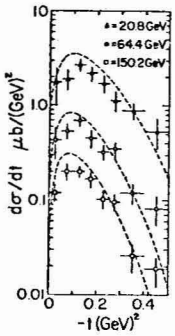

Figure 13. Representative differential cross sections. The dashed lines are the predictions of Irving and Michael (Ref. 25) which are based on 6-GeV/c data.

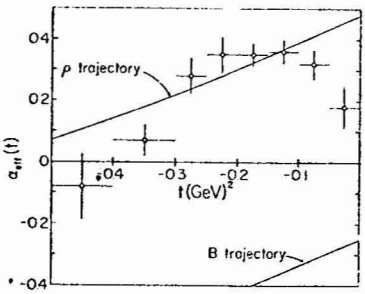

Figure 14. The effective Regge trajectory. The ρ trajectory is taken from Ref. 19 and the B trajectory is the one assumed in Ref. 25.

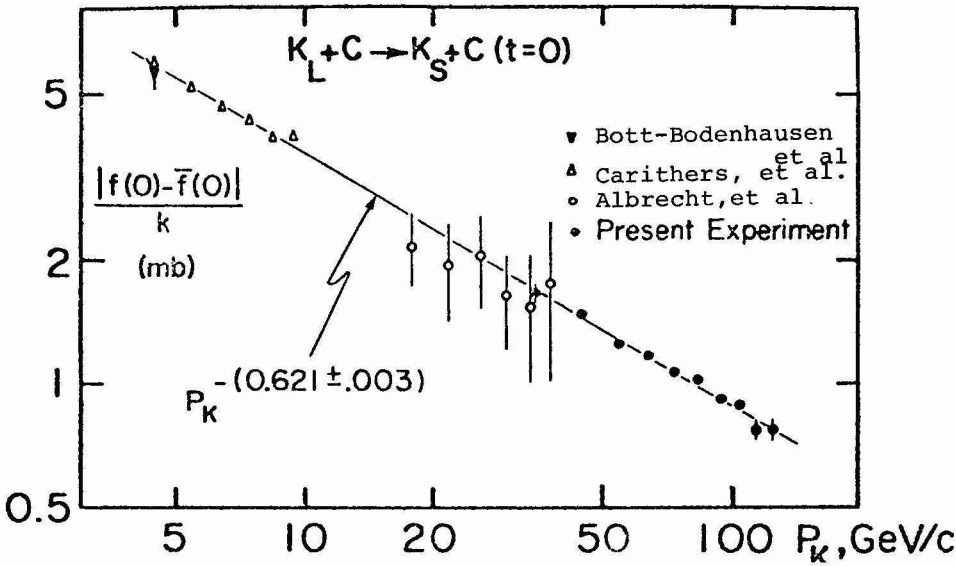

Figure 15a.

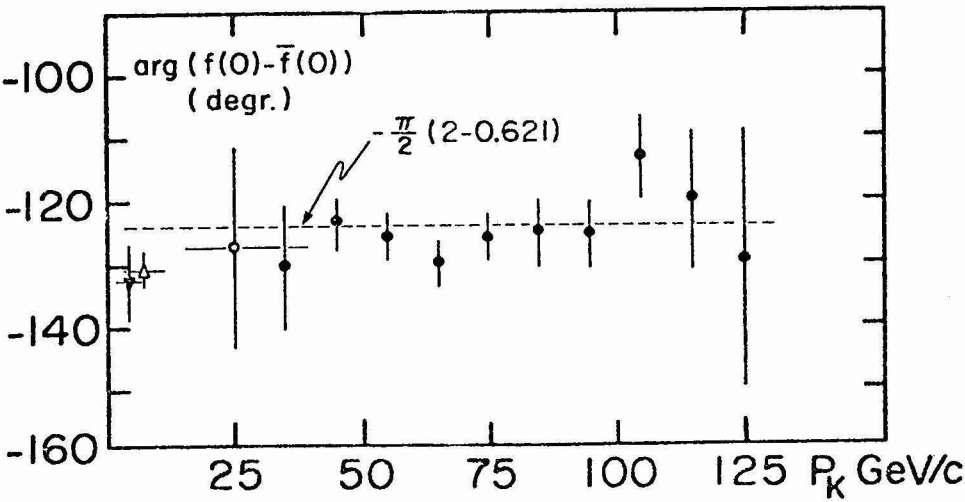

Figure 15b.

$|f-\bar{f}|/k$ and $\arg(f-\bar{f})$ vs. P_k for all carbon data. The arg $(f-\bar{f})$ data of Ref. 28 are plotted for clarity as a single point, given in Ref. 28. The solid line is the best fit to P_k^{-n}. The dashed line is the phase predicted by the measured exponent n.

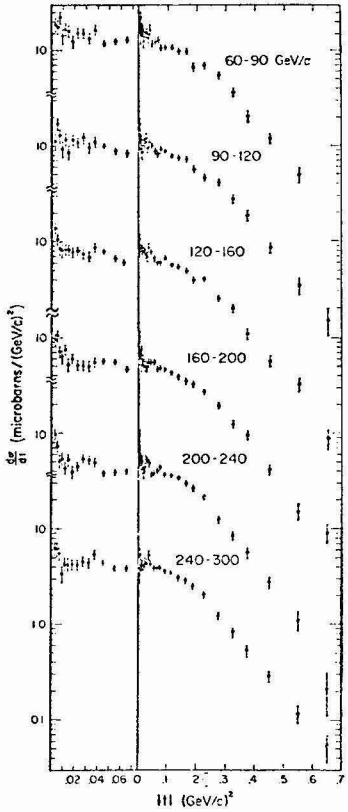

Figure 16. n-p charge-exchange absolute cross-sections. The errors shown are statistical only. Small-momentum-transfer data are shown in an expanded |t| scale for ease in viewing.

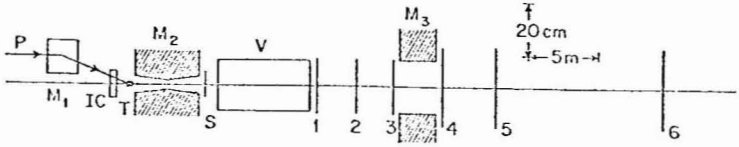

Figure 17. Elevation view of the Fermilab neutral hyperon beam. 300-GeV protons are incident from the left. M_1 is the restoring magnet for production-angle variation. IC and T are ion chamber and Be target. M_2 is the collimator and sweeper. S is a veto counter; V is the decay vacuum; and 1-6 are multiwire proportional chambers. M_3 is the analyzing magnet.

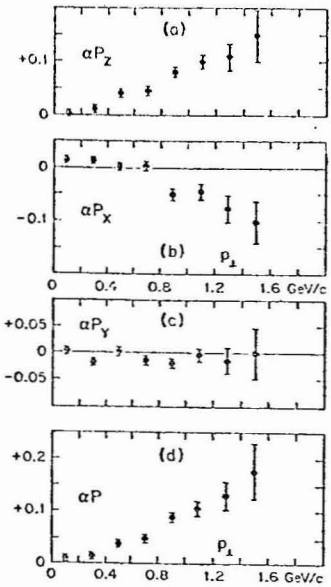

Figure 18. Three components and magnitude of the $\Lambda^0 \rightarrow p + \pi^-$ asymmetry as a function of Λ^0 transverse momentum.

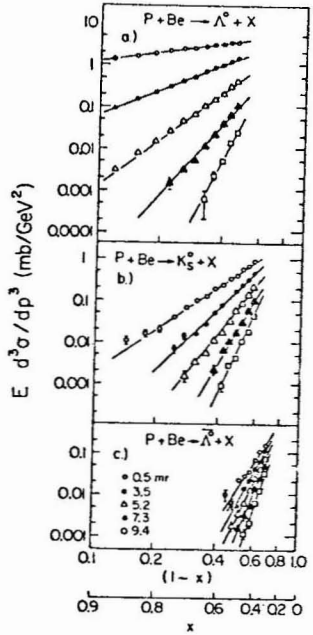

Figure 19. Inclusive production of Λ^0, K^0_S and $\bar{\Lambda}^0$ by 300 GeV protons on beryllium.

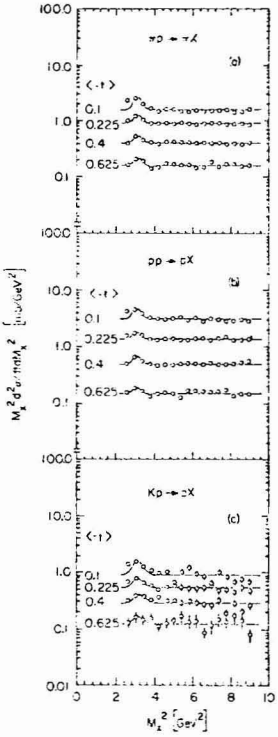

Figure 20. (a) The invariant cross section $M_X^2 d^2\sigma/dt\, dM_X^2$ in mb/GeV^2 for $\pi^+p \to p^+X$ plotted vs M_X^2 in GeV^2.

(b) The invariant cross section for $p^+p \to p^+X$,

and

(c) For $K^+p \to K^+X$. Data at 140 and 175 GeV have been combined.

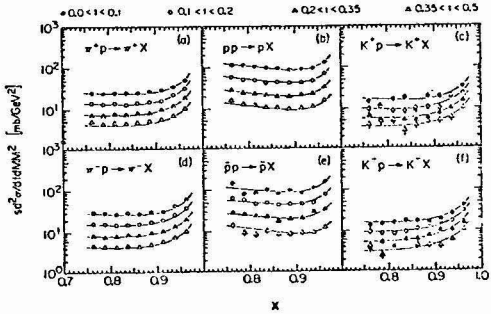

Figure 21. Inclusive cross sections at 70-GeV/c incident momentum for the ranges of momentum transfer indicated. The curves show the results of the fits described in the text.

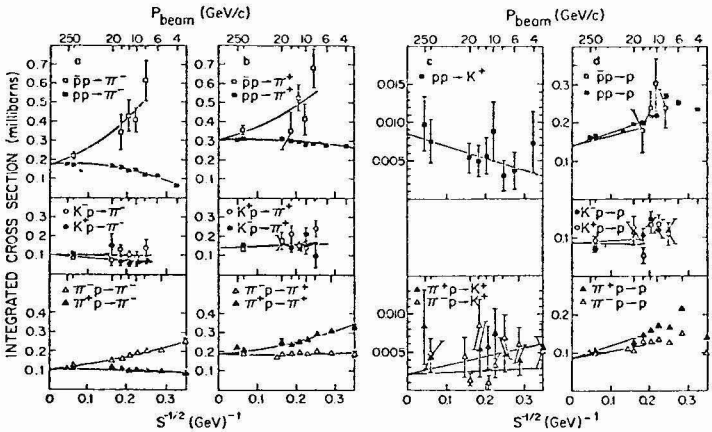

Figure 22. Cross sections integrated over the apparatus acceptance, for the production of (a) π^-, (b) π^+, (c) K^+, and (d) p. The solid lines are fits to $A + Bs^{-1/2}$ or $A+B^{-1/2}+Cs^{-1}$ as described in the text. The tick marks on the abcissa at the top of each part of the figure correspond to the beam momenta at which the cross sections were measured.

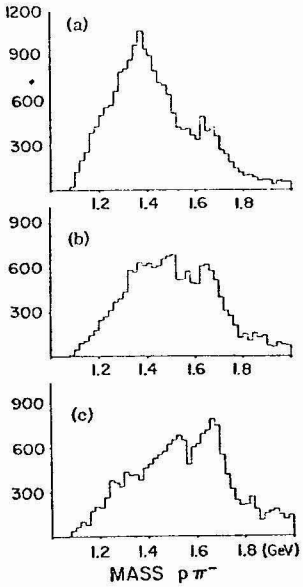

Figure 23. Mass spectra of $p\pi^-$ pairs in hydrogen, integrated over a 50-300 GeV/c neutron momentum band, displayed as a function of t. (a), (b), and (c) correspond to $|t|$ bands of 0.02-0.08, 0.08-0.20, and 0.20-1.00 GeV^2, respectively.

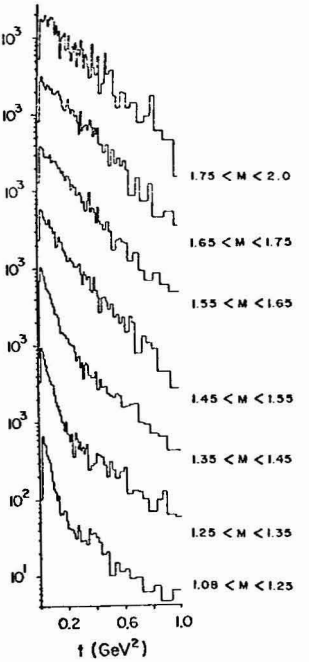

Figure 24. Distributions in $|t|$ for seven mass bands of the $p\pi^-$ system: <1.25, 1.25-1.35, 1.35-1.45, 1.45-1.55, 1.55-1.65, 1.65-1.75, and 1.75-2.0 GeV.

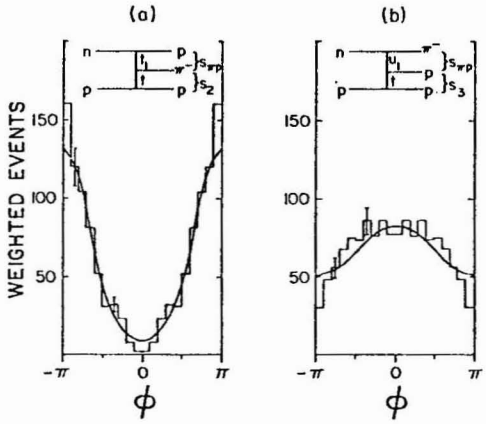

Figure 25. Projected ϕ distributions for (a) $\cos\theta>0.8$ and (b) $\cos\theta<-0.8$. The Deck diagrams expected to dominate in these regions of $\cos\theta$ are shown above the data. The curves are calculations of Deck contributions described in the text.

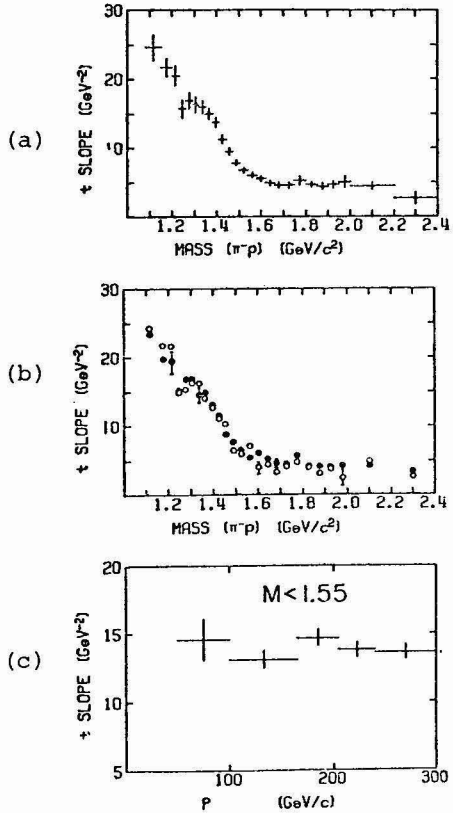

Figure 26. Slope parameter in t as a function of the mass of the produced ($p\pi^-$) system. Data for all momenta are given in graph (a). (b) contains the results of (a) split up according to incident neutron momentum; solid circles are for data above 200 GeV/c. (c) displays the variation of the B parameter with incident momentum for data with M < 1.55 GeV.

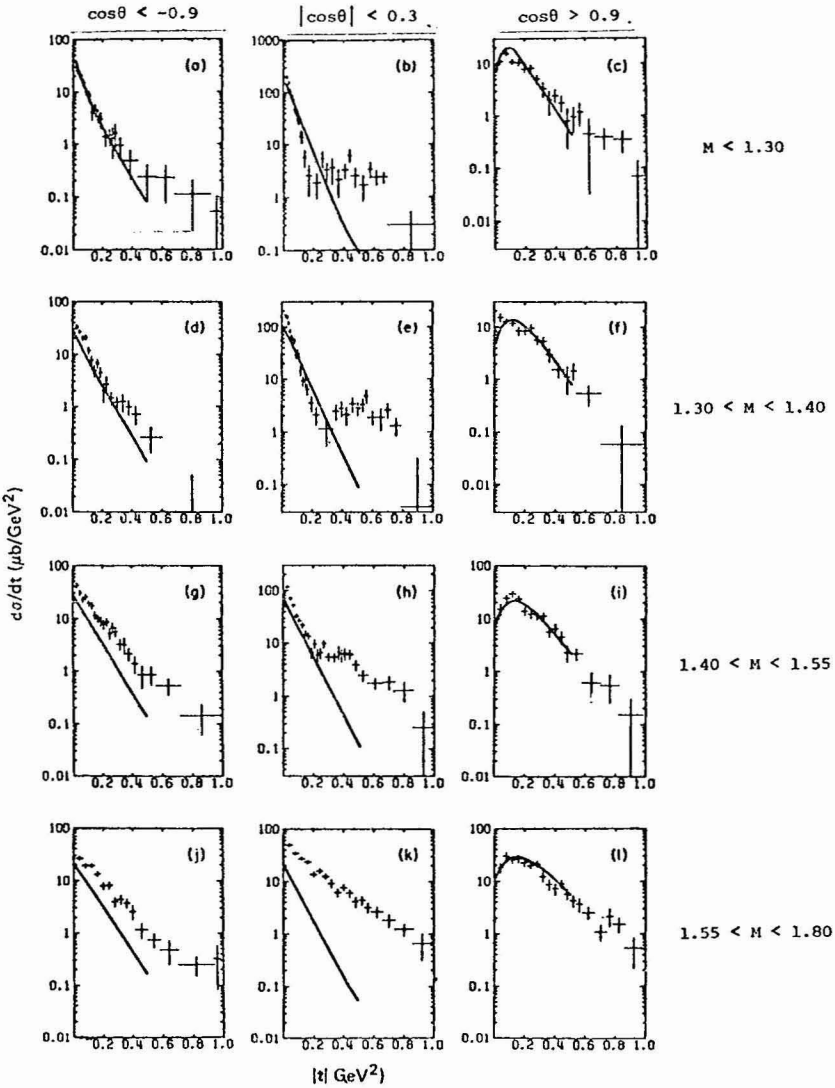

Figure 27. Momentum transfer distributions as a function of the Gottfried-Jackson angle for different regions of M. Curves are calculations taken from a model proposed in Reference 46.

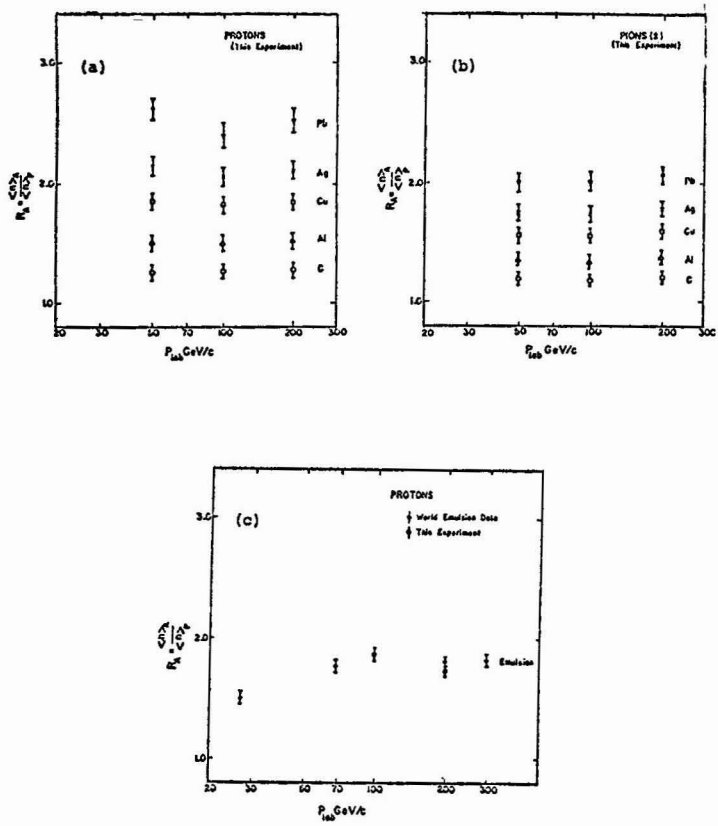

Figure 28. Energy dependence of R_A for various targets.
(a) Incident protons at 50, 100 and 200 GeV.
(b) Incident π^+ at 50 and 100 GeV and π^- at 200 GeV.
(c) Proton-emulsion over the energy range 25 to 300 GeV. The world emulsion data are obtained from Reference 50.

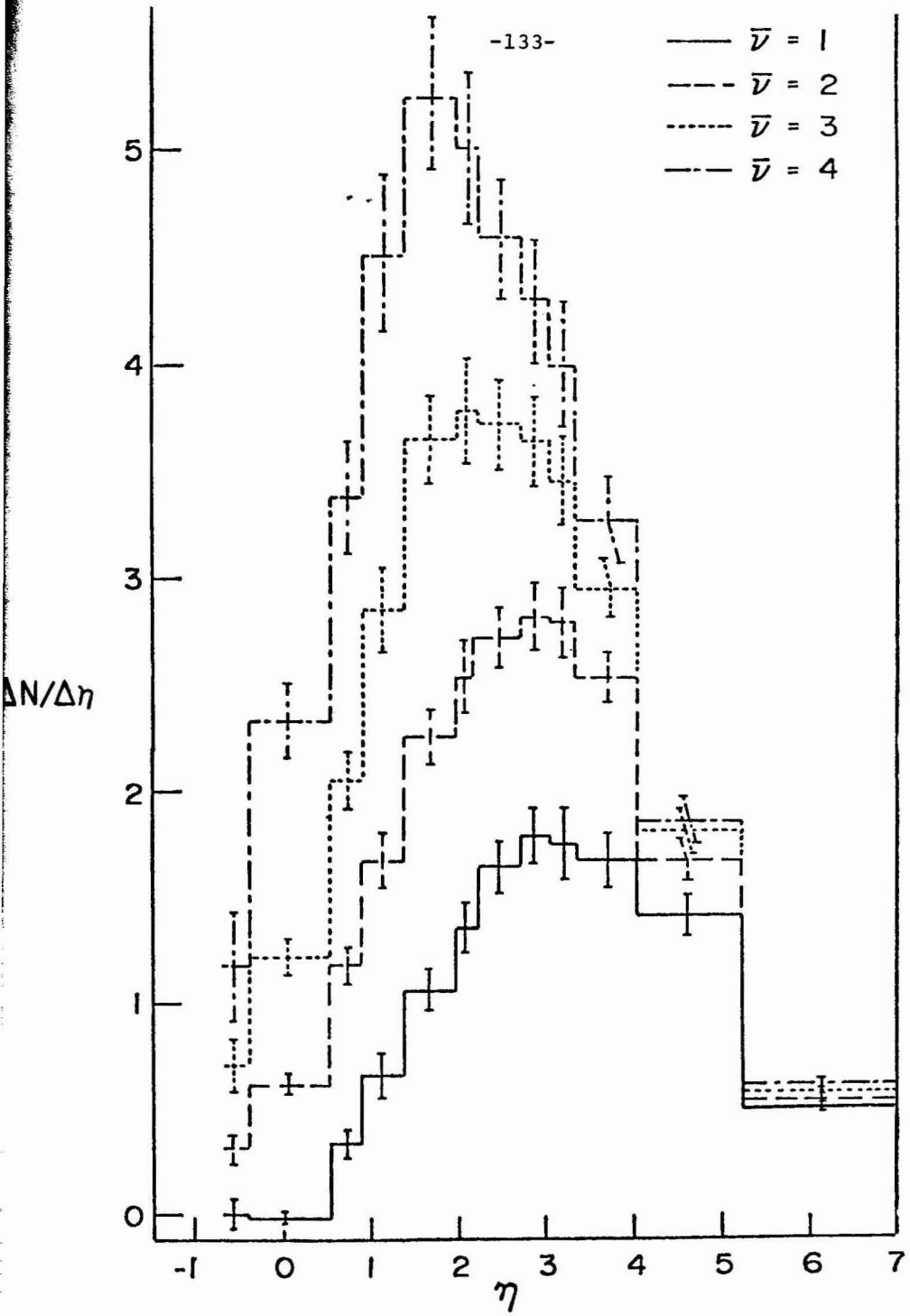

Figure 29. Pseudorapidity distributions for various values of $\bar{\nu}$ in 200 GeV proton-nucleus interactions.

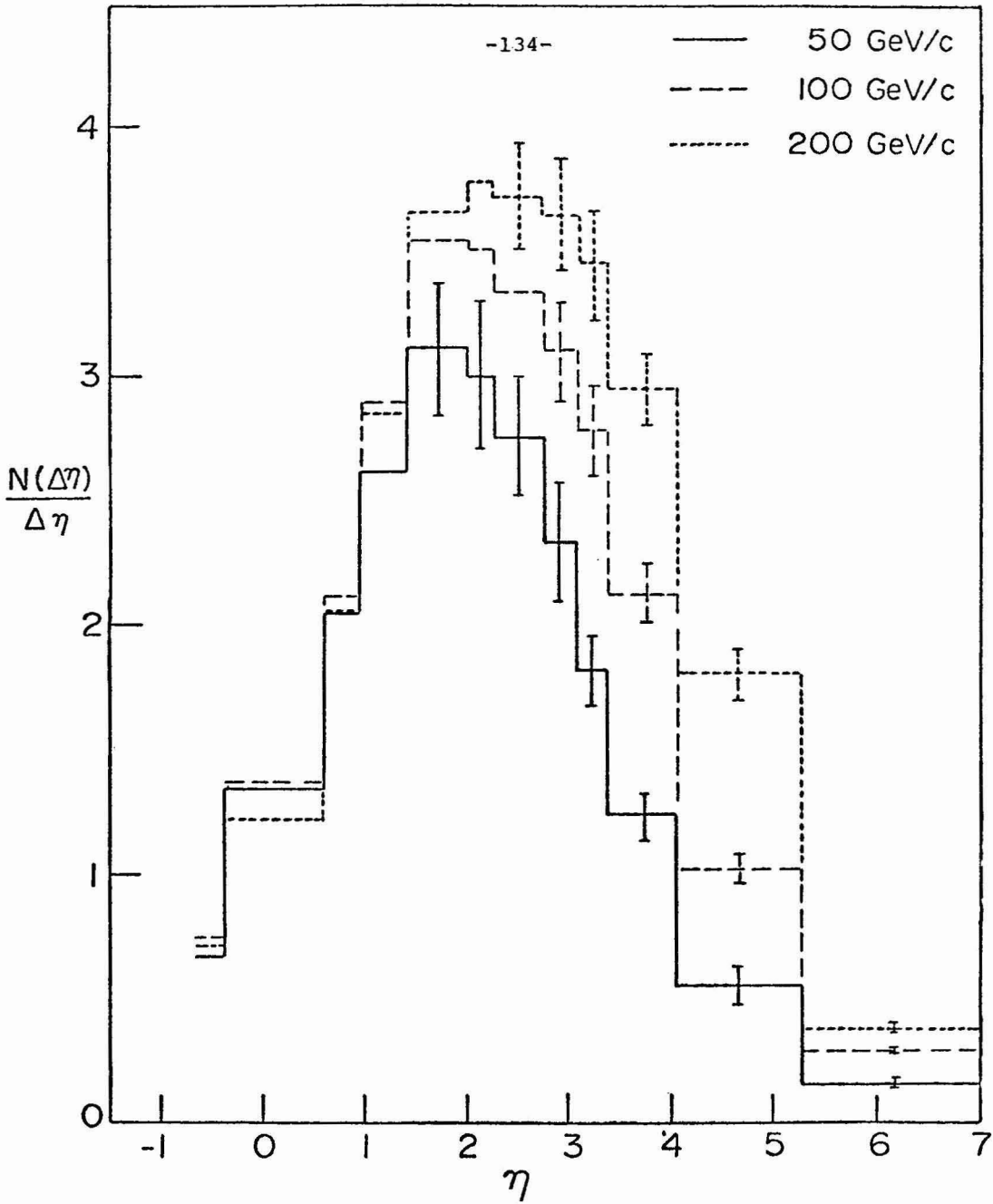

Figure 30. Energy dependence of pseudorapidity distributions for the $\bar{\nu} = 3$ data. In the interest of clarity, only typical errors are shown.

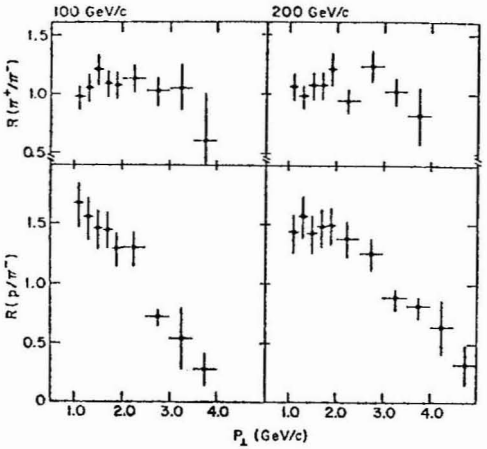

Figure 31. Ratios of invariant cross sections as described in the text versus P_t.

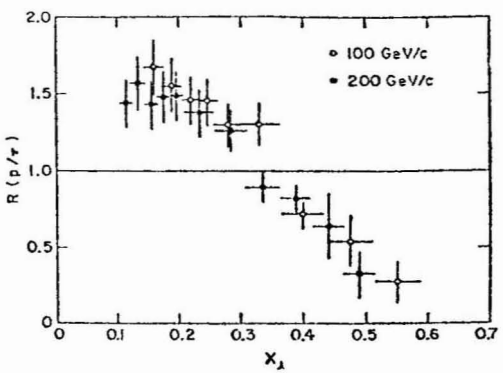

Figure 32. Ratio of invariant cross sections versus x_t for $pp \rightarrow \pi^0 X$ and $\pi^- p \rightarrow \pi^0 X$ at 100 and 200 GeV/c.

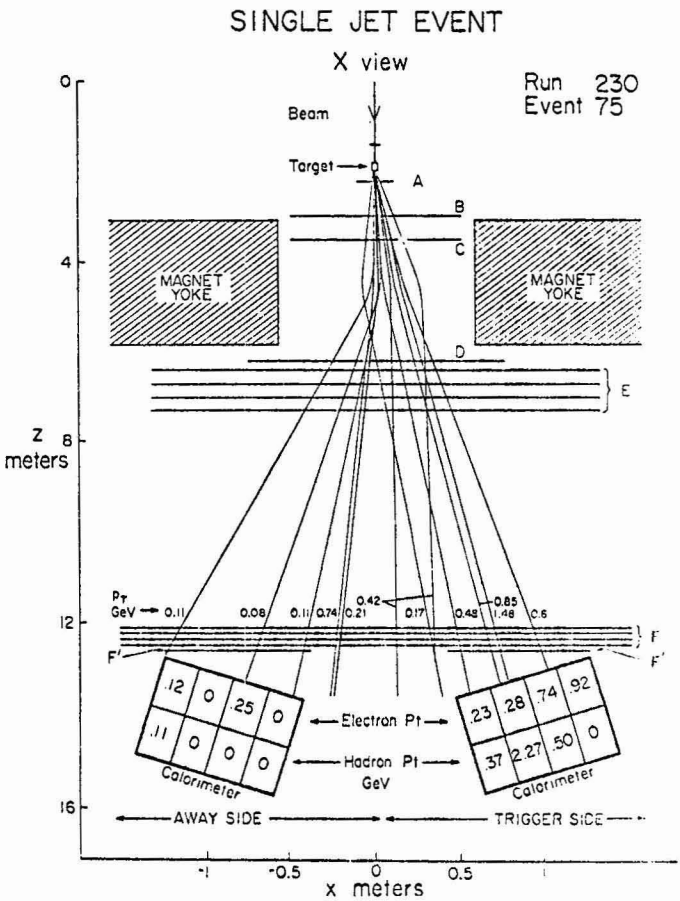

Figure 33. Plan view of the spectrometer, with the transverse dimensions magnified by a factor of 4. The tracks from a typical event are also shown. A, B, C, D and F' indicate proportional planes, while E and F are spark chambers. A 22 cell gas Cerenkov counter between the E and F stations is omitted for clarity.

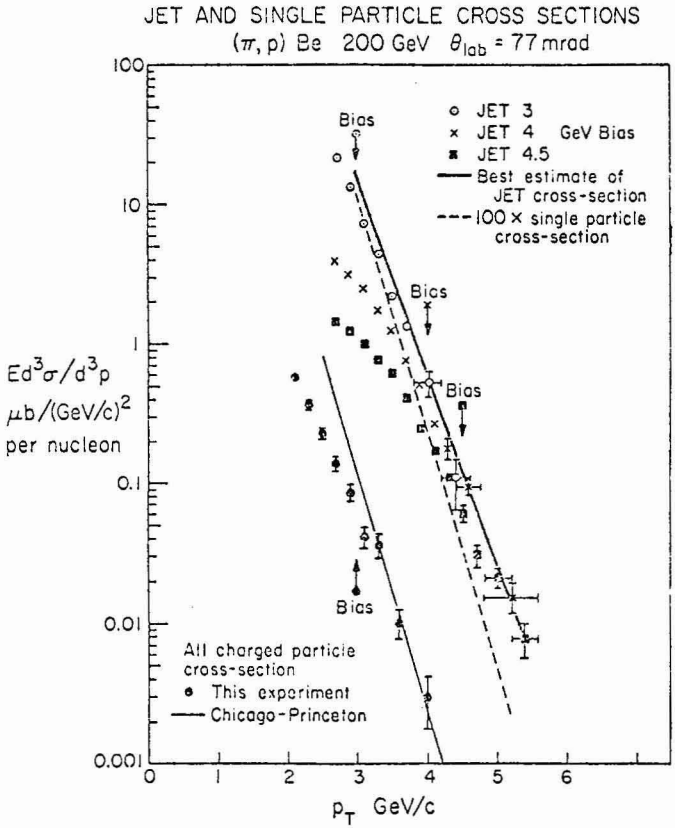

Figure 34. The single particle and jet cross sections averaged over the cms rapidity y region .1 to .44.

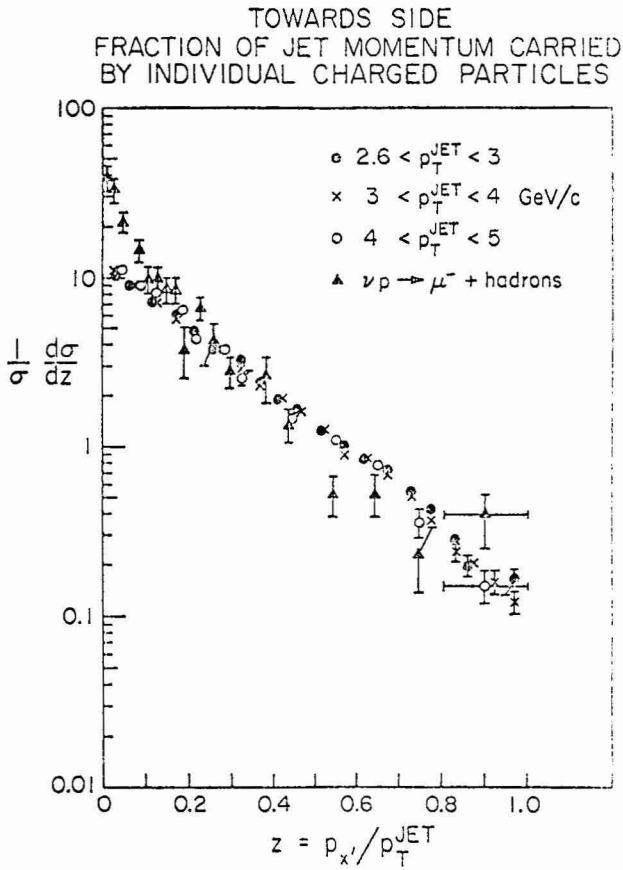

Figure 35. The distribution in transverse momentum fraction z for individual charged particles is shown for three jet P_t ranges. It is compared with the analogous distribution from neutrino scattering[59].

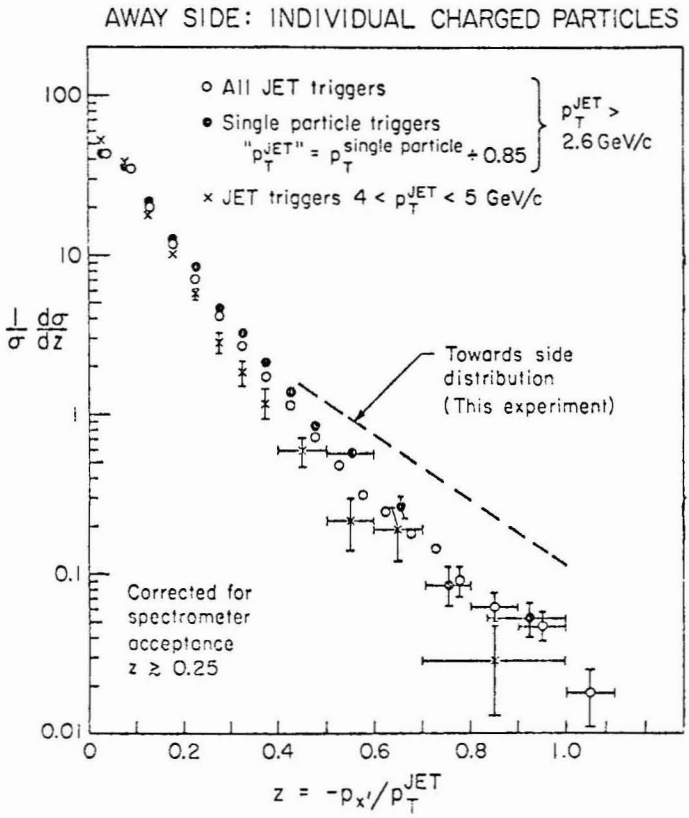

Figure 36. Distributions in momentum fraction z for particles on the away side for both jet and single particle triggers.

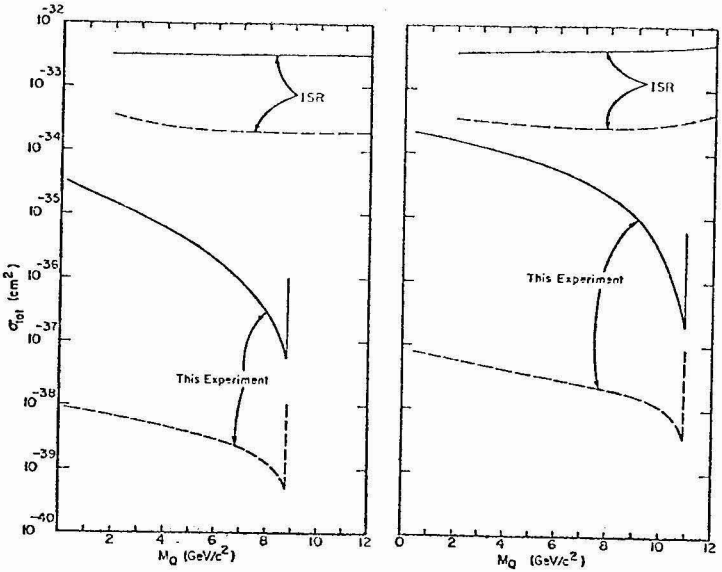

Figure 37. Upper limits on total cross section for fractionally charged particle production. (a) Charge -1/3; (b) charge -2/3. Solid lines, limits obtained assuming four-body phase space (with an isotropic center-of-mass angular distribution). Dashed lines, limits with the four-body phase space constrained by a multiplicative factor of $\exp(-6P_t)$, where P_t is the transverse momentum in GeV/c. Shown are results from this experiment and from Bott-Bodenhausen et al. (Ref. 62) at the CERN intersecting storage rings.

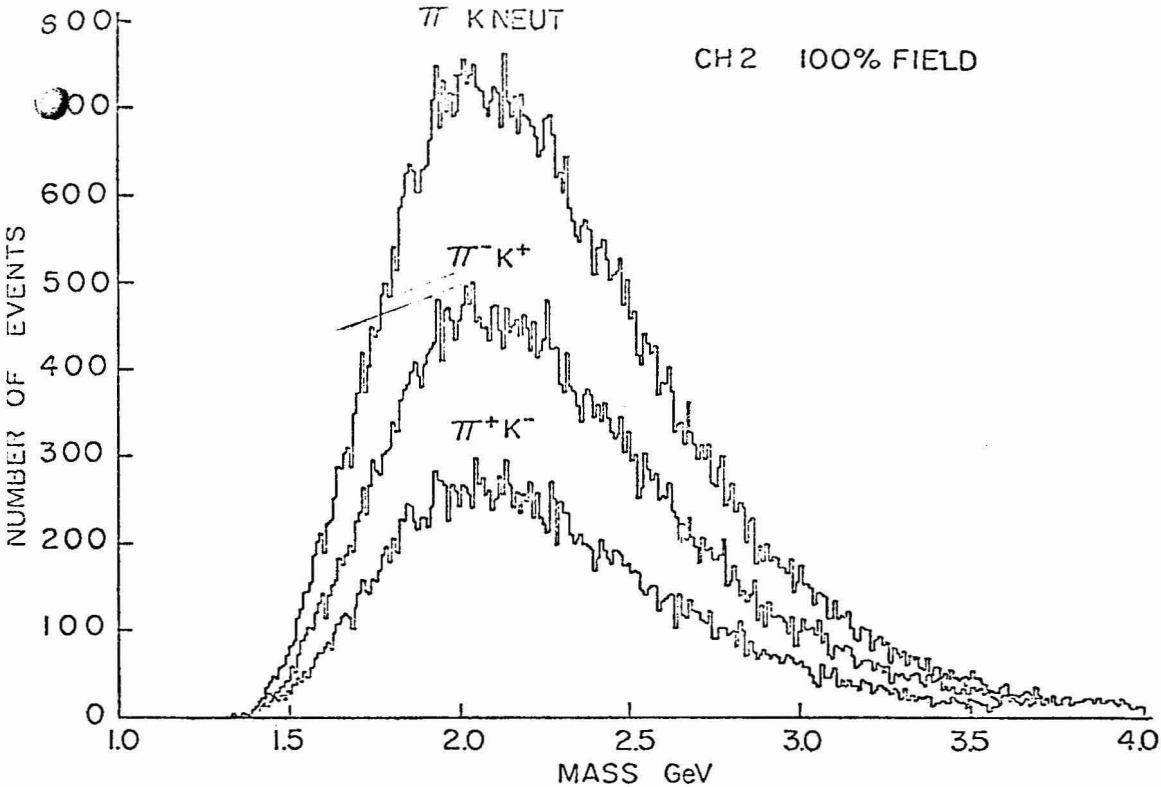

Figure 38. πK spectra: CH_2 target, 100% magnetic field.

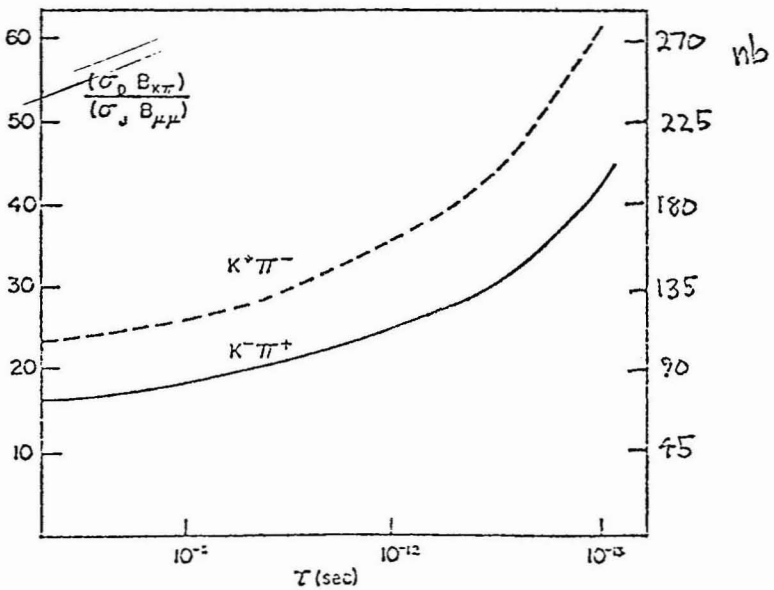

Figure 39. Sensitivity of "long-lived" search in units of $\sigma_J \cdot B_{\mu\mu}$ versus lifetime of D^0.

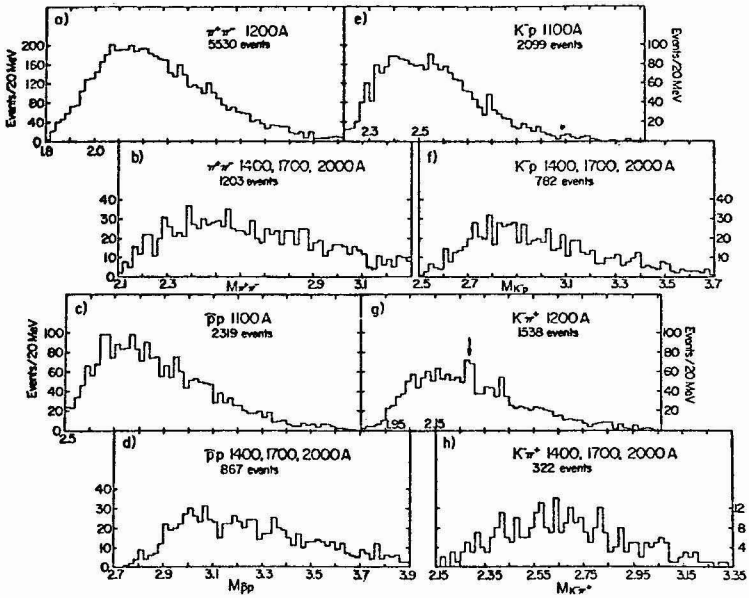

Figure 40. $\pi^-\pi^+$, $\bar{p}p$, $K^-\pi^+$ mass distributions from (a), (c), (e), (g) the lowest mass settings and (b), (d), (f), (h) the three higher mass settings of the spectrometer.

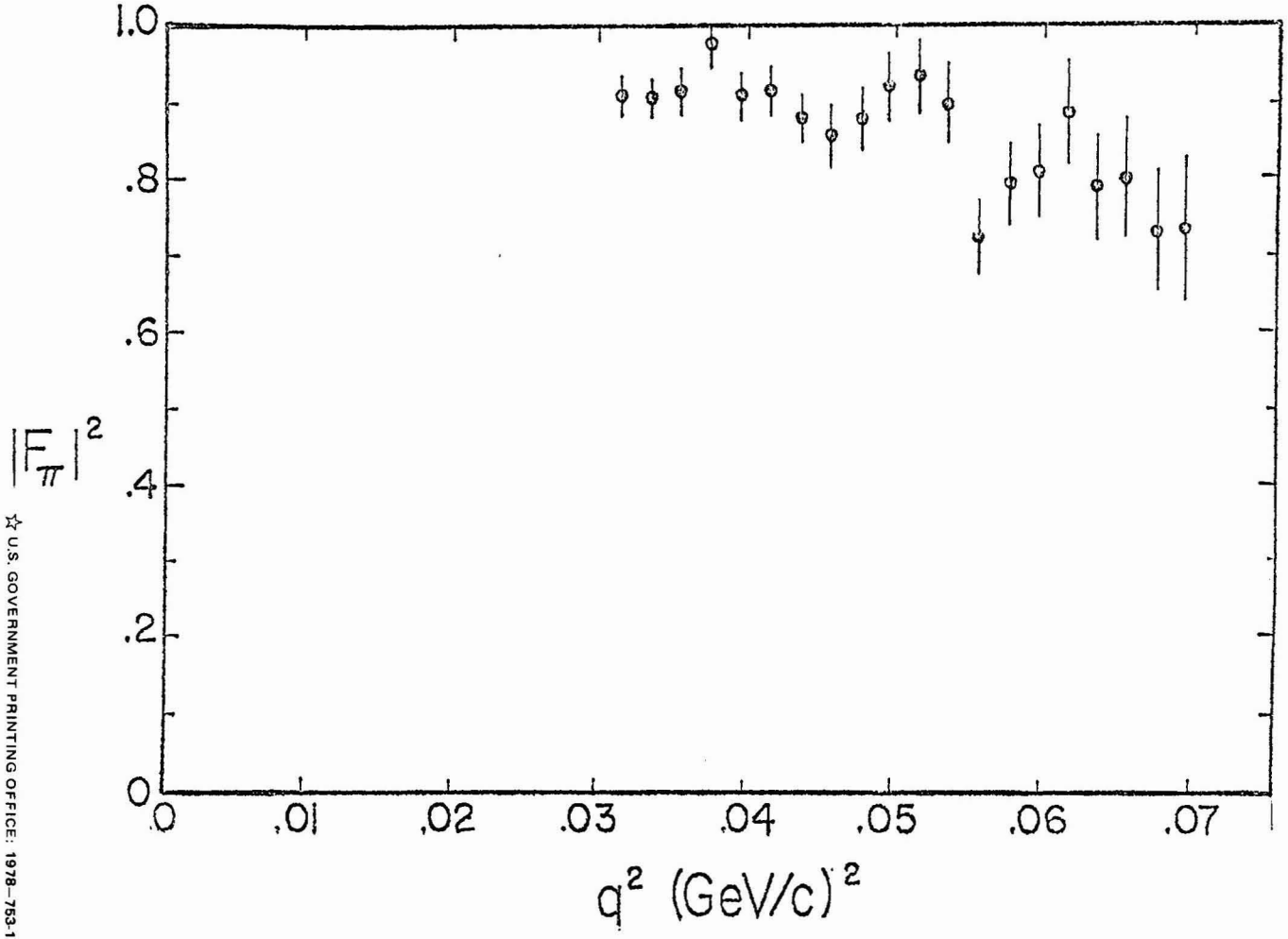

Figure 41. The pion form factor.

☆ U.S. GOVERNMENT PRINTING OFFICE: 1978—753-171